



CLIMATE  
CHANGE  
AGRICULTURE AND  
FOOD SECURITY

**CGIAR Research Program on  
Climate Change, Agriculture and Food Security (CCAFS)**

**Climate Change in East African Agriculture:  
Recent Trends, Current Projections, Crop-  
Climate Suitability, and Prospects for Improved  
Climate Model Information**

**February 2012**

**Richard Washington & Helen Pearce**



**Correct citation:**

Richard Washington & Helen Pearce. 2012. Climate Change in East African Agriculture: Recent Trends, Current Projections, Crop-climate Suitability, and Prospects for Improved Climate Model Information. CGIAR Research Program on Climate Change, Agriculture and Food Security (CCAFS). Copenhagen, Denmark. Available online at: [www.ccafs.cgiar.org](http://www.ccafs.cgiar.org).

Published by the CGIAR Research Program on Climate Change, Agriculture and Food Security (CCAFS).

CCAFS Coordinating Unit - Department of Agriculture and Ecology, Faculty of Life Sciences, University of Copenhagen, Rolighedsvej 21, DK-1958 Frederiksberg C, Denmark. Tel: +45 35331046; Email: [ccaafs@cgiar.org](mailto:ccaafs@cgiar.org)

Creative Commons License



This Report is licensed under a Creative Commons Attribution – NonCommercial–NoDerivs 3.0 Unported License.

This publication may be freely quoted and reproduced provided the source is acknowledged. No use of this publication may be made for resale or other commercial purposes.

© 2012 CGIAR Research Program on Climate Change, Agriculture and Food Security (CCAFS).

**DISCLAIMER:**

This report has been prepared as an output for Theme 4 Integration for Decision Making under the CCAFS program and has not been peer reviewed. Any opinions stated herein are those of the author(s) and do not necessarily reflect the policies or opinions of CCAFS. The geographic designation employed and the presentation of material in this publication do not imply the expression of any opinion whatsoever on the part of CCAFS concerning the legal status of any country, territory, city or area or its authorities, or concerning the delimitation of its frontiers or boundaries.

All images remain the sole property of their source and may not be used for any purpose without written permission of the source. All figures and maps are produced by the authors, unless otherwise noted.

## **Abstract**

The climate of East Africa is investigated and the implications of climate change on agriculture are assessed. The ability of General Circulation Models (GCMs) to reproduce the observed climate was investigated to establish how reliable future climate and associated crop growth projections might be. Current temperatures are simulated adequately, while the ensemble of models captures precipitation more robustly than any single model. The simulated spatial distributions of ten major crops grown in the region were generally similar to observed. A warmer future is projected in all models, along with a wetting trend in some areas projected to occur mainly during the short rains. Current crop distributions may be more affected by temperature changes in the future than by rainfall changes; this may favour crops with higher temperature thresholds (for example cassava and pigeon pea). Crops with cooler optimal thresholds (for example maize and millet) may be adversely affected by higher temperatures. Changes in the severity and frequency of extreme events in the region, while uncertain, could have substantial impacts on crop yields and food production.

## **Keywords**

General Circulation Model; climate; crop suitability; temperature threshold.

## About the authors

**Richard Washington** is Professor of Climate Science at the School of Geography and the Environment and Fellow of Keble College, University of Oxford. His research interests are in climate change and variability, particularly in Africa and the global tropics. He has degrees from the University of Natal and University of Oxford and taught at the University of Natal and University of Cape Town. His doctorate was on African rainfall variability and change, which was undertaken jointly between the University of Oxford under Professor Alayne Street-Perrott and Chris Folland's group at the Hadley Centre of the UK Meteorological Office. He took up a University Lectureship position and Fellowship at Keble College in 1999, and a Readership in 2006. Richard is Co-Chair World Climate Research Program African Climate Variability Panel (CLIVAR-VACS) 2006-2010 and served as a panel member of CLIVAR-VACS from 2003-2006. Richard leads the development of the CLIVAR Africa Climate Atlas. **Contact:** [richard.washington@ouce.ox.ac.uk](mailto:richard.washington@ouce.ox.ac.uk)

**Helen Pearce** is a DPhil student in the Climate Systems and Policy research cluster at the University of Oxford under the supervision of Professor Richard Washington. **Helen's current research focuses** on the East African region, using a combination of observed and model data to develop understanding of the climate system in this area. She is specifically concentrating on how the technique of Self-Organising Maps can be used to classify states of different climatic variables during the short rains season. **Contact:** [Helen.pearce@ouce.ox.ac.uk](mailto:Helen.pearce@ouce.ox.ac.uk)

# Contents

1. Introduction.....	6
2. The Observed Climate of East Africa.....	7
2.1 Description of datasets.....	8
2.2 East African climate - the basic state.....	8
2.3 Observed variability and trends.....	11
2.4 Climatic Extremes.....	18
3. Key Food Crops of East Africa.....	21
3.1 Crop selection.....	21
3.2 Crop growth thresholds.....	22
3.3 Results.....	23
4. Climate Models and the East African Climate.....	28
4.1 Model selection.....	28
4.2 Model simulation of the observed climate.....	30
4.3 Model climatology 1970 to 1999.....	31
5. Model derived crop growth thresholds.....	34
6. Model Climate Projections for the 21 <sup>st</sup> Century.....	36
6.1 Previous studies.....	36
6.2 Model projections.....	38
7. Future Climate Scenarios and the Impact of Crop Growth in East Africa.....	43
8. Summary and Conclusions.....	47
Appendix 1.....	50
Appendix 2.....	60
Appendix 3.....	66
References.....	87

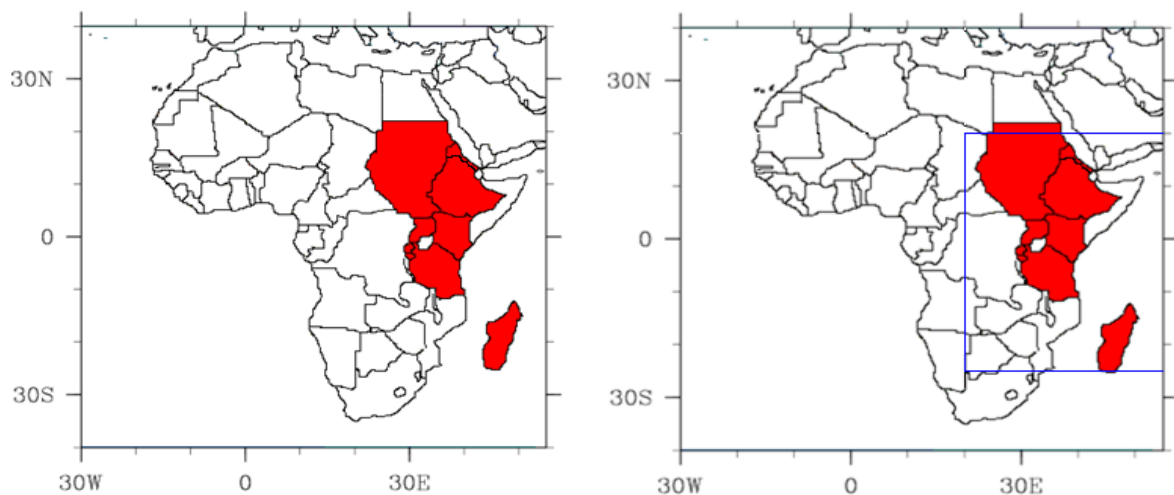
## Acronyms

AOGCMs	Atmosphere-Ocean General Circulation Models
CMIP3	Climate Model Intercomparison Project 3
CRU	Climatic Research Unit
DJFM	December, January, February, March
ENSO	El Nino Southern Oscillation
FAO	United Nations Food and Agricultural Organization
GCMs	General Circulation Models
IOD	Indian Ocean dipole
IPCC AR4	Intergovernmental Panel on Climate Change Fourth Assessment Report
ITCZ	Intertropical convergence zone
JJA	June, July, August
MAM	March, April, May
NCEP	National Centre for Environmental Prediction
OND	October, November, December
RCMs	Regional Climate Models
SLP	Sea level pressure
SRES	Special Report on Emissions Scenarios
SST	Sea surface temperature
SSTA	Sea surface temperature anomaly

# 1. Introduction

The question of potential changes to climate over the 21<sup>st</sup> century under increasing anthropogenic greenhouse gas emissions is a pressing one. This is particularly true where communities are heavily reliant on crops grown regionally, introducing significant food security and local management concerns and thus increasing the need for information about current projections of change and how this may impact on agriculture. One such region, and the focus of this study, is East Africa, with the consensus being that the impact of climate change on agriculture will impact significantly on development challenges of this continent (Thornton et al. 2009). The focus of this report is on a domain including Burundi, Eritrea, Ethiopia, Kenya, Madagascar, Rwanda, Sudan, Tanzania and Uganda and as such covering the region contained between 20°E and 60°E, 25°S and 20°N. This domain, highlighting the focus countries, is shown in Figure 1.1. Precipitation events in East Africa occur due to convective events linked to the migration of the intertropical convergence zone (ITCZ) about the equator leading to a bimodal annual cycle over much of East Africa with just one precipitation season to the north of the domain (Mutai and Ward 2000).

**Figure 1.1: The study domain employed in this report**



In Section 2, this report will begin by introducing the climate of the region, looking at annual cycles in temperature and precipitation, seasonal variations and climatic extremes. Trends in these measures over the second half of the 20<sup>th</sup> century will also be examined. The quality of the data employed herein and the impact this may have on the findings of this report will be discussed. In Section 3, selected crops of key agricultural importance in East Africa will be mapped to show their current spatial distribution in the region. The climatic thresholds and

limits for the production of each crop will also be introduced as a basis for analysis as to suitability of the region to continue to grow these crops in future. Section 4 will evaluate the ability of selected coupled general circulation models (GCMs) from the Climate Model Intercomparison Project 3 dataset (CMIP3) to reproduce the observed 20<sup>th</sup> century climate (climatology, variability and trends) as outlined in section 2. Section 5 employs the crop growth thresholds established in the previous section in order to evaluate the magnitude of model error over the East African region. In particular, the effect that this error has on the simulation of crop growth regions under current conditions in the GCMs in comparison to the crop maps plotted in Section 4 will be assessed. In Section 6 GCM climate change projections for the 21<sup>st</sup> century over East Africa are introduced. Preceding analysis of the output from the GCMs employed in this study there will be an examination of the current state of climate model science, focusing on the robustness and uncertainties of model projections. Analysis will be carried out focusing on three ‘time slices’ of the 21<sup>st</sup> century (2030s, 2050s and 2090s) and using three Special Report on Emissions Scenarios (SRES) emissions scenarios ranging from the high emissions A2 scenario through the A1B to a more conservative B1 scenario. In Section 7 the potential regions of growth of our selected crops under climate change projections for the domain will be analysed and discussed. The climatic thresholds and limits established for each crop will be again applied to the model output, this time during the 21<sup>st</sup> century in order to establish the potential risks to food security in East Africa under anthropogenic climate change. Again, three time slices and three SRES scenarios will be the focus. In Section 8 the research outcomes of the report will be summarised, key conclusions are reviewed and areas for further work are discussed.

## **2. The Observed Climate of East Africa**

In this section, background climate of the East African domain will be outlined, focusing on the variables of temperature and precipitation. Additionally, seasonal variability of the climate and trends of the region over the last half century will be examined. The East African focus regime has a climate regime distinct to the rest of the continent, with the movement of the ITCZ having a significant influence on the precipitation regime (Anyah and Semazzi 2006). With Giannini et al. (2008) highlighting that atmosphere-ocean general circulation models (AOGCMs) of different international modelling groups represent the African climate to varying degrees, with no universally accepted strategy on how to best weight the models

when they are used to simulate anthropogenic climate change scenarios it therefore indicates the importance of initially establishing current climatic conditions over the region prior to looking into future projections.

## 2.1 Description of datasets

Table 2.1 details the observed and reanalysis datasets of temperature and precipitation used in this study. The main surface temperature dataset used (mean, maximum and minimum) was the University of East Anglia’s Climatic Research Unit (CRU) gridded dataset (resolution 0.5° by 0.5° or about 55km at the equator). For precipitation, two reanalysis datasets were employed. These were the National Centre for Environmental Prediction (NCEP) and Japanese Reanalysis (JapRe) products.

**Table 2.1: Details of observed and reanalysis datasets**

Data	Dataset	Period available	Resolution	Key Papers
Land surface temperature	CRU TS2.1 (CRU)	1901-2002	0.5° x 0.5°	Mitchell and Jones 2005
Precipitation and temperature	National Centre for Environmental Prediction (NCEP)	1948-2010	1° x 1°	Kalnay et al. 1996
Precipitation	Japanese Reanalysis (JapRe)	1948-2006	0.5° x 0.5°	Hirabayashi et al. 2008

## 2.2 East African climate - the basic state

As previously stated, the precipitation cycle of East Africa is dominated by convective events associated with the migration of the ITCZ, with the annual precipitation cycle lagging the solar insolation cycle by approximately one month (Black et al. 2003). For many of the (more southerly) focus countries, precipitation falls mostly in the boreal spring [March, April, and May (MAM)] and autumn [October, November, and December (OND)], referred to as the long and short rains respectively (Mutai and Ward 2000) with precipitation falling in co-location with the migration of the ITCZ. Further north in the domain over much of Ethiopia, Sudan and Eritrea, at the most northerly limit of the ITCZ annual cycle there is a unimodal annual precipitation cycle with the primary rainy season falling during the boreal summer months [June, July and August (JJA), approximately]. Additionally, over much of Ethiopia there are preceding rains from March followed by a pause before the main rains begin (Verdin

et al. 2005). At the south of the domain lies Madagascar. Here, the ITCZ lies over the north part of the country during austral summer [December, January, February, and March (DJFM)] and this period therefore constitutes the main rainy season. The southernmost part of Madagascar has a low precipitation climatology and can be classified as a desert region (Jury et al. 1995).

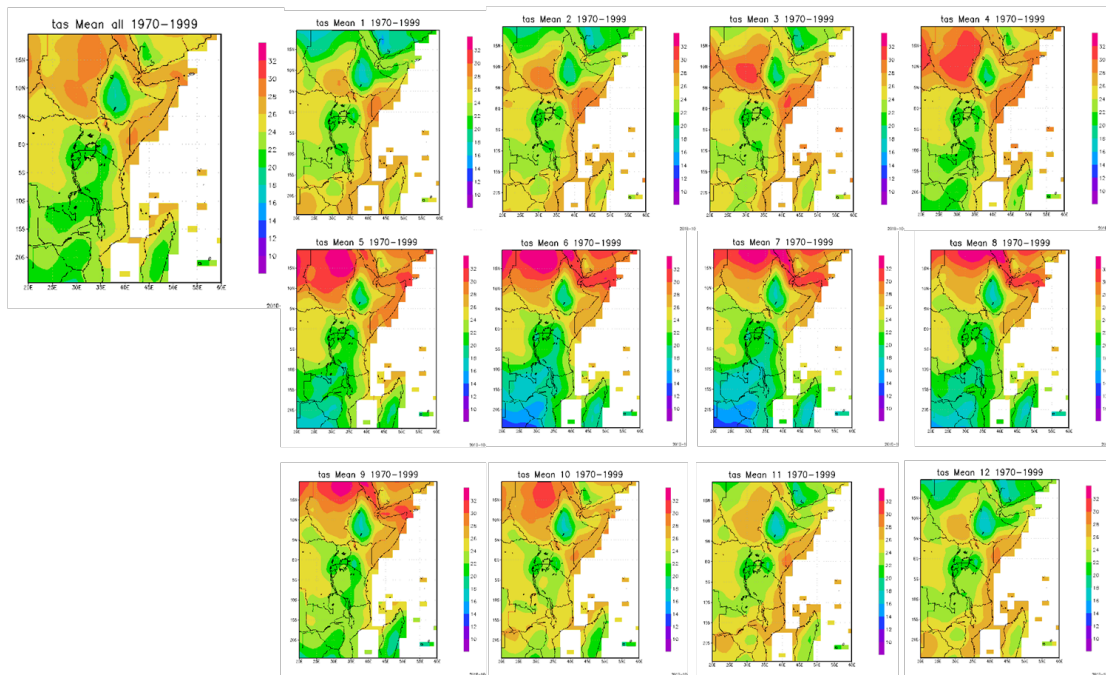
Interannual precipitation variability over the East Africa arises from a complex interaction between sea surface temperature anomalies (SSTAs), large scale atmospheric patterns, synoptic scale weather disturbances, tropical cyclones and subtropical anticyclones, extratropical weather systems, wave perturbations and free atmosphere variations (Mutai and Ward 2000). Relative to the long rains, the short rains tend to have stronger interannual variability, greater spatial coherence across a large area and more significant associations with El Nino Southern Oscillation (ENSO); warm El Nino events are associated with increased rain with negative anomalies occurring during La Nina events (Mutai and Ward 2000). The link to ENSO can be further connected to outbreaks of moist South Atlantic westerly flows, which are linked to anomalous precipitation over the region and tend to increase/decrease during El Nino/La Nina episodes respectively (McHugh 2006). This applies to all of the continental focus countries with the exception of Sudan (Schreck and Semazzi 2004). However, the connection between Madagascan precipitation and El Nino episodes is debated. Whilst Jury et al. (2003) argued that El Nino can be accompanied by wetter conditions over the island (following the teleconnection over the larger East African region); Ingram and Dawson (2005) link drought episodes in southern Madagascar to El Nino events, citing the 1982–3 and 1994–5 events as examples. This emphasizes the complex forcings and climatic controls in the East African region. A further control on East African precipitation is the Indian Ocean dipole sea surface temperature (SST) variability mode. Increased precipitation on the Indian Ocean coast of East Africa is linked to warm SSTAs in the western equatorial Indian Ocean, with SSTAs of the opposite sign present around Indonesia (McHugh 2006). In addition, topography also has a significant influence on the distribution of precipitation at a sub-regional scale (Oettli and Camberlin 2005).

### **2.2.1 Temperature**

Figure 2.1 shows the annual temperature climatology for the period 1970–1999 and the seasonal cycle for the wider East African domain. For the year as a whole, the highest

temperatures are found north of the Equator, where climatological mean temperatures are between 24 and 26°C with the exception of Ethiopia where they are between 18°C and 24°C. Ethiopia largely has temperatures similar to those seen south of the equator. Of the focus countries, the lowest mean temperatures are found in Madagascar where the warmest month of January has mean temperatures of 24°C and the lowest mean temperatures of 18°C are found in the austral winter months of June to August.

**Figure 2.1: Annual and monthly observed temperature climatology for the region**



The annual cycle has greatest amplitude in the north of the region over Sudan with mean temperatures in excess of more than 32°C from May to September but only 14°C in boreal winter. In contrast, the East African coastline of Kenya and Tanzania has a much less defined annual cycle, with mean temperatures consistently remaining in the region of 22°C to 26°C throughout the year. Ethiopia has relatively cool temperatures in comparison to the surrounding countries due to the highland areas of high relief. The landlocked countries of the domain; Uganda, Rwanda and Burundi, have both consistent and moderate mean temperatures throughout the year in the region of 20–26°C, with their equatorial location meaning there is little seasonal variation in mean temperatures.

### 2.2.2 Precipitation

Figures 2.2a and 2.2b (the NCEP and JapRe reanalysis precipitation datasets) show the 1970–1999 regional precipitation climatology and seasonal cycle. The primary feature of the

seasonal precipitation cycle is the movement of the intense centre of precipitation governed by the migration of the ITCZ from around 15°S in January to a northward maximum at approximately 10–15°N in the boreal summer months, from June to August before returning back across the equator, following the strongest insolation, in boreal winter.

Within the focus countries, there are several different precipitation regimes across the domain. Several of the East African countries, Tanzania, Uganda, Kenya, Burundi and Rwanda and southern Ethiopia have a bimodal precipitation regime, with precipitation seasons from March to May (the long rains) and October to December (the short rains) associated with the seasonal passage of the ITCZ. In the NCEP reanalysis the precipitation peaks at between 5 and 9 mm/day, with more intense precipitation values of up to 11 or 12 mm/day in the JapRe dataset. This is a common pattern over all regions and months of the domain, with the JapRe dataset showing consistently heavier daily precipitation than the NCEP dataset and having a more northerly peak of precipitation associated with the seasonal migration of the ITCZ. Sudan, northern Ethiopia and Eritrea in contrast have one main precipitation season, in boreal summer (approximately June–September, with peak intensity in July–August) when the location of the ITCZ is at its northward maximum. Sudan, being the northernmost country in the domain, has a very large precipitation gradient from desert regions in the north with less than 75 mm annual precipitation to the equatorial zone in the south with a precipitation climatology of 1200 to 1800 mm (Osman and Shamseldin 2002). Madagascar has a unique annual precipitation pattern in comparison to the other countries in the domain, with a long rainy season from November to April over the austral summer with peak precipitation values of 10 mm/day in NCEP in January and 12 mm/day in January in the JapRe dataset. This rainy season is followed by a dry season from May to October.

## **2.3 Observed variability and trends**

### **2.3.1 Short term variability**

Figure 2.3 shows patterns of annually averaged CRU temperature, NCEP precipitation and JapRe precipitation averaged over the region. For temperature, whilst there is significant interannual variation, the general trend is towards warmer mean temperatures. In particular the increase is especially evident from approximately 1970 onwards. In contrast, both the NCEP and JapRe precipitation datasets show no clear overall trend, but do exhibit significant

interannual variability, with a climatological precipitation mean of between 2.3 and 3.1 mm/day throughout the second half of the 20<sup>th</sup> century.

**Figure 2.2: Annual and monthly precipitation climatology (in mm/day) for the region taken from the (a) NCEP and (b) JapRe reanalysis datasets**

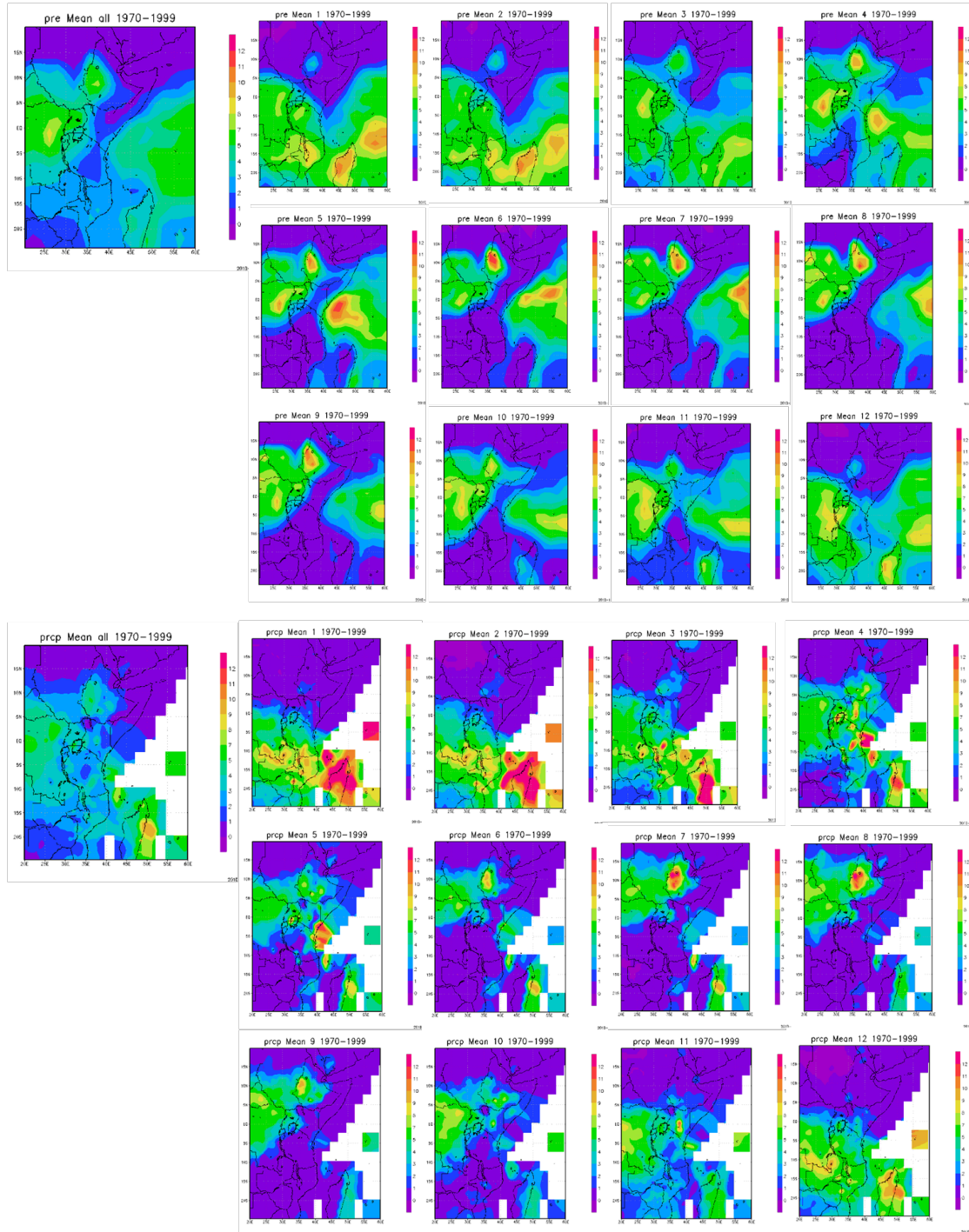
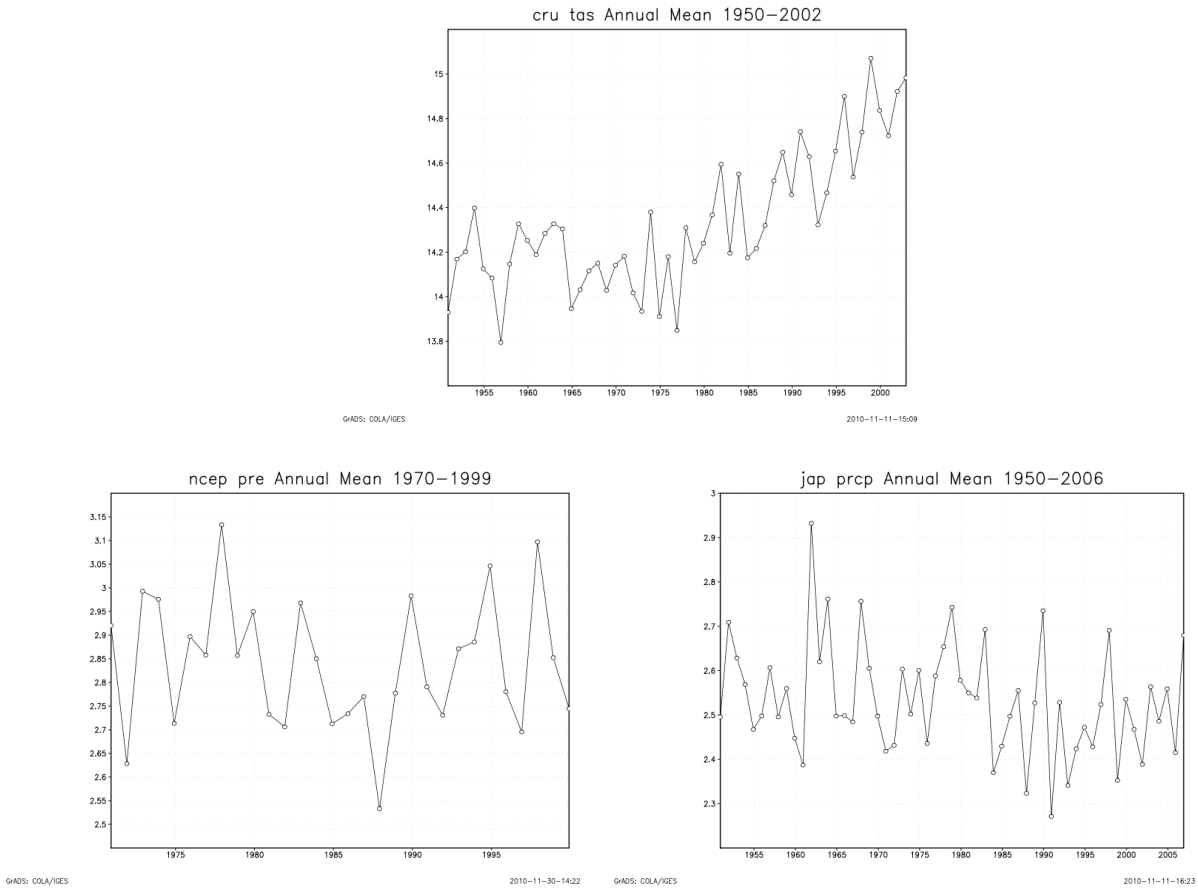


**Figure 2.3: Annual average precipitation and temperature, averaged over the region for (a) temperature, (b) precipitation (NCEP) and (c) precipitation (JapRe)**



There is considerable interannual variability in the East African climate, with greater interannual variability being associated with the short OND rains than the long MAM rainy season (Camberlin and Philippon 2002). There are two key modes of interannual variability in the region. ENSO is the first. The documented teleconnection with ENSO is both direct (atmospheric teleconnections) and indirect (through the response of the Indian and Atlantic Ocean basins) (Giannini et al. 2008). The strength of this interannual relationship is strongest in the short OND rains, when there is a positive relationship between South Pacific circulation variability and East African precipitation that is statistically significant at the 99% confidence level. However, there is also statistically significant (at the 98% level) relationship with the long MAM rains; in this case the relationship exhibits a negative correlation with the long rains over East Africa decreased during El Nino events (McHugh, 2006). McHugh (2006) demonstrates that during El Nino events outbreaks of moist South Atlantic westerly flows over East Africa are increased. These anomalous westerlies during El Nino episodes prevent

the inflow of thermally stable subsiding air masses from the Indian Ocean. This therefore increases low level moisture convergence, decreases lower troposphere stability and so increase cloudiness and precipitable water anomalies during the short OND rainy season (McHugh 2006).

A second mode that has a significant impact on East African interannual precipitation variability, particularly in the short OND rains, is the Indian Ocean dipole (IOD).

Ummerhoffer et al. (2009) conclude that anomalously high rains during OND are primarily associated with local warm SSTs in the western Indian Ocean, with the cooler eastern part of the dipole much less crucial. This occurs because the warm sea surface temperature anomalies induce a co-located area of low sea level pressure (SLP) over the western Indian Ocean and East African coast. These SLP anomalies induce enhanced westerlies over central Africa and onshore anomalies that converge over equatorial East Africa. These influences combine to increase latent heat flux, atmospheric moisture content and local convection (Ummerhofer et al. 2009). These events are known as a positive IOD mode. Conversely, during the negative IOD mode East Africa receives less precipitation than normal during the OND rainy season (Behera et al. 2005).

In contrast to the short OND rains, the long MAM rains show much weaker teleconnections to external modes of variability, partially due to the incoherent spatial and temporal precipitation anomalies seen during this period, although there may be connections on a more local scale. For example, eastern Ethiopian precipitation is negatively correlated with southwest Indian Ocean tropical cyclone activity and northern Ethiopian and Eritrean precipitation in spring may be connected to movement of mid latitude ridge-trough systems (Riddle and Cook 2008).

### **2.3.2 Decadal variability and observed trends**

Global mean temperatures have increased by  $0.74^{\circ}\text{C} \pm 0.18^{\circ}\text{C}$  over the past century (1906–2005) with an accelerated rate of warming of  $0.07^{\circ}\text{C}/\text{decade}$  over the past 50 years on average (IPCC AR4 2007). With this in mind and the current focus on anthropogenic climate change it is important to evaluate trends in the climate over East Africa that may be attributable to increases in greenhouse gases over recent decades. Christy et al. (2009) analyse 20<sup>th</sup> century station temperature over Kenya and Tanzania and conclude that from 1946–2004 trends in maximum temperature are near zero, whereas minimum temperature sees a significant positive trend over the same period. This shows a decrease in the diurnal temperature range,

which over Sudan and Ethiopia has decreased by between 0.5°C and 1°C since the 1950s (Caminade and Terray 2006). There have been several studies into trends in the region over the second half of the 20<sup>th</sup> century. Schreck and Semazzi (2004) identify a precipitation trend mode over East Africa characterised by positive anomalies to the north of the region and negative to the south with the axis of this trend located on a northwest to southeast orientation from the Ugandan border with the Democratic Republic of Congo in the west to the Indian Ocean coast around Zanzibar in the east. They do not go as far as to attribute this pattern occurring during the short rains to global warming but suggest instead a strong potential connection (Schreck and Semazzi 2004). A largely positive 20<sup>th</sup> century trend in basin precipitation around Lake Victoria has been identified (Kizza et al. 2009). The authors also note the significant influence of the short OND rains on annual precipitation variability, with most stations having a significant annual trend also having exhibited a coincident significant trend in OND precipitation.

However, there are also conflicting studies that suggest decreases in precipitation during key growing seasons in East Africa. For example, Funk et al. (2008) conclude that Ethiopia, Kenya, Burundi and Tanzania saw precipitation decline during the 1979–2005 period. They suggest that this may be due to Walker circulation anomalies that have arisen as a result of increased tropical Indian Ocean precipitation (due to relatively high warming of SSTs in this region). These Indian Ocean anomalies are associated with atmospheric ridging and anticyclonic moisture circulation over Eastern Africa which disrupts the main onshore moisture flows. Furthermore, the CMIP ensemble experiments suggest that anthropogenic increases over the late 20<sup>th</sup> century are likely responsible for the Indian Ocean warming that they propose induces drying over the East Africa seaboard (Funk et al. 2008). A particularly strong decline to the order of 35–45 percent of the 1950–1979 mean precipitation through much of central and eastern Ethiopia and Kenya has been noted (Williams and Funk 2010). This trend is reinforced by data which suggests that drying has been amplified at high elevations, for example at the summit of Kilimanjaro (Mölg et al. 2009).

In addition to trends in mean statistics, for agriculture the onset of the wet season is also important. Kniveton et al. (2009) investigate trends in the start of the wet season over Africa from 1978–2002. Over Madagascar, in common with much of Africa, there is a trend towards a later start to the rainy season of up to 0.5 days a year. In continental East Africa the trend is

more mixed with some isolated locations showing an earlier start to the rainy season (Kniveton et al. 2008). These different studies indicate the complex nature of trends in the East African region, reinforcing the fact that different seasons may see contrasting trends in mean figures over the 21<sup>st</sup> century.

Figures 2.4, 2.5a and 2.5b show the decadal changes in CRU temperature and NCEP and JapRe precipitation respectively from 1961–2000. Averaged annually over this period, most of the domain sees a warming trend of between 0.1 and 0.6°C/decade. There is a small region of no change or very slight cooling trend (+0.1°C to -0.2°C/decade) but this is located over the Democratic Republic of Congo and so not one of the focus countries of this study. There is also a region on the Indian Ocean coast of Tanzania and Kenya that sees very little change in mean temperatures during this period. The greatest positive trend in temperature is seen to the north of the domain and measures between 0.3 and 0.6°C/decade, focused over Sudan and extending into Ethiopia and Uganda. The other focus countries of this study, inland Kenya and Tanzania, Burundi, Rwanda, Madagascar and Eritrea see a positive trend of between 0.1 and 0.3°C annually over the period 1961–2000.

From month to month, the spatial pattern of trends is very similar to that described for annual trends, with the magnitude of positive temperature trends being the main variable on the seasonal level. The greatest positive trend is observed in the north of the region in the later part of the year from August to December, with the trend reaching up to 1.1°C/decade in August. This time of year also sees an accentuation of the positive temperature trend over the remainder of East Africa, although to a lesser extent than in the North. The only months where the north of the domain does not have the largest positive trends are January and February where the area of greatest trend migrates south over Uganda and southern Sudan and measures 0.6°C/decade. During these months the northern region sees a slight negative trend of between 0 and -0.2°C/decade. For all individual months, the temperature trend in the remainder of the focus countries is largely consistent and with that of the annually averaged figures.

In contrast, precipitation trends from 1961–2000 show much less coherence, especially between the NCEP and JapRe datasets. The NCEP data (Figure 2.5a) shows an annually averaged drying trend of 0 to -1.1 mm per day/decade over all of the focus countries except Madagascar (where a positive trend of up to 0.6 mm per day/decade is recorded). In

comparison, the JapRe dataset indicates no clear trend on an annually averaged basis with trends across the region of between -0.3 mm and +0.3 mm per day/decade.

Analysing the monthly patterns, the divergence in the magnitude of trends between the NCEP and JapRe datasets continues. In the NCEP data the greatest decreases over the East African region are found during the long rains from March and continuing into June with decreases of up to -1.8 mm per day/decade, the centre of this trend being focused on southern Sudan, Ethiopia, Uganda, Rwanda and Burundi. Though much of the region exhibits negative trends across these years there are some positive trends evident in Ethiopia from 0.0 to 0.9 mm per day/decade from October to December.

Madagascar is an anomaly relative to the rest of the domain, with a positive precipitation trend of up to 1.8 mm per day/decade in annual precipitation totals and the greatest increases recorded in January and February in the NCEP dataset. However, in the JapRe dataset Madagascar does not exhibit a consistent positive trend over the year, with January and February seeing negative trends of up to 1.8 mm per day/decade in direct contrast to the NCEP data. Furthermore the East African short MAM rains see a slight positive trend of up to 0.8–0.9 mm per day/decade. These differences in apparent trends in precipitation between the two reanalysis dataset highlight the problems of creating an accurate record of precipitation over East Africa.

**Figure 2.4: Temperature trend from the CRU dataset from 1961-2000. Trends are in °C/decade**

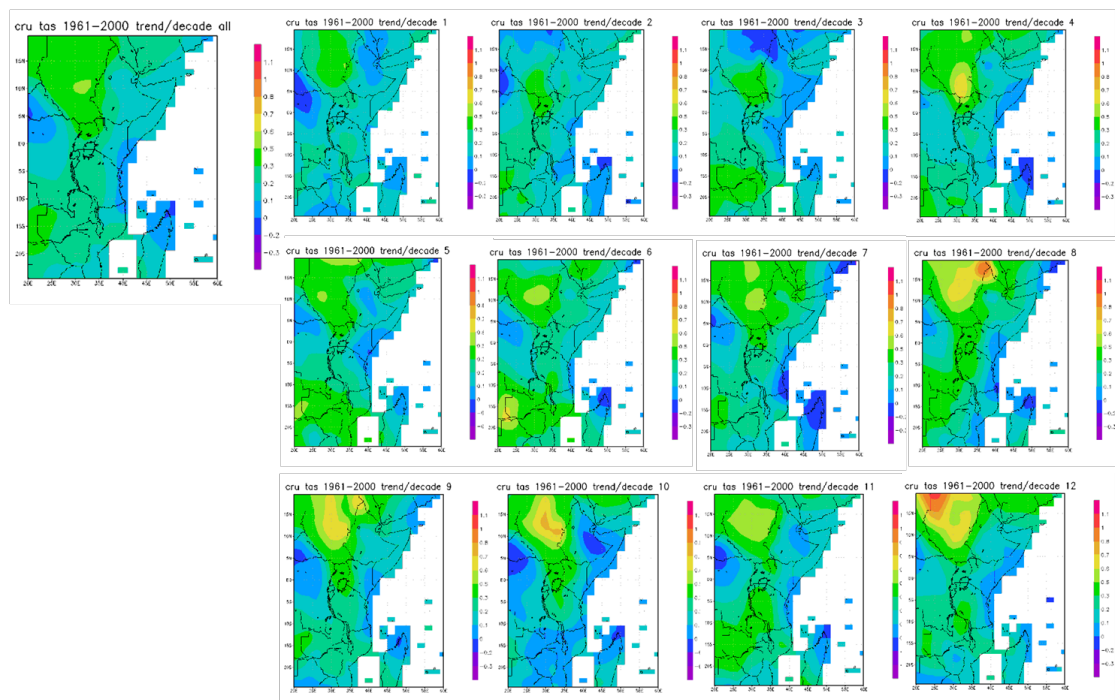
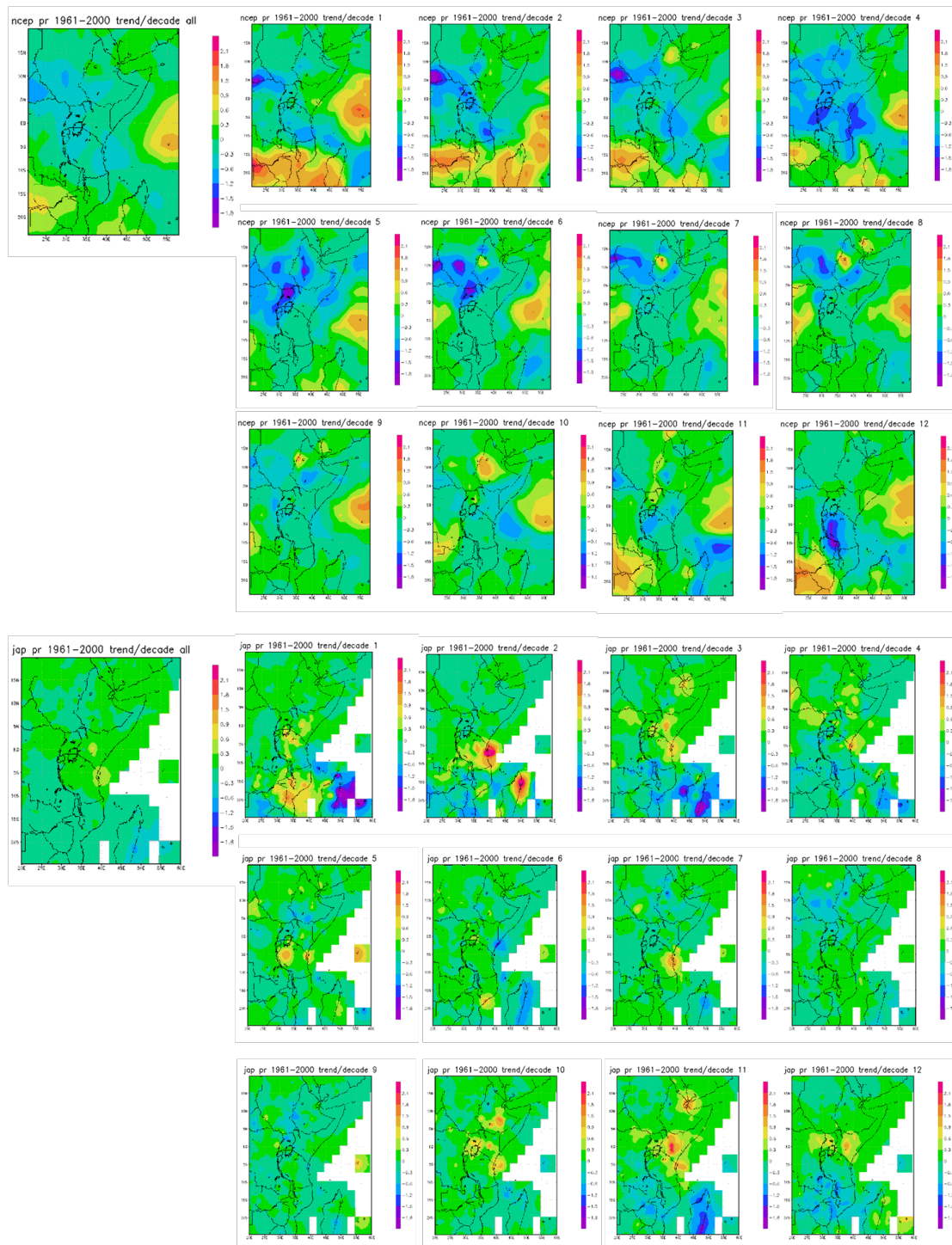


**Figure 2.5: Precipitation trend for (a) NCEP and (b) JapRe datasets. Trends are in mm/decade.**



## 2.4 Climatic Extremes

Variability and change in climatic extremes are also of significance to agricultural production, with indices discussed here chosen due to their relevance to key crops grown in East Africa (introduced in Section 3). Easterling et al. (2000) suggest that societal infrastructure is

becoming more sensitive to climatic extremes, for example through cultivation and settlement on marginal lands and so, in some cases, extreme conditions (such as droughts, flooding or heatwaves) can have greater impact on crop yields than optimal mean conditions.

Furthermore, it has been suggested that the impact of climate change will be felt most strongly through changes to intensity and frequency of extreme events (Kharin et al. 2007). Analysing extreme events is more difficult than mean conditions partially due to the lack of observed daily data at the regional level; in the tropics particularly, such data is often unavailable which prohibits an accurate analysis of extreme events (Kiktev et al. 2003). Additionally, it appears that model differences are the primary source of uncertainty in simulation of current extremes in models, with simulation of extreme precipitation events in the tropics being particularly problematic (Kharin et al. 2007).

Under anthropogenic warming, it is likely that the intensity and frequency of extreme events will increase. Here, the occurrence of 95% single day precipitation events in NCEP and JapRe precipitation (Figure 2.6a and b), 95% maximum single day temperature events in CRU (Figure 2.7) and 5% minimum single day CRU temperature events (Figure 2.8) are analysed. The difficulties and uncertainties in modelling extreme events are highlighted above through comparing the JapRe and NCEP trends for the 1970–1999 climatology period. The spatial distribution of climatological precipitation for both reanalysis datasets is similar, with the most intense 95% maximum precipitation events in the region in western Ethiopia and the eastern coastal part of the domain, particularly eastern Ethiopia, Kenya and Tanzania experiencing lower 95% maximum precipitation peaks. However, the magnitude of the 95% maximum precipitation events differs significantly between the NCEP and JapRe datasets. In line with the climatology for the two reanalysis datasets, the JapRe dataset peaks at much higher values with the 95% maximum events having a magnitude of between 30 and 35 mm/day in contrast to between 20 and 25 mm/day in NCEP over the same region. Turning to trends in these events for the period 1970–1999, the two datasets produce trends of opposite sign over central Sudan, with a negative trend of up to 10% in the NCEP dataset and a positive trend in the JapRe data. Elsewhere over our focus countries, the NCEP data has a slight negative trend in maximum precipitation events (up to 2%). In contrast, the JapRe dataset shows no clear trend in 95% events over the region, although there is a tendency for the coastal areas to show slight positive trends (2%/decade) with a slight negative trend further inland. Over Madagascar, the JapRe dataset indicates a slight decreasing trend in the

magnitude of 95% maximum precipitation events whereas NCEP there is a positive trend over most of the country other than a small area of decreasing intensity in these events in the north. This inconsistency in trends can at least be partially attributed to the short climatology period of only thirty years, which for a variable with high interannual variability such as precipitation, can lead to the appearance of artificial and inconsistent trends.

**Figure 2.6: Climatologies and percentage trends during the 1970-1999 period of 95% daily precipitation events taken from (a) NCEP and (b) JapRe. The trend figures are percent per decade trends.**

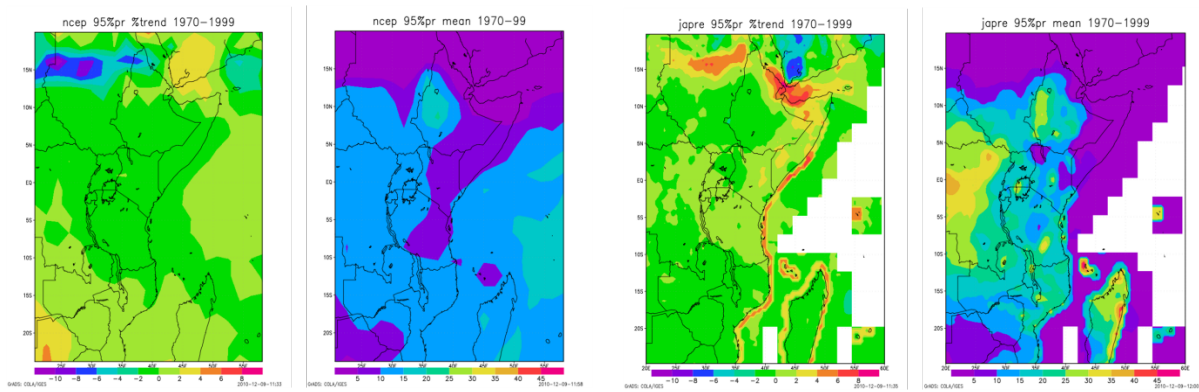
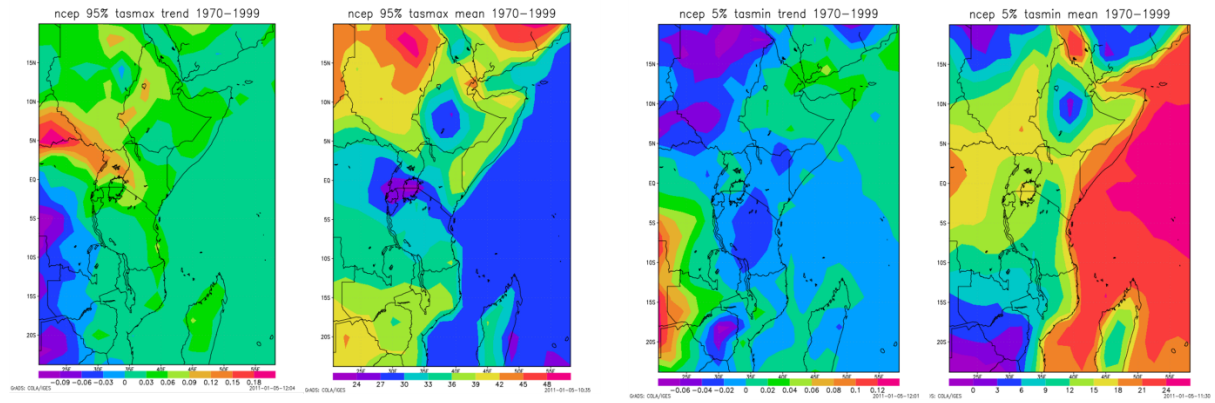


**Figure 2.7 (left) and Figure 2.8 (right): Trends for 95% maximum temperature and 5% minimum temperature events. Trends are in degrees per decade.**



The Ethiopian highlands are the location for both the coldest 5% minimum temperature events and the lowest maximum temperature events, with the climatology figure between 0 and 6°C and 24 and 30°C respectively. Temperature maximums are found in northern Sudan and peak at 48°C, with southern Sudan having the second highest temperature peaks of 42°C. In terms of the 5% minimum temperature events, aside from the centre over Ethiopia low minimum temperatures are also found over central Sudan with the remainder of the focus countries

having temperature minimums of between 6 and 18°C. In terms of percentage change, trends in temperature extremes are relatively small, but consistent across the focus region. As would be expected given the forcing effect of increasing greenhouse gas concentrations at the end of the 20<sup>th</sup> century, 95% maximum temperatures have increased by up to 0.18°C decade over East Africa, with Uganda, Rwanda and Burundi the centre of this increase. There is also a slight cooling trend in the extreme minimum temperatures of East Africa, with this being most apparent over central Tanzania (-0.06°/decade).

### **3. Key Food Crops of East Africa**

In this section, some key agricultural food crops produced in the East African region will be introduced. The optimum, and also extreme, thresholds for the growth of these crops will be examined alongside the current distribution of production over the domain. This will allow the identification of areas which may already be climatically marginal where, if production is currently occurring, may face food security concerns in the near future. This approach also highlights whether the potential for production is being realised across the region, and introduces the possibility of regions where non climatic factors may play a considerable role in production if there are regions where current conditions appear optimal for cultivation but the current distribution of growth does not match this.

#### **3.1 Crop selection**

Crops were selected based on their financial value to the specified countries in the East African region, with consideration also made to those which were particularly important from a food security perspective. Additionally, crops which were grown across the majority of the countries in this fairly diverse domain were prioritised. Table 3.1 shows the selected crops, their total value to the region (internationally standardised prices), and the number of the countries in the domain where the crop is grown (there are a total of 9 countries in the domain).

**Table 3.1: Crops selected for this study, their value across the East African region and number of the study countries they are grown in. Values are from United Nations Food and Agriculture Organization (FAO).**

Crop	Total value (\$1000s)	No. countries grown in
Maize	1 277 201	8
Cassava	1 142 874	6
Bananas	980 947	7
Sorghum	938 746	7
Rice	896 989	5
Sweet Potatoes	728 192	8
Wheat	447 076	6
Potatoes	413 219	7
Millet	247 345	3
Pigeon Pea	99 863	4

### **3.2 Crop growth thresholds**

A review of available grey literature was undertaken to establish optimal and extreme thresholds for growth of each crop. Key values are shown in Table 3.2.

The primary thresholds used relate to temperature and precipitation; optimum temperature range, optimum precipitation range, optimum minimum temperature, optimum average minimum temperature, absolute/optimum maximum temperature and absolute precipitation range. The thresholds are then used to create masks which depict the geographical limits of growth of each crop within the East African region. To expand, for each crop individually, each variable (for example optimum temperature range) is taken in turn and the established range is applied to the observational and reanalysis data to create a mask with two possible values; 0 when the condition is not met, and 1 when it is. In this example this will create a map shaded where the data is within the optimal temperature range, indicating that the optimal cultivation conditions for this variable exist for the crop. This process is then repeated for each variable and the maps layered to indicate the relative suitability for growing the crop over different parts of the domain (high values indicate greater suitability for production). However, where there are absolute thresholds (such as absolute minimum precipitation) this indicates that the area is not suitable for the cultivation of a particular crop even if other optimal conditions are met.

The following plots are produced with respect to the 1970–1999 climatology:

- Optimum temperature range
- Absolute precipitation range
- Optimum precipitation range
- Optimum minimum temperature (single lowest instance of daily minimum temperature during relevant months)
- Optimum average minimum temperature (applicable to all crops except cassava, millet and sorghum, and combined with optimum minimum temperature in one mask where both conditions are satisfied)
- Absolute/optimum maximum temperature (applied to all crops except millet and sorghum)

### **3.3 Results**

The plots for these masks applied to the climatology period are shown in Appendix 1, Figures A1 to A10, with separate climatology plots being shown for the NCEP and JapRe precipitation datasets. The highest numbers correlate directly with the greatest number of criteria being satisfied.

**Banana:** In common with all of the crops, the primary limiting factor on growth is precipitation; however it would be possible to grow bananas outside of the indicated climatological area through irrigation. Optimum growing conditions (with NCEP reanalysis precipitation) are found in the west of the domain, from northern Tanzania up through Burundi and Rwanda and into western Ethiopia, and also over Madagascar. The JapRe precipitation dataset indicates optimum growing conditions are similarly co-located but over a smaller region.

**Cassava:** Under both precipitation datasets indicate suitable conditions for cultivating cassava are found across most of the East African domain, with the exception of northern Kenya and eastern Ethiopia. Optimal conditions for cassava are located in Madagascar and the western part of the domain, although high suitability values for cassava growth are found over all of the focus countries.

**Maize:** Maize has limited areas of optimal growth in the East African domain, restricted to the Indian Ocean coastline of Kenya and Tanzania and much of southern Sudan under both

reanalysis precipitation datasets. Although not an absolute limit on cultivation, tropical growth maize prefers very warm minimum temperatures (20°C) which are not found over much of the domain which could limit yield.

Millet: Optimal growing conditions for millet are located where precipitation is relatively low in comparison to the other crops. Therefore, optimal conditions for millet growth are found in eastern Ethiopia, Kenya and Tanzania, with suitable conditions found along the eastern part of the domain. The impact of the differences between precipitation datasets are more evident here, with precipitation limits in the JapRe set leading to the inclusion of Rwanda, Burundi and northern Tanzania within the millet growth domain where it is excluded by the NCEP dataset. The Agro-Maps Database (Figure 3.11) indicates that millet can be grown in these countries.

Pigeon Pea: Both the NCEP or JapRe reanalysis datasets indicate that pigeon pea can be cultivated under optimal conditions over much of East Africa. This is primarily attributable to the ability of pigeon pea to withstand large variations in precipitation and temperature.

Potato: Optimal conditions for growing potatoes are not found anywhere in the East African region, due to warmer than ideal mean temperatures found at this latitude. Furthermore, potatoes cannot tolerate waterlogging and so most suitable conditions with both NCEP and JapRe precipitation are found in Kenya, eastern Ethiopia and eastern Tanzania along the Indian Ocean coastline and also in a belt across southern Sudan.

Rice: For both NCEP and JapRe datasets, the optimal area in the domain for rice growth is in southern Sudan where there an optimal combination of significant annual precipitation and very high minimum temperatures. However, rice could also be grown over most of the East African domain and Madagascar, especially if irrigation systems are utilised.

Sorghum: In contrast to most of the selected crops, temperature instead of precipitation may be the main limiting factor for sorghum cultivation in the region. This crop prefers very high mean temperatures which can be found mainly over Sudan, making this the optimal region for its growth. Sorghum can however tolerate a large absolute precipitation range allowing it to be grown over much of the East African region, especially over Kenya and eastern Ethiopia.

Sweet potato: Optimal regions for growth of sweet potato are similar under both the NCEP and JapRe datasets and are co-located where lower mean average temperatures are located in

the south of the domain over Tanzania, Uganda, Burundi, Rwanda and Madagascar. However, sweet potatoes require minimum annual precipitation of 750 mm which means in the NCEP dataset much of Kenya and Tanzania is unsuitable for sweet potato cultivation although this is not the case under JapRe.

Wheat: Both precipitation datasets indicate that much of the East African domain is deemed unsuitable for the cultivation of wheat due to the narrow absolute precipitation limits. This means the optimal areas for wheat cultivation are where total precipitation values are lowest over eastern Ethiopia and Kenya and a band across central Sudan in both datasets, with much of eastern Tanzania also falling within the optimal growth domain in the NCEP dataset.

**Table 3.2: Growth limits of the crops investigated in this study**

CROP	Optimal Avg Temp	Max Temp	Min Temp (single day)	Optimal Avg Precip	Max Avg Precip	Min Avg Precip	Capacity to deal with waterlogging/ saturation?	Capacity to deal with drought?	Growing period	Altitude	Photo-sensitivity	Harvest
Millet (Pearl)	20-28		12	250-600 (500+ for forage)	1200	125	No waterlogging, esp in summer	Yes, but needs rain late in devt and cannot tolerate extreme drought	70-80	<1500m		Late summer
Cassava	22-28	<30av for 8m	10	1000-4000	5000	500	No	Yes, up to 2-3 months	365	<1500m	<13h light	All year
Sorghum (lowland)	28-31		15	450-750		300(?)	Yes	Yes, but not in 60 days after planting	90-120	<1500m	>12h light	Late summer
Pigeon Pea	18-29	35+	10	650-1500	2500+	250	No	Yes, can deal with <650mm, esp after first 2 months	90-120 (up to 365 as annual)	<2000m	Short days optimal	June/July
Rice (African)	25-30	40 av	10,20 (av)	700-1100		500	No	Not in pollination or later growth	100-120	<1500m		Late summer
Wheat	10-24	30		400-650	750	250			100-190	<2800		
Sweet Potato	20-25	350	15	750-1000		750	No	Yes, after first 60 days	90-210	<2800m	<13h light	
Potato	15-20	30	10	500-700	1200	350		Not towards the middle/end of the cycle	90-150	Mostly >1200 in East Africa		Dec-Feb/Jun-Jul (planted at onset rainy season)

Figure 3.11 shows the concentration of growth of crops in East Africa as taken from the FAO Agro-Maps database (<http://www.fao.org/landandwater/agll/agromaps/interactive/page.jsp>). In many cases, though not all, the spatial extent of crop growth is comparable with the optimal areas indicated in Figures 3.1 to 3.10. One particularly notable exception is pigeon pea. The climatological maps indicate that conditions would be optimal for this crop over most of East Africa whereas the FAO maps shows it being grown in just two small regions in southern Tanzania. This could indicate that a focus could be made on a shift in the type of crops traditionally grown in East Africa to expand to new types of cultivation under a changing climate.

**Figure 3.11: FAO Agro-MAPS crop ranges for the most recent year available**



Source: Images from <http://www.fao.org/landandwater/agll/agromaps/interactive/page.jsp>

In addition to these maps indicating where mean climate conditions are suitable for the cultivation of each crop, extreme weather conditions may also impact the ability to cultivate crops across the region. For example, most of these crops cannot deal with waterlogging and so an increase in maximum precipitation events could have a considerable impact. There was no clear trend in this measure in the latter half of the 20<sup>th</sup> century but potential changes to this

and other extreme measures in the future should be considered in relation to future agricultural production strategies in the region.

## **4. Climate Models and the East African Climate**

As stated by Caminde and Terray (2010), similarities between observed conditions and climate model simulations of the 20<sup>th</sup> century are necessary; but not sufficient for us to have confidence in future projections. In recent years significant improvements have been made to GCMs, with the evolution from purely atmospheric models to those including oceans, land surface processes, ocean-ice interactions and many parameterisations of sub grid scale processes, with AOGCMs representing the only method to simulate future climate (Herrera et al. 2006). However, the influences on the African climate are multiple and complex, with models able to represent the climate this region with varying degrees of adequacy. One way to try and reduce uncertainty related to differing simulations is to use a multimodel ensemble, based on the hypothesis that the averaging of models using different parameterisations will cancel out differences with no physical basis whilst retaining information from robust responses (Giannini et al. 2008). Despite these limitations, the use of models is crucial to evaluate potential changes to African climate and crop cultivation in East Africa specifically. The use of models is also key to attribution studies. In order to more adequately understand the mechanisms and influences through which observed patterns are formed, models must be able to reproduce the background climate state from which idealised forcing experiments can be compared. If the key variables and driving mechanisms of change cannot be identified through such studies, the ability to verify the plausibility of future projections is decreased (Giannini et al. 2008).

### **4.1 Model selection**

An evaluation of the Intergovernmental Panel on Climate Change Fourth Assessment Report (IPCC AR4) models is undertaken for this report. An initial cross-section of models was chosen based on the availability of all required data and resulted in 8 models being selected (shown in Table 4.1). Also employed is an ensemble output of the dataset which includes all of the CMIP3 models, not just the 8 analysed individually in this study. The use of an ensemble can reduce uncertainty in our projections; the mean and median of the CMIP3 models has a lower error under climatology conditions in almost all variables than individual

models (Gleckler et al. 2008). Gleckler et al. also note that not all models are equally skilful in simulating the climatological annual cycle and variance of monthly anomalies. Over the tropics the CCCMA, MPI and GFDL models (all used here) are found to have superior performance with overall errors on the order than 5% less than typical, and up to 30% less than poorly performing models over this region, although questions still remain as to how well relatively good mean performance translates to simulation of basic variability characteristics (Gleckler et al. 2008).

**Table 4.1: Models employed in the study (from Gleckler et al. 2008)**

Modelling Group	Model designation	AGCM horizontal/ vertical resolution	OGCM horizontal/ vertical resolution	Key papers
Canadian Centre for Climate Modelling and Analysis	cccma_cgcm3_1 "CCCMA"	T63 L31	1.4 x 0.94 L29	Flato and Boer, (2001), McFarlane et al., (2005)
Center National Weather Research	cnrm_cm3 "CNRM"	T63 L45	182 x 152 L31	Salas-Melia et al., (2005)
Commonwealth Scientific and Research Organisation	csiro_mk3_0 "CSIRO"	T63 L18	1.875 x 0.84 L31	Gordon et al., (2002)
U.S. Dept. Of Commerce/NOAAb/ Geophysical Fluid Dynamics Laboratory	gfdl_cm2_0 "GFDL"	T45 L24	1 x 0.33-1 L50	Delworth et al. (2006), Gnanadesikan et al. (2006), Wittenberg et al. (2006), Stouffer et al. (2006)
Goddard Institute for Space Studies, NASA	giss_model_e_r "GISS"	4 x 5	4 x 5	Schmidt et al., (2005)
Meteorological Institute, University of Bonn, Meteorological Research Institute of KMA, Model and Data Groupe at MPI-M	miub_echo_g "MIUB"	T30 L19	T42 L20	Legunkte and Voss (1999)
Max Planck Institute for Meteorology	Mpi_echam5 "ECHAM"	T63 L32	1 x 1 L42	Roeckner et al. (2006)
Meteorological Research Institute	mri_cgcm2_3_2_a "MRI"	T42 L30	2.0 x 0.5- 2.0 L23	Yukimoto et al. (2001)

Climate model projections of East Africa are not just influenced by the ability of models to simulate conditions over the region. As discussed in Section 2, one of the main drivers of

interannual climate variability in the region is ENSO and so the accurate simulation of this mode is also crucial to future climate projections. However, this connection is often not adequately simulated in models (Hulme et al. 2001). A model that has fitted these criteria, although not used in this study, is the SINTEX-F1 model which captures features of the East African climatology well and also simulates the Indian Ocean dipole and ENSO systems realistically (Behera et al. 2005).

## **4.2 Model simulation of the observed climate**

There have been several studies over the East Africa region that employ regional climate models (RCMs). One of the first studies to successfully customise an RCM over this domain was published in 1999 by Sun et al. They utilised the NCAR RegCM2 model and managed to reproduce interannual precipitation variability for most years from 1982–1993. These developments have been built upon since then. Kaspar and Cubasch (2008) use the regional climate model CLM to evaluate the quality of simulated precipitation, concluding that the seasonal precipitation cycle is adequate in all configurations they test although absolute values are very much influenced by choices of schemes. The importance of different configurations of climate models can be further demonstrated by the need to include a three-dimensional lake model coupled with the RCM to obtain a more realistic simulation when simulating climate in the vicinity of Lake Victoria (Song et al. 2004).

In the examination of rainy season onset over the Greater Horn of Africa with the regional model MM5, the climate model replicated a consistent picture in comparison to three observed dataset (satellite and gauge based (Riddle and Cook 2008). A further study is that of Anyah and Semazzi (2007). The authors use the ICTP-RegCM3 model to evaluate the East African short OND rains. They find that the simulated monthly and seasonal precipitation climatologies and interannual variability is relatively consistent with observations. The model is in particular agreement with observed data over northern Uganda, central Tanzania and the East African coast. In contrast the model underestimates precipitation over northeastern Kenya and overestimates it over the Lake Victoria Basin. Additionally the simulation is poorer over the central Kenyan highlands where model resolution seems to affect the simulation. Positively, RegCM3 successfully maintains the connection between regional precipitation and global interannual modes of variability, namely ENSO and the Dipole Model Index (Anyah and Semazzi 2007).

## 4.3 Model climatology 1970 to 1999

The climatologies of the models selected for analysis are now reviewed. The 20c3m experiments from the models (forced with historical emission values) are used to evaluate the replication of the observed climatology in each model.

### 4.3.1 Temperature

Figure 4.1 shows the ensemble temperature cycle. Table 4.2 broadly summarizes the individual model climatologies for each model employed. In general, the spatial distribution of temperature patterns is relatively well simulated, even if the absolute temperature values are less well represented in some models. The ensemble dataset of CMIP3 models provides a good overall representation of the CRU data for the climatology period in terms of the spatial and temporal patterns of the most intense temperatures throughout the year. However, the ensemble tends to underestimate high temperatures, for example over central Sudan in May, and similarly overestimates some colder regions as well, indicating the model ensembles generally have a slight negative temperature bias.

**Figure 4.1: Annual and monthly ensemble temperature climatology for the region**

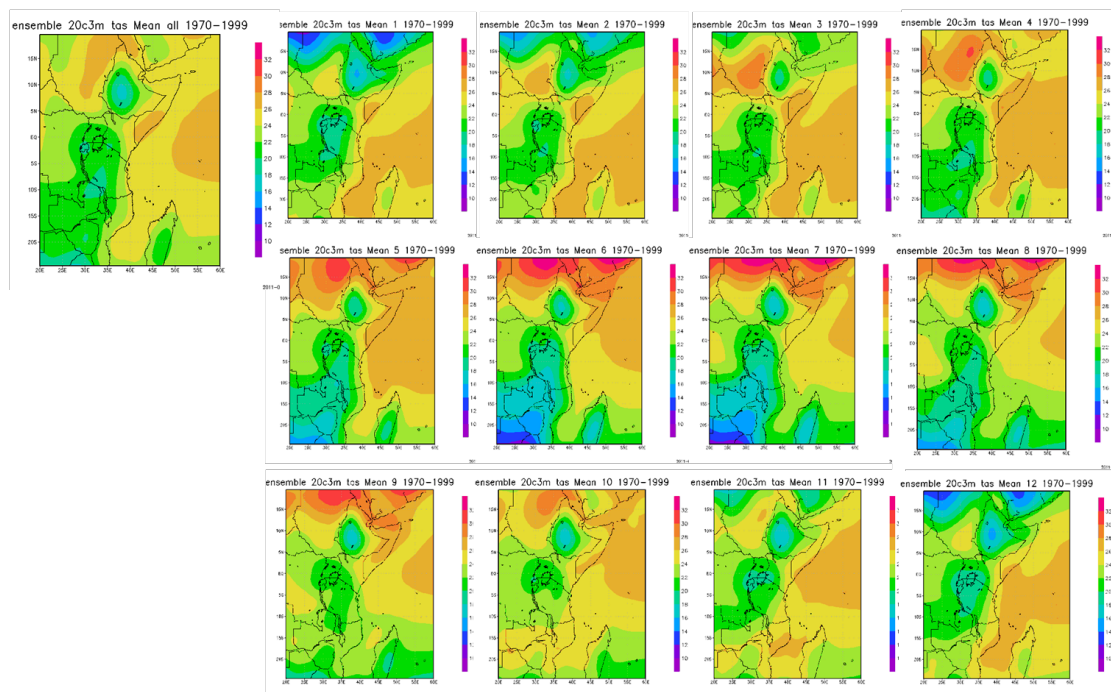


**Table 4.2: Summary of model performance with respect to reference climatologies**

Model	Temperature	Precipitation
CCCMA	Generally too cold across East Africa, especially over Uganda/Rwanda/Burundi/Tanzania region	Good location of most intense precipitation but fringes of precipitation extend too far north consistently
CNRM	Is consistently too cool by between 2 and 4°C across the whole region	Again, good location of most intense precipitation but extent of precipitation covers too much of the domain most of the year
CSIRO	Again, good spatial depiction but slightly too cool across East African	Good depiction of annual cycle but precipitation intensity generally underestimated
GFDL	Good for both spatial patterns and temperature, especially between July and November	Good annual cycle but overestimates precipitation intensity over land between October and May
GISS	Good spatial patterns, tends to too warm temperatures inland over most of the domain but too cool along the coast	Extremely excessive precipitation over most of the domain
MIUB	One of the better representations of temperature for both magnitude and spatial patterns	Annual cycle moves north too early and too far, and precipitation intensity underestimated
MPI	Good spatial pattern but too great an intensity i.e. tends to too warm and too cold depending on the month	Good annual spatial precipitation pattern but intensity is consistently underestimated over land
MRI	Less distinct spatial pattern than some other models but good representation of	Generally shows a good spatial location for the annual cycle and also good intensity of precipitation

### 4.3.2 Precipitation

The ensemble precipitation cycle is depicted in Figure 4.2. Over the whole year, the ensemble precipitation cycle is a reasonable approximation to the reanalysis datasets. In addition, the seasonal cycle of precipitation is well represented, although the model ensemble cannot reproduce the same intensity of precipitation as seen in the observed datasets over the location of greatest convection throughout the year. Furthermore, the band of precipitation retreats south too early in the model ensemble, with a centre of precipitation remaining over Ethiopia until October/November in the reanalysis datasets, but only until September in the model ensemble.

Figure 4.2: Annual and monthly ensemble precipitation climatology for the region

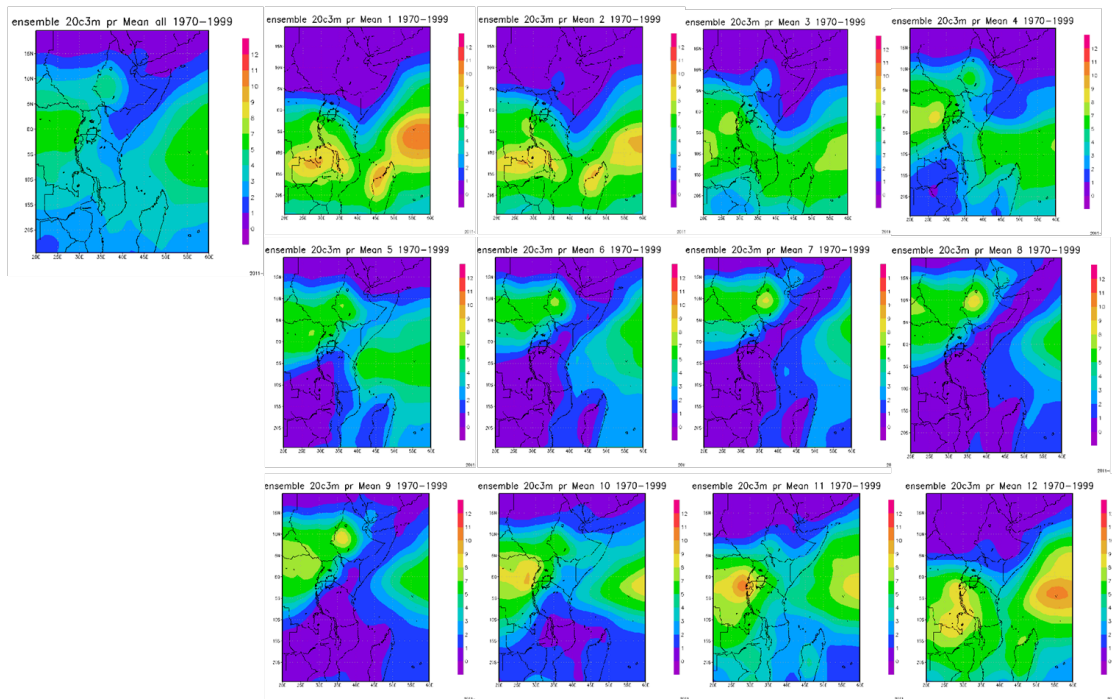


Figure 4.3: The annual precipitation cycle averaged zonally across the domain for the 1970-99 period

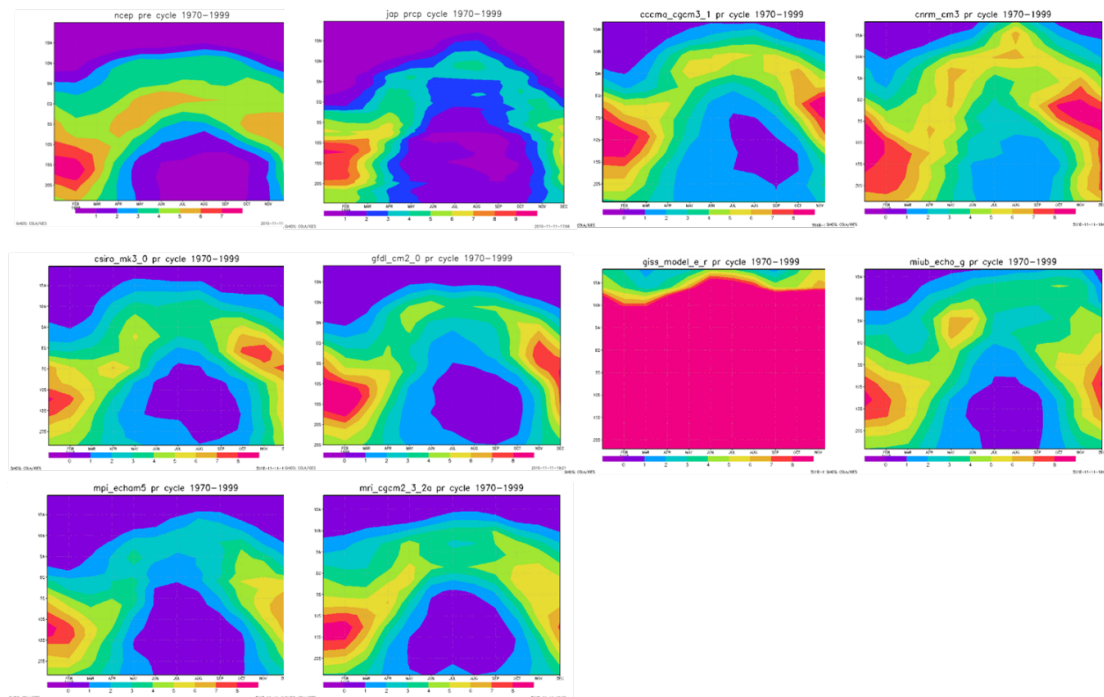


Figure 4.3 shows the climatological cycle of precipitation across the domain for the NCEP and JapRe reanalysis datasets and the selected models for the climatology period. Despite the slight difference between the two observed cycles, it is still evident that the majority of models produce an annual cycle that moves too far north, with precipitation spread across a large part of the domain during most of the year, causing it to be overestimated in places. The models producing the most realistic annual cycles during this period are the MPI and MRI models.

## 5. Model derived crop growth thresholds

Employing the same approach as used in Section 2, the domain masking exercise is repeated for the 8 models and the ensemble output. This allows for examination of the impact of model errors on simulated crop growth regions under current (1970–1999) climatic conditions. These plots are shown in Appendix 2, Figures B1 to B10 for both the model ensemble and each model. For reference, the climatic crop growth maps using both the NCEP and JapRe precipitation datasets are included for each crop.

**Banana:** The ensemble output follows the climatological growth region well, although the optimum area in the ensemble is slightly smaller and does not extend into Uganda. The southern border of growth is further south in the ensemble due to the precipitation distribution biases in the models. The individual models exhibit greater variation in their representation of current banana growth regions though almost all manage to locate the optimal area for banana growth well.

**Cassava:** Cassava is a crop that can be widely grown over East Africa and the model ensemble domain reflects this. One key difference is that the precipitation distribution in the models suggests that cassava can be grown over northern Kenya and eastern Ethiopia when observed precipitation makes these regions inappropriate for cassava cultivation. This is reflected in the individual models with the most realistic precipitation regimes

**Maize:** The key optimal region of maize growth over central-southern Sudan is well replicated by the model ensemble as are other areas of varying suitability. As with cassava, the weakest element of the model simulation of the crop cultivation region is in eastern Ethiopia and northern Kenya where the models overestimate precipitation. However, half of

the individual models robustly capture the precipitation limitations on maize growth in this region.

Millet: Almost all the selected models successfully simulate the optimal region of millet growth covering parts of Sudan, Ethiopia, Kenya and Tanzania. The model ensemble is also able to replicate this with success. The millet growth domain is well represented in the GCMs for the climatological period.

Pigeon Pea: Pigeon pea is a crop that can be widely cultivated over the East African region and the model ensemble growth area reflects this very well. Almost the whole domain has optimal conditions for pigeon pea to be grown with the exception of the Ethiopian highlands. Individual models also simulate these conditions robustly, with the exception of the GISS model (which is affected by poor precipitation representation).

Potato: Potato is a crop that cannot be grown optimally anywhere in East Africa, although there are areas where several conditions are satisfied and cultivation may be possible. These areas are largely in a band running through central-southern Sudan and down the eastern coastal countries in the focus region. The ensemble replicates this pattern well; successfully pinpointing rain limited areas (Uganda, Rwanda, Burundi and western Ethiopia) where cultivation is not possible.

Rice: The model ensemble is generally successful at simulating the main cultivation regions for rice in East Africa. However, as with other crops, the overestimation of precipitation in the models means that suitable conditions are simulated further into Kenya and Tanzania than in the observed/reanalysis data. At the individual model level, most have some ability to simulate the main cultivation regions, though only the CSIRO and MIUB models follow the observed/reanalysis domains such that southern Sudan is indicated to be an optimal rice growing region.

Sorghum: The model ensemble generally manages to pick up on the limited areas suitable for the cultivation of sorghum, although this does not extend down into the coastal region of Tanzania where conditions are also found to be appropriate in the observed climatology. Most of the individual models also have success in this area.

Sweet Potato: Precipitation is a primary limiting factor in the cultivation of sweet potato over the eastern part of the domain (eastern Ethiopia, Kenya and Tanzania). The overestimation of

the precipitation cycle in most models means that the ensemble crop domain does not fully recognise this although several of the individual models do. The general pattern, however, is successfully simulated in both the ensemble and individual models.

Wheat: Whilst the model ensemble is successful in reproducing the ‘T’ shape over the north of the domain where cultivation is possible, the precipitation cycle deficiencies in the models lead to it being located slightly too far northwards in the ensemble, with optimal growth areas located in southern Kenya and Tanzania not recognised. The best simulations of the crop growth area in individual models are found in the CSIRO and MPI models.

The crop thresholds discussed here are based on climatological mean conditions. Whilst these form a baseline for establishing whether a region may be suitable for cultivation of a particular crop, climatic extremes such as drought or heavy precipitation events can impact negatively on yields and must also be considered.

## **6. Model Climate Projections for the 21<sup>st</sup> Century**

### **6.1 Previous studies**

The most recent Intergovernmental Panel on Climate Change Assessment Report (IPCC 2007) projects a warmer future under all non-mitigation scenarios for all models, with a multimodel global average temperature increase of 3.4°C (2.0°C-5.4°C) under the high emissions A2 scenario by 2090–2099 relative to 1980–1999 (IPCC 2007). Furthermore, all models used in the IPCC AR4 with an A1B scenario show temperature increases over East Africa during all seasons that are larger than the global average response (Doherty et al. 2010). With regards to precipitation, it is hypothesised that the increase in anthropogenic greenhouse gas concentrations will lead to an intensification of the hydrological cycle leading to both increases and decreases in local mean precipitation levels and an intensification of higher order precipitation events (Trenberth et al. 2003). The IPCC (2007) suggests that one of the more robust projected precipitation changes is of an increase in precipitation over East Africa. Eighteen out of 21 models used in the IPCC report project an increase in precipitation over this domain in the core of this region (to the east of the Great Lakes). Hulme et al (2001) find that very few regions of Africa experience a projected precipitation change outside that of natural variability under the B1 scenario. East Africa is an exception to this with increases of 5-30% projected during boreal winter (DJF) months. For the high emissions A2 scenario

this projected percentage wetting increases to up to 50 or 100% over parts East Africa. The authors urge caution about changes to precipitation associated with ENSO due to difficulties in simulating this mode of variability (Hulme et al. 2001).

However, whilst there is much evidence to support a wetter future in the East African region, there is also evidence to the contrary. One study suggests that East African precipitation will decrease by 5-10% during JJA under the B1 scenario, and ‘significantly’ decline over parts of the Horn of Africa (Hulme et al. 2001). Williams and Funk (2010) hypothesis that climate models project increased precipitation over the focus region due to the models projecting more ‘El-Nino like’ conditions, traditionally associated with increased precipitation in East Africa, though crucially this connection is only strong in the short rains. Instead, the authors suggest that the drying trend observed during the short MAM rains towards the end of the 20<sup>th</sup> century, and attributed to tropical Indian Ocean warming, will continue during the short rains over the 21<sup>st</sup> century irrespective of whether warm ENSO episodes do also occur more frequently (Williams and Funk 2010). This opposing hypothesis highlights the importance of seasonal precipitation variability with East Africa; the presence of two distinct rainy seasons over many of the focus countries makes it necessary to consider changes in seasonal precipitation and not just annual conditions.

Madagascar has a different climate regime to the continental part of the East African domain, and consequently the climate change projections differ. The projected median changes for Madagascar suggest that precipitation will increase during the summer months of January to April, although the results are inconsistent over the northwest of the country. From May onwards a drying trend is projected in southern Madagascar, with this trend also affecting eastern parts of the island from June to September, with increased precipitation projected for the rest of Madagascar projected to remain wetter (Tadross et al. 2008). The whole of Madagascar is projected to warm over the 21<sup>st</sup> century, with the lowest increases seen in coastal regions and to the north, and the greatest projected increases of at least 1.5°C by 2046–2065 in southern and inland Madagascar. In terms of cyclone activity, projected changes are inconsistent for most of the year (January to August). However from September–December there are projected to be fewer cyclones over Madagascar in the early part of the season. This is coupled with a projected increase in cycle intensity of up to 17% (Tadross et al. 2008).

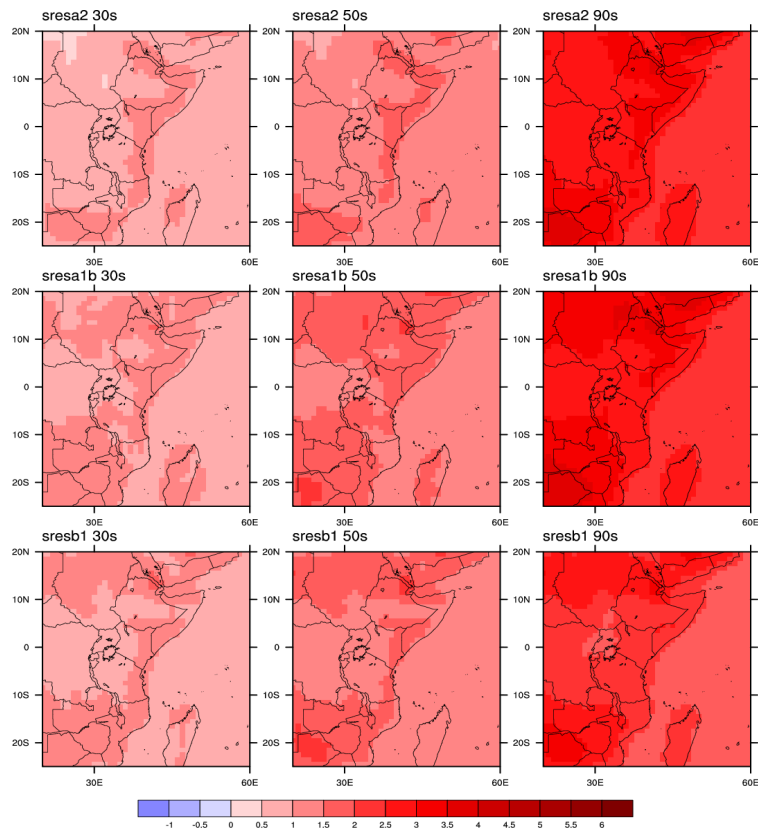
## 6.2 Model projections

In this study, in order to provide a comprehensive spectrum of climate change projections and indicate the extent of uncertainty surrounding global emissions futures, three SRES scenarios are employed. These are the B1, A1B and A2 scenarios, which represent low, medium and high emission paths respectively. Three ‘time slices’ are selected; the 2030s (2030–2039 inclusive), the 2050s (2050–2059) and the 2090s (2090–2099). It is to be expected, in the case of robust models, that changes will increase in magnitude both over time and through to the highest emissions scenario. For example, the smallest change should be present in the low B1 2030s time slice with the greatest change seen during the 2090s under the A2 SRES scenario.

### 6.2.1 Temperature

Figure 6.1 shows climatological temperature anomalies for the ensemble output relative to the 1970–1999 climatology for the three SRES scenarios and three time slices. As would be expected, the universal pattern of the domain is one of warming, with temperature increasing as the 21<sup>st</sup> century progresses to a peak of up to approximately 4°C across the region under the SRESA2 scenario in the 2090s for the ensemble. Individual models all exhibit similar warming trends as the 21<sup>st</sup> century progresses, but of differing magnitudes and spatial patterns. In some models there is warming of more than 5.5°C by the 2090s in the A2 scenario, particularly over Ethiopia and Sudan. By contrast, under the conservative B1 emissions scenarios temperatures show an increase of 2.5 to 3°C by the 2090s in the ensemble, but a range of between 1 and 3°C in the individual models.

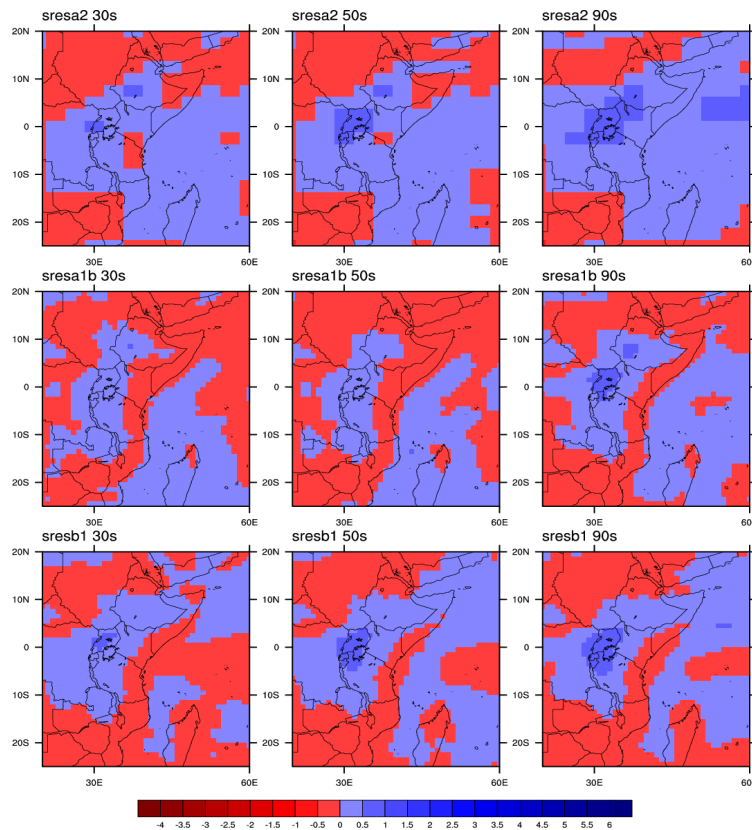
**Figure 6.1: Temperature anomalies (in °C) from the model ensemble for the 2030s, 2050s and 2090s under sresa2, sresa1b and sresa1 scenarios relative to a 1970-99 climatology.**



### 6.2.2 Precipitation

Figure 6.2 shows climatological precipitation anomalies for the ensemble output relative to the 1970–1999 climatology for the three SRES scenarios and the three time slices. For precipitation, the ensemble data shows a consistent spatial pattern of change over the 21<sup>st</sup> century for the whole year over the East African region. This pattern suggests an increase in precipitation over the majority of the countries of interest with the biggest change of 1.5 mm/day projected over the Ugandan region extending into the surrounding countries. Of our focus countries, the only place projected to see a decrease in the daily precipitation climatology is Sudan and parts of the coastal regions of Tanzania and Kenya in the lower emissions scenarios. In contrast, the signal of precipitation change for Madagascar is less clear; by the 2090s the high emissions A2 scenario suggests a slight increase (+0.5 mm/day) in daily precipitation whereas the more conservative B1 scenario indicates a slight drying may occur.

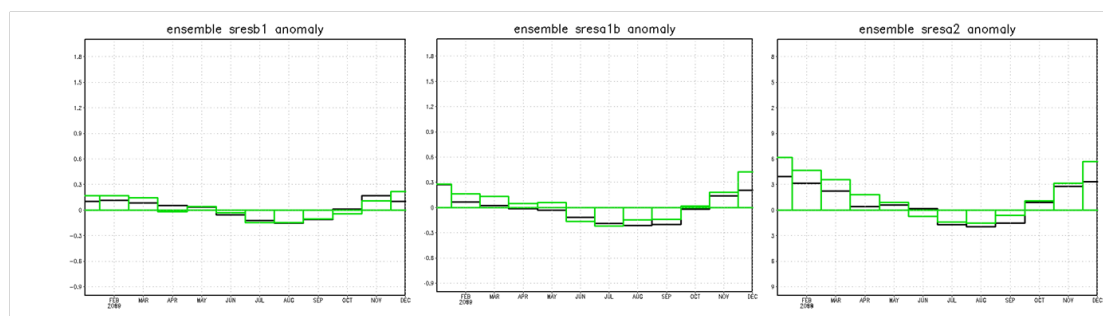
**Figure 6.2: Precipitation anomalies (in mm/day) from the model ensemble for the 2030s, 2050s and 2090s under sresb1, sresa1b and sresa2 scenarios relative to a 1970-99 climatology.**



For individual models and seasons the patterns are much more varied. During the long OND rains most models do show a similar pattern to the ensemble yearly pattern, with projections pointing to increased daily precipitation over much of East Africa. However, during the short MAM rains several models (CCCMA, CSIRO, GFDL and MPI) project decreased precipitation of up to 2 mm/day in Ethiopia under the A2 scenario by the 2090s. This pattern is also evident in the lower emissions scenarios in some models for this season, with the mixed trends in this season highlighting the uncertainty surrounding model precipitation simulations. Moving into the boreal summer months of June to August, a dominant pattern again emerges amongst the models. For this season, the projections converge on a drier future with up to 1.5 mm/day less precipitation projected over much of the East African continent and Madagascar. In general, it appears that projected increases in precipitation are co-located with those places where projected temperature increases are least.

Figure 6.3 shows total monthly precipitation anomalies over the region for the 2050s and 2090s. The anomalies for each month emphasize some of the seasonal patterns outlined above. The ensemble patterns are consistent between scenarios, with the pattern strengthened under the highest emissions A2 storyline. As previously noted, the dominant projection is for increased precipitation between October and May of up to 0.6 mm/day with the maximum increases projected for November to March, but for slight decreases in precipitation (approximately -0.15 mm/day) projected during boreal summer. Most of the individual models show similar overall patterns to this, but with considerable variations in the magnitude of the projected change. Notable exceptions include the CSIRO model where the projections are inconsistent in direction from month to month, the GFDL model where the dominant signal through most of the year is for drying in all scenarios and the MRI model where drying is also more dominant.

**Figure 6.3: Precipitation anomalies in the Sahel region, relative to a 1970-99 baseline. Figures for the 2050s are black and the 2090s are green.**



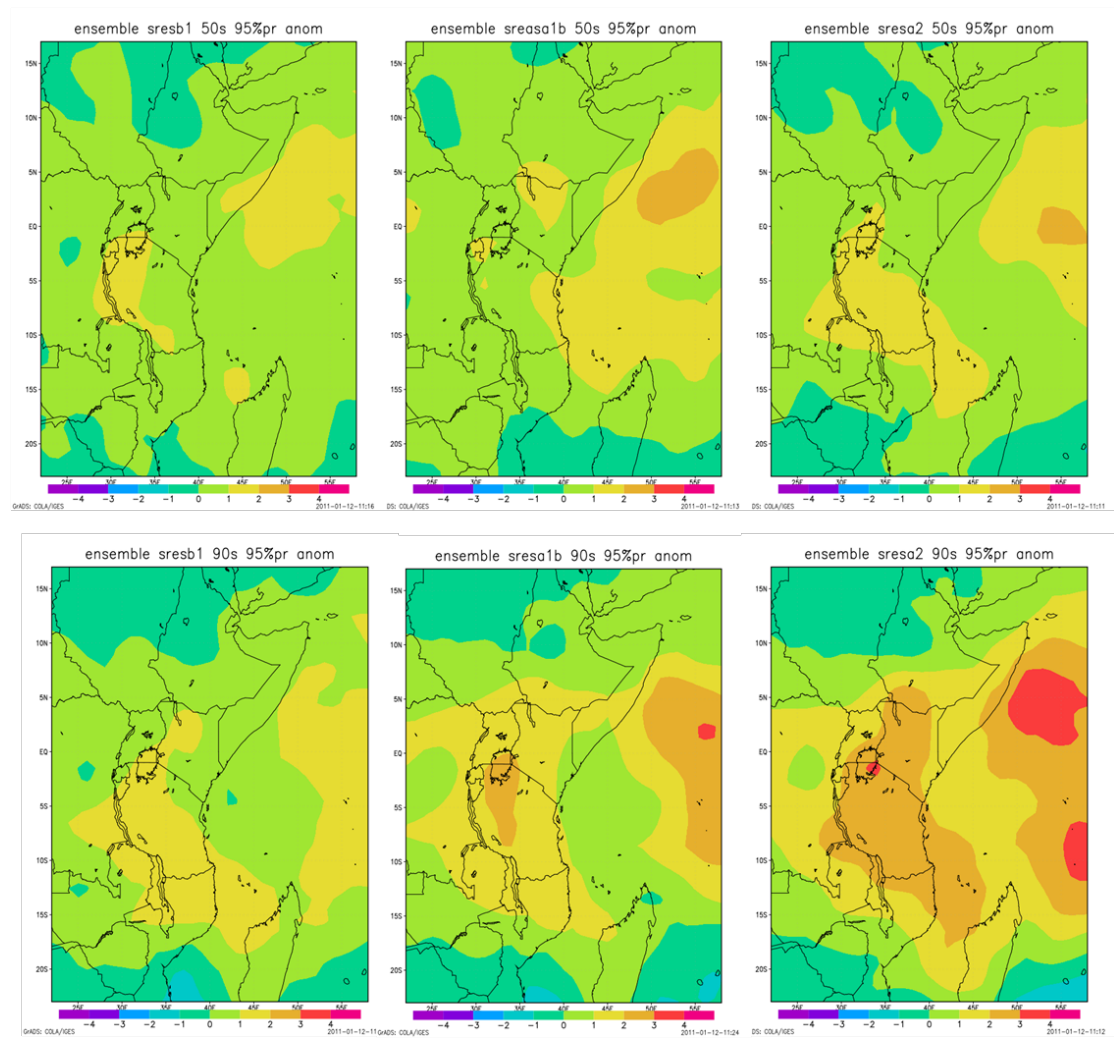
### 6.2.3 Extremes

Research on future changes in extreme climate events in Africa is limited (IPCC 2007). The IPCC estimate that by the end of the 21<sup>st</sup> century the number of extremely wet seasons in East Africa will increase to one in every five (IPCC 2007). Globally, it is suggested that relative changes to precipitation extremes will be greater than changes to mean precipitation and concurrently the return period of such events is reduced (Kharin et al. 2007). Kharin et al (2007) also conclude that changes in warm extremes tend to follow changes in temperature of the climatologically warmest month.

The 95% ensemble precipitation anomalies for all three scenarios for the 2050s and 2090s are shown in Figure 6.4. Over East Africa, the dominant signal that emerges by the 2090s (particularly in the A2 scenario), is one of increased intensity of the most extreme

precipitation events. The centre for this projected change is in the centre of the domain in Kenya and Tanzania but an increase in the magnitude of these extreme precipitation events is projected over the majority of the focus countries of between 1 and 4 mm/day relative to the 1970–99 climatological events. The only exception is over Sudan where a small decrease (-1 mm/day) in the intensity of the heaviest precipitation events is projected under all SRES scenarios by the 2090s.

**Figure 6.4: Anomalies in the 95% precipitation event threshold, averaged across the model ensemble. Figures are in mm/day.**



## 7. Future Climate Scenarios and the Impact of Crop Growth in East Africa

Applying the same approach as in Section 5, the output from our chosen models and the ensemble data is used to evaluate potential changes to crop growth regions in East Africa. Given the errors seen in the climatological model crop cultivation domains seen in Section 5, anomalies are derived relative to the model climatologies for the 2030s, 2050s and 2090s with respect to their 1970–1999 climatologies. These model derived anomalies are then applied to the observed and reanalysis 1970–1999 climatologies. Finally the same crop growth thresholds as defined earlier are applied to the data to create potential future cultivation domains over the region. This methodology means that the projections are not affected by bias in the model 20c3m runs and thus provide a more robust assessment of impact of climate change on crop growth domains in East Africa. Daily data is not available for the 2030–2039 period. Therefore, two different crop domain plots have been produced, so that in addition to the plots including all data for the 2050s and 2090s there are also plots for all periods excluding the minimum temperature data. Cold extremes are projected to warm, globally, about 30–40% faster than warm extremes, and so the importance of minimum temperature limitations will diminish at the 21<sup>st</sup> century progresses (Kharin et al. 2007). This means that although some projections exclude minimum temperature measures due to lack of available daily data this should not be problematic.

Figures C1 to C10 in show the ensemble crop domains for the three selected SRES scenarios in comparison to the observed climatologies using both the NCEP and JapRe precipitation datasets, thus providing both forcing and initial condition uncertainty in the projections. For each crop and each reanalysis dataset there are two different domains shown, one including the minimum temperature measures for the 2050s and 2090s and one excluding minimum temperatures domains for all three time slices of the 21<sup>st</sup> century (2030s, 2050s and 2090s).

Banana: The absolute extent of the crop growth domain does not change significantly in the ensemble output through the 21<sup>st</sup> century. The plots based on the NCEP climatology show a significantly larger area suitable for cultivation and this remains the case through the three periods of analysis. Using the NCEP reanalysis climatology by the end of the 21<sup>st</sup> century all three scenarios show an extended area of western Ethiopia where optimal conditions for

banana cultivation are satisfied and this could represent a region of opportunity for this widely exported crop. Additionally there may be opportunities for growth in Uganda, Burundi, Rwanda and the westernmost fringes of Tanzania and Kenya. Madagascar is also projected to continue to have a suitable climate for banana cultivation over the next century. The projections remain comparable when the JapRe derived climatology is used as the baseline. All currently suitable areas continue to be so under anthropogenic warming with some expansion around the fringes of the suitable climatic regions, representing a possible opportunity for expansion of cultivation or increasing of yields in these regions. The plots excluding minimum temperature, as expected, do not show any deviation from this pattern. For all crops minimum temperature is expected to become less significant as a limiting factor under anthropogenic warming as the 21<sup>st</sup> century progresses.

Cassava: As with banana cultivation, changing mean climatic conditions over the 21<sup>st</sup> century do not appear to adversely impact on the climatic suitability of current optimal cassava growing regions. Taking firstly Madagascar, whilst the northern half of the island currently has optimal conditions for cassava cultivation, by the 2050s under all scenarios and with both the NCEP and JapRe reanalysis datasets as a base, the whole of the island is expected to have conditions optimal for the cultivation of cassava (excluding non-climatic factors). Over mainland East Africa, the late 20<sup>th</sup> century had suitable conditions for cassava growth over the entire focus region except central to northern Sudan, where production was limited by precipitation. This remains the case during the 20<sup>th</sup> century and the bounds of production are not significantly affected by projected changes in climate. More specifically, however, with the NCEP reanalysis as the base, the region for optimal cultivation (where all ideal conditions for growth are satisfied) contracts by the 2090s. This contraction occurs at the northern boundary of cultivation in southern Sudan and measures up to about 5° under the A2 scenario in the 2090s, a significant amount. The diminishing suitability of southern Sudan to cultivate cassava is also projected when the JapRe dataset is used as a base, and although the region may still have acceptable climatic conditions for cultivation, the lack of ideal projections for this area could indicate potential impacts on yields.

Maize: Under current climatic conditions maize experiences optimal growth conditions in very few regions in East Africa. This is a scenario which is not projected to change significantly over the 21<sup>st</sup> century; and in fact the small region of southern Sudan where

conditions were optimal contracts using both base datasets and under all scenarios by the 2090s. Elsewhere, however, over the remaining mainland focus countries the suitability of the mean climate increases slightly, although still does not reach optimal levels indicating that maize may not be a suitable crop to cultivate in this region over the 21<sup>st</sup> century.

Millet: In common with maize (and in contrast to cassava and banana) the projections for mean climate suitability of East Africa for millet cultivation is that the region will become less optimal and therefore less likely to provide high yields of this crop. Madagascar is not currently a region where millet can be grown under natural climate conditions and this continues through the 21<sup>st</sup> century under all climate change scenarios. On the continent, the main region of optimal growth under current conditions in eastern Ethiopia and Kenya contracts under all scenarios and whilst the region still meets the majority of the mean climate criteria for successful cultivation, yields may be adversely affected. However, under both the NCEP and JapRe precipitation bases, the over extent of cultivation is projected to remain largely unchanged. When the plots excluding minimum temperature are considered, the outlook remains very similar, with optimal areas for millet cultivation contracting significantly as the 21<sup>st</sup> century progresses, reinforcing the argument that minimum temperature is a less significant limiting influence on crop growth in East Africa under global warming scenarios.

Pigeon Pea: As discussed previously, pigeon pea is currently an underutilised crop in East Africa, with relatively limited cultivation despite optimal conditions for growth existing over much of the region. By the end of the 21<sup>st</sup> century it is still projected that much of East Africa will have optimal mean climatic conditions indicating a potential opportunity for diversification of agriculture. The one country where cultivation is not projected to remain optimal in a warmer climate is southern Sudan, however conditions here continue to meet the majority of optimal climatic parameters.

Potato: Potato cultivation does not thrive under the very warm temperatures found over East Africa and even under current climatic conditions no areas in East Africa can be classified as optimal for the cultivation of this crop. It therefore follows that with increasing temperatures projected over the 21<sup>st</sup> century opportunities for potato cultivation are likely to diminish. The most significant change seen in the domain is when the NCEP precipitation dataset is used as a base and a narrowing of a suitable band across mid-southern Sudan and into Ethiopia is

observed, which is especially evident in the 2090s under the A2 scenario. This is also evident where JapRe is used as the base reanalysis dataset, but to a lesser extent. Otherwise, the ensemble projections do not indicate any significant changes in the extent of potato cultivation over the region; with northern Madagascar, Uganda, Rwanda and Burundi outside the limit of potential potato cultivation regions throughout the 21<sup>st</sup> century due to insufficient precipitation falling in those areas.

Rice: It is projected that changes associated with increasing anthropogenic emissions may increase opportunities for rice cultivation over the 21<sup>st</sup> century. The most significant projected change is over the western part of the domain where the region of optimal conditions expands significantly. The second region where optimal conditions appear to expand is over coastal regions of Tanzania and northern Madagascar. The main limit on cultivation in East Africa is precipitation, especially over eastern Ethiopia and Kenya and these regions remains limited in this regard at the end of the 21<sup>st</sup> century, although irrigation may increase cultivation opportunities here. Based on these projections, it is concluded that rice cultivation may become more feasible and sustainable by the end of the 21<sup>st</sup> century in East Africa.

Sorghum: Whilst there are few areas of optimal cultivation conditions during the climatology period for the growth of sorghum, the conditions across the whole of the East African focus region (except northern Sudan) appear suitable for some cultivation. With the total extent of potential cultivation remaining the same under both NCEP and JapRe base conditions it is not projected that prospects for sorghum cultivation will decrease under any scenario.

Furthermore, areas of eastern Kenya, eastern Ethiopia and central Sudan are projected to develop optimal cultivation conditions by the 2090s regardless of the scenario employed which may signal further opportunity to develop this crop. As with previous crops, the plots excluding minimum temperatures show very similar optimal and suitable areas of cultivation, reinforcing that this is not likely to be a limiting factor to growth in the immediate future.

Sweet Potato: The overall extent of the sweet potato crop growth area remains the same over the 21<sup>st</sup> century, however the previously optimal areas of cultivation are uniformly decreased in size with these less suitable mean conditions indicating the potential for decreased yields. Whether the NCEP or JapRe reanalysis dataset is used a basis for the climatology, by the end of the 21<sup>st</sup> century no optimal cultivation regions remain in the East African domain.

Wheat: Precipitation levels limit factor on wheat cultivation in East Africa under current climatic conditions, with only a small band of suitable conditions along the coastal regions and stretching across into central Sudan. This band remains at the end of the 21<sup>st</sup> century but under the NCEP climatology is significantly narrowed. Furthermore, no new opportunities for cultivation are projected in the ensemble crop domains, suggesting that with projected increases in temperature during the 21<sup>st</sup> century, shifting focus to crops where optimal yields are found under higher temperatures may produce better yields in locations where wheat is currently cultivated.

## 8. Summary and Conclusions

This report has investigated climate change and crop cultivation potential over an East Africa domain of Burundi, Eritrea, Ethiopia, Kenya, Madagascar, Rwanda, Sudan, Tanzania and Uganda. Current climatological crop growth domains have been investigated and the implications that anthropogenic climate change will have on the suitability of the region to continue to grow these crops at the end of the 21<sup>st</sup> century have been analysed. A cross-section of eight CMIP3 models and an ensemble were analysed to establish how realistic their simulation of current crop growth domains were and to see how much confidence could be placed in their future projections.

The climate of East Africa is dominated by convective precipitation associated with the seasonal migration of the ITCZ across the equator, leading to three main precipitation regimes over the focus domain of 20°E to 60°E and 25°S to 20°N. For many of the focus countries this results in a bimodal precipitation regime with precipitation falling mostly in boreal spring (March to May, known as the long rains) and autumn (October to December, the short rains). To the north of the East African domain, Ethiopia, Eritrea and southern Sudan have one rainy season from June to September coinciding with the peak of northwards migration of the ITCZ. In the south of the domain Madagascar has a primary rainy season from December to March when the ITCZ is located over the north of the island. The south of the country receives very little precipitation. Interannual variability in East Africa is strongly linked to the El Nino Southern Oscillation and the Indian Ocean Dipole mode.

The East African climate is complex and different climate models reproduce it with varying degrees of fidelity. As such, eight separate models and an ensemble of the CMIP3 models

were employed in this study. Generally, the selected models are able to simulate temperatures adequately, although many models exhibited a slight cool bias, including the ensemble. Precipitation is less well represented in the models. Many locate the general spatial and temporal pattern of precipitation but model biases are greater than for temperature. The ensemble output captures precipitation most robustly but does not capture the most intense precipitation and the band of precipitation associated with the ITCZ retreats southwards too early in boreal autumn. Generally the models have an annual cycle that migrates too far north and covers too great an area.

Ten key crops currently grown in the East African domain were selected and their climatological growth limits were investigated using the observed and reanalysis datasets. The spatial extent of growth shown in the FAO Agro-Maps database was comparable in many cases to that produced by this technique. This analysis also indicated that pigeon pea may have significantly greater potential for development in the region than is currently being utilised if cultivation is not restricted by other factors. The replication of these crop growth areas based on the 20c3m model runs generally followed approximately the same spatial patterns as observed data, but there were some key differences due to the inadequate simulation of climatological precipitation patterns in the models.

Under anthropogenic climate change a warmer future is projected in all models, with the most significant changes observed in the high emissions A2 scenario by the 2090s over Ethiopia and Sudan. East Africa is one of the few regions where average precipitation projections converge, in this case to a wetter mean future. On closer analysis it emerges that this wet trend is mainly projected to occur during the short OND rains with evidence to suggest that the long MAM rains may decrease. Results for the eight individual models tend to support this; whilst most show increased precipitation in the short OND season, several (CCCMA, CSIRO, GFDL and MPI) point to a drier long MAM rainy season, with projected decreases in precipitation of up to 2 mm/day during the long MAM season. The projections for Madagascar are more mixed, with increases or decreases in precipitation amongst projections depending on the scenario both in the model and ensemble outputs.

The impact these projected changes may have on agriculture in the region appears to be highly variable. The projected increases in mean precipitation result in the absolute extent of growth of many primary crops in the model projections remaining very similar to the late 20<sup>th</sup>

century climatology period. Changes in optimal growth areas are therefore more closely related to the increase in temperatures and how these relate to optimal growing conditions for each crop. Some crops, such as bananas, cassava, pigeon pea and rice, see an expansion of optimally suitable areas as a result of relatively high temperatures being optimal for their growth. In contrast, crops with cooler optimal conditions (maize, millet, potato, sorghum, sweet potato and wheat) may be less optimally suited to a warmer East African climate and whilst it may remain possible to cultivate these crops, higher temperatures may adversely impact on yields. It is also necessary to consider changes to extremes, which whilst uncertain could lead to more flooding and waterlogging, a trend which would impact all crops grown in the region.

Overall, when considering climate conditions in isolation, the outlook for the cultivation of key food crops in East Africa is variable. Crops suited to warmer conditions may thrive whilst yields for crops suited to more temperate climates may suffer. It should be noted that significant uncertainty remains over possible changes to extreme events in the region, any changes to which may impact yields even more than changes in mean conditions.

# Appendix 1

Figure A1: Thresholds of production across the region, as realised from mean climatic conditions, for banana. Maps are provided using both the (a) NCEP and (b) JapRe precipitation reanalyses, both use the CRU temperature dataset.

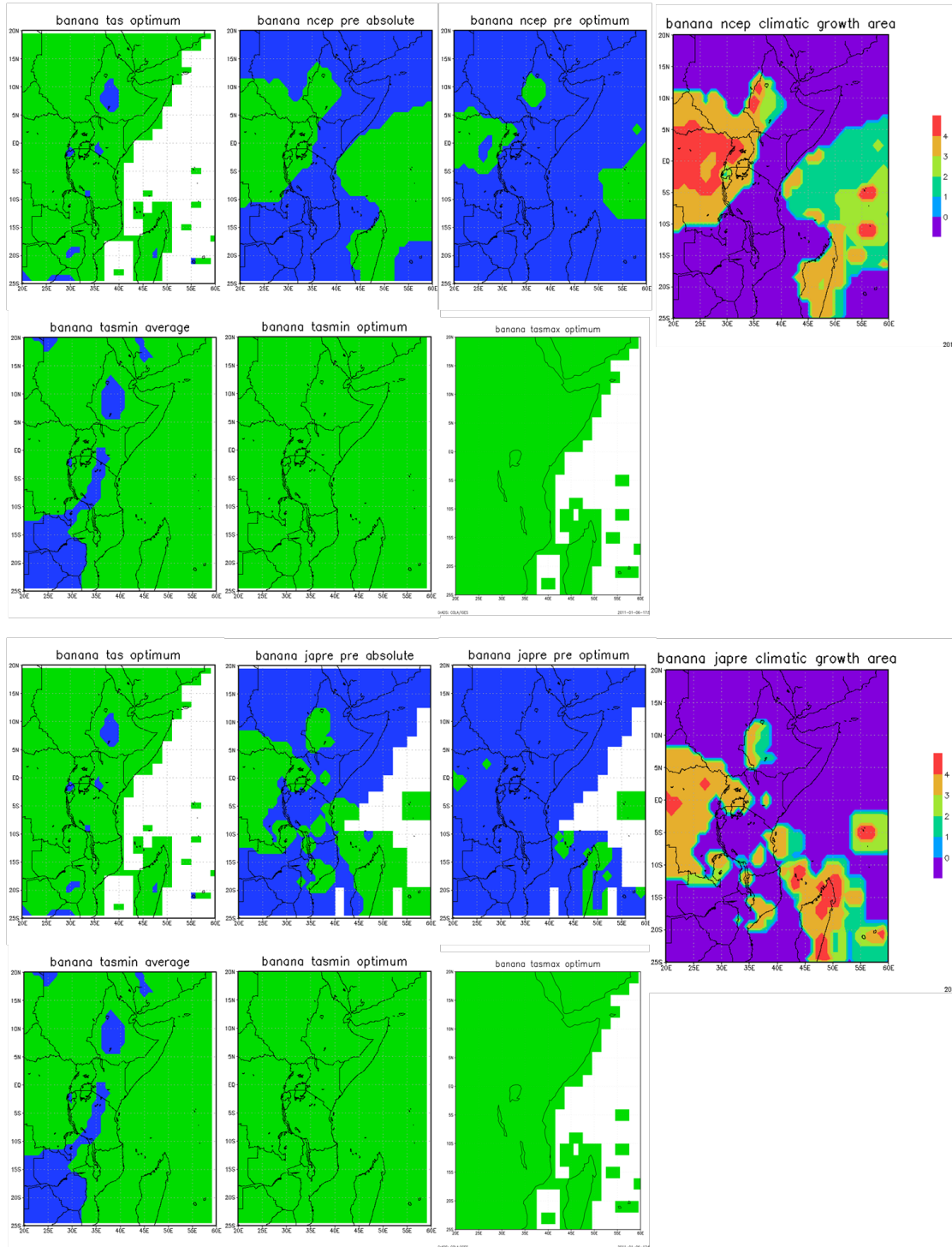
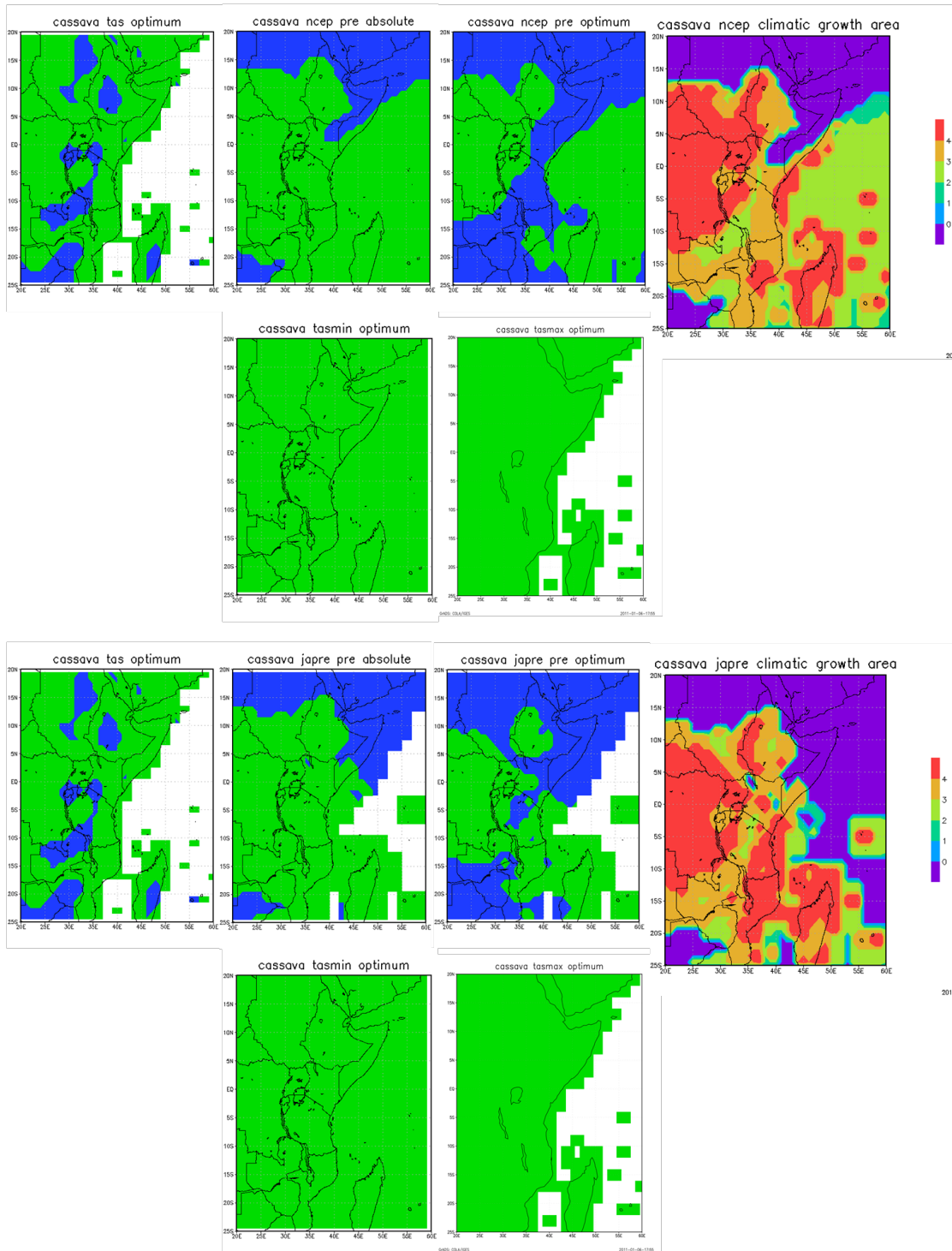
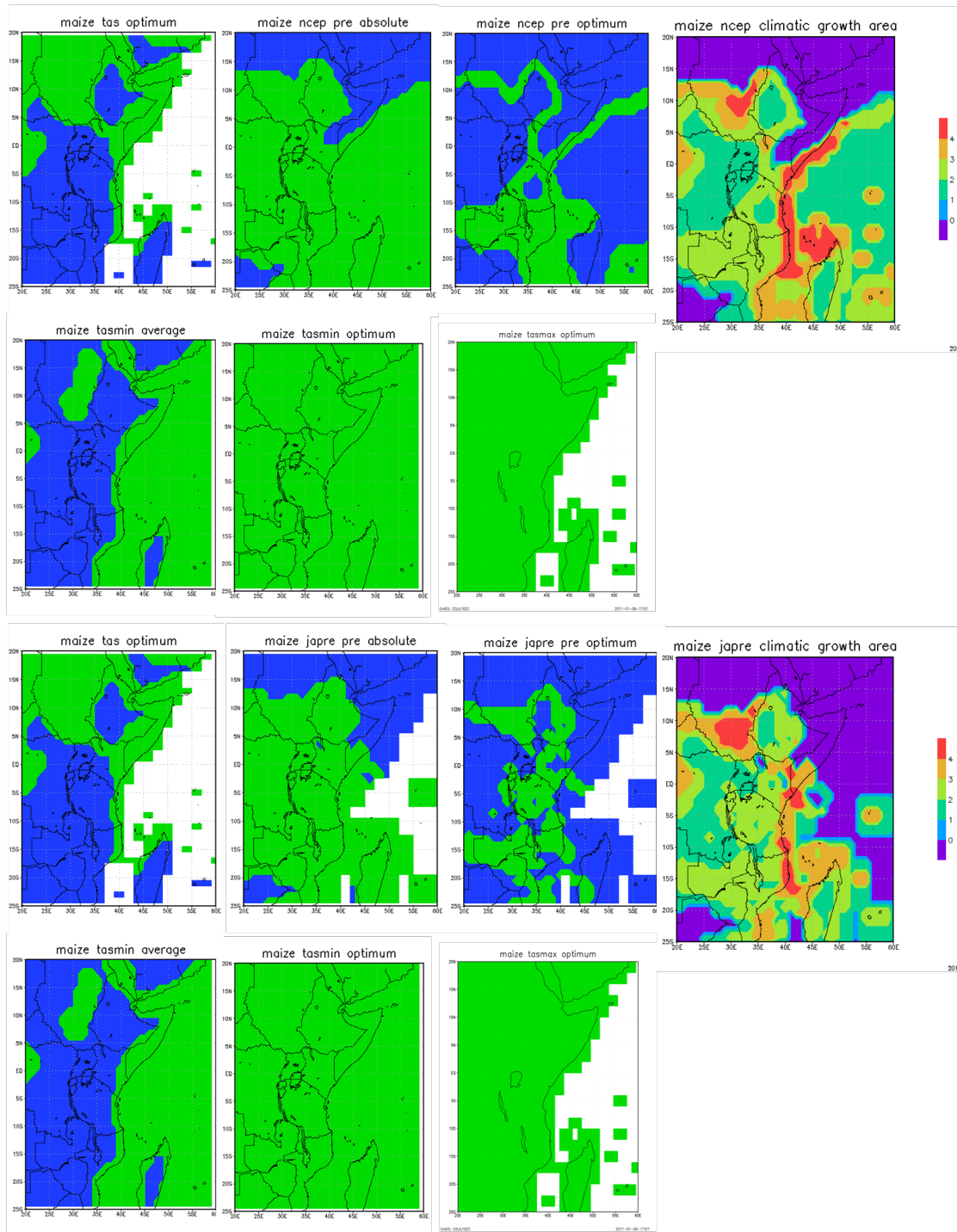


Figure A2: Thresholds of production across the region, as realised from mean climatic conditions, for cassava. Maps are provided using both the (a) NCEP and (b) JapRe precipitation reanalyses, both use the CRU temperature dataset.



**Figure A3: Thresholds of production across the region, as realised from mean climatic conditions, for maize. Maps are provided using both the (a) NCEP and (b) JapRe precipitation reanalyses, both use the CRU temperature dataset.**



**Figure A4: Thresholds of production across the region, as realised from mean climatic conditions, for millet. Maps are provided using both the (a) NCEP and (b) JapRe precipitation reanalyses, both use the CRU temperature dataset.**

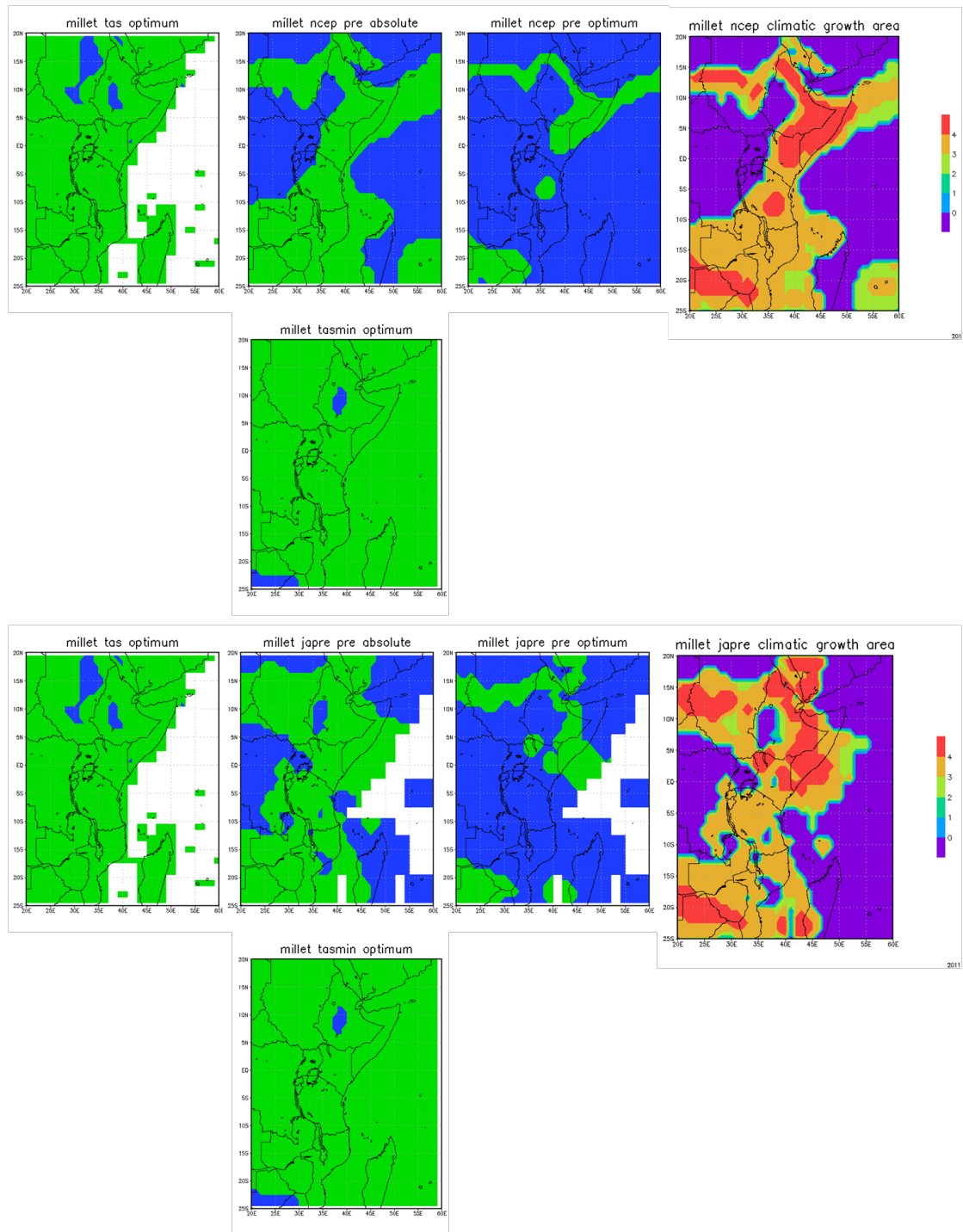


**Figure A5: Thresholds of production across the region, as realised from mean climatic conditions, for pigeonpea. Maps are provided using both the (a) NCEP and (b) JapRe precipitation reanalyses, both use the CRU temperature dataset.**

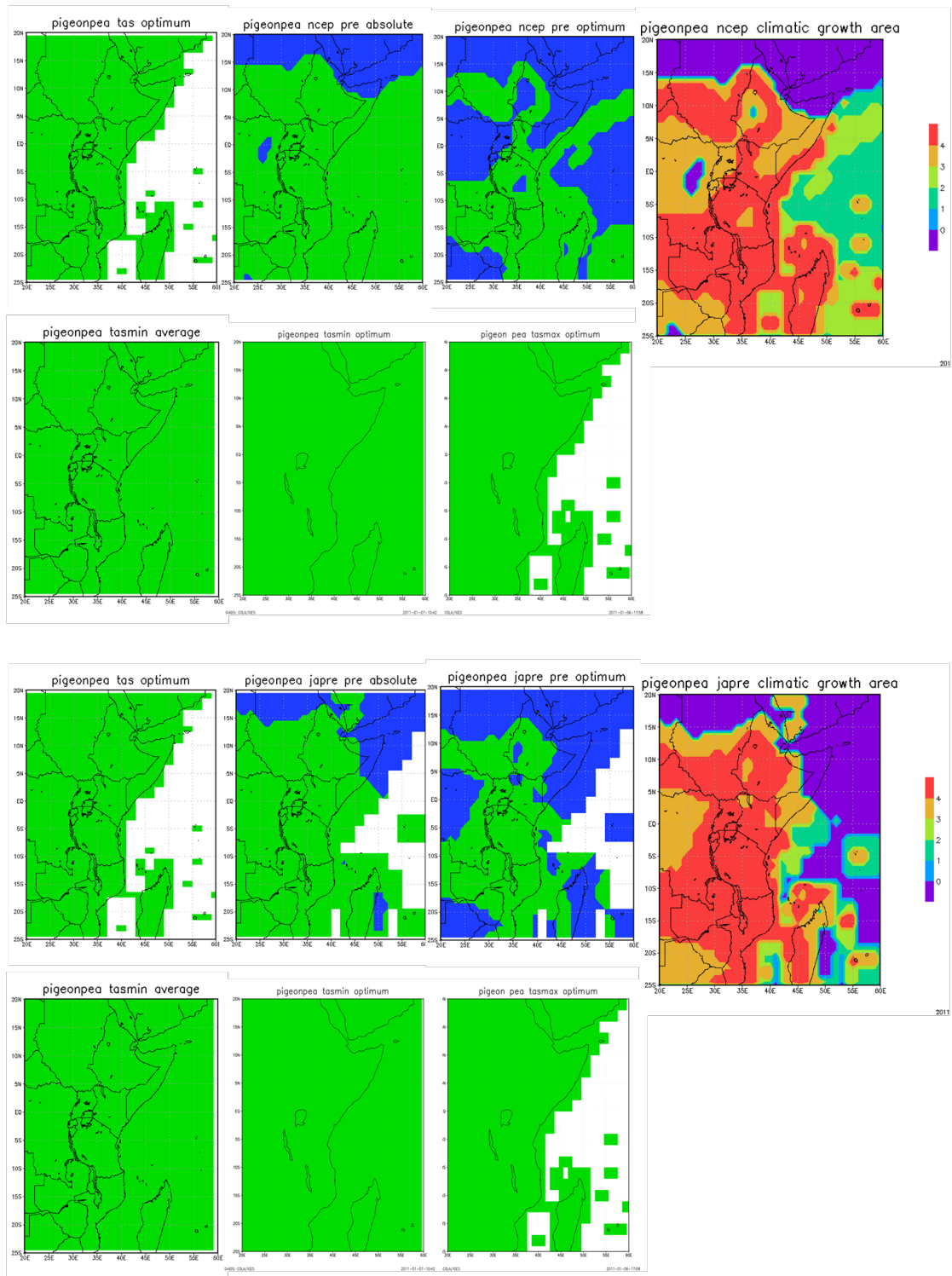


**Figure A6: Thresholds of production across the region, as realised from mean climatic conditions, for potato. Maps are provided using both the (a) NCEP and (b) JapRe precipitation reanalyses, both use the CRU temperature dataset.**

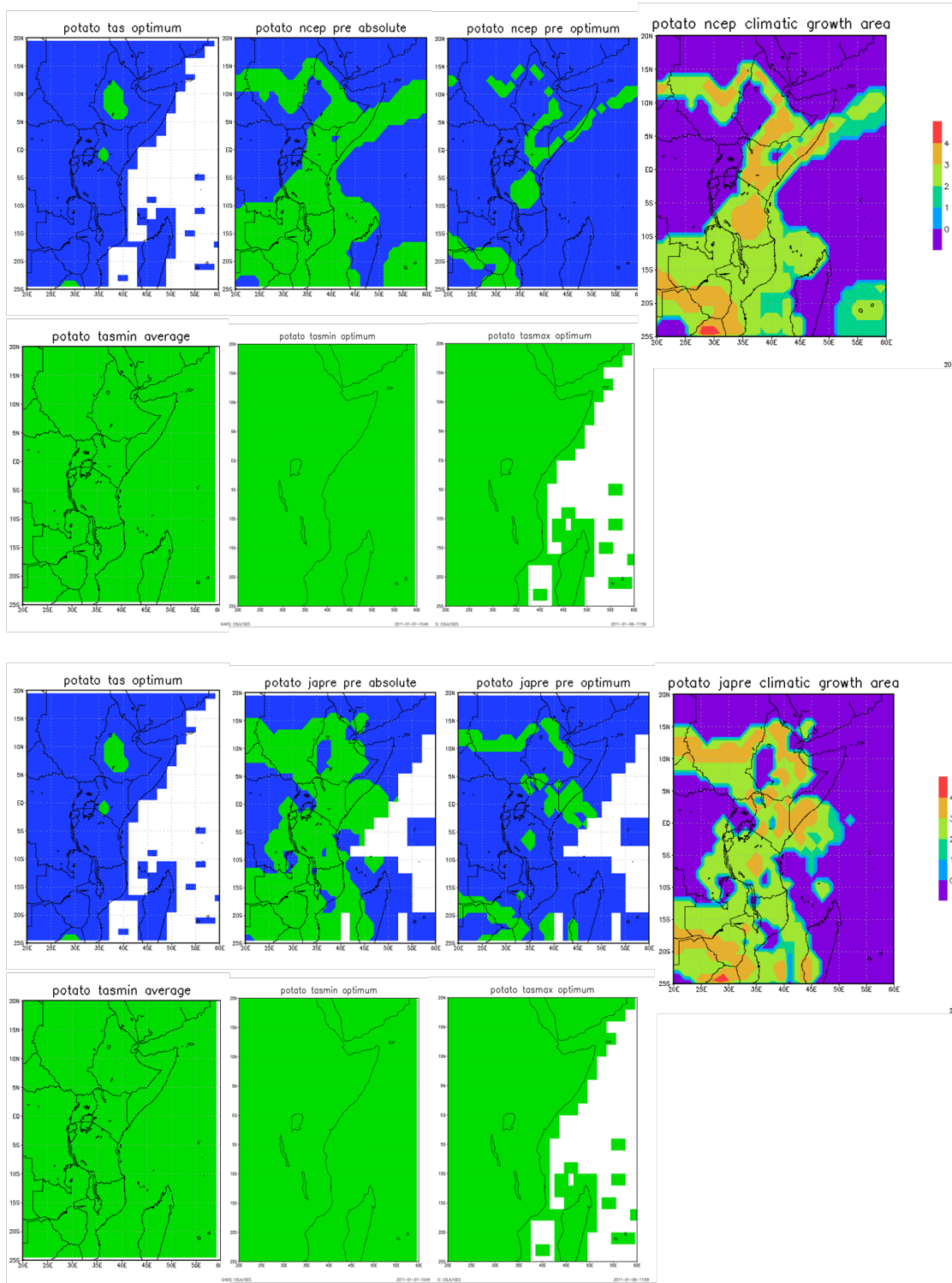


**Figure A7: Thresholds of production across the region, as realised from mean climatic conditions, for rice. Maps are provided using both the (a) NCEP and (b) JapRe precipitation reanalyses, both use the CRU temperature dataset.**

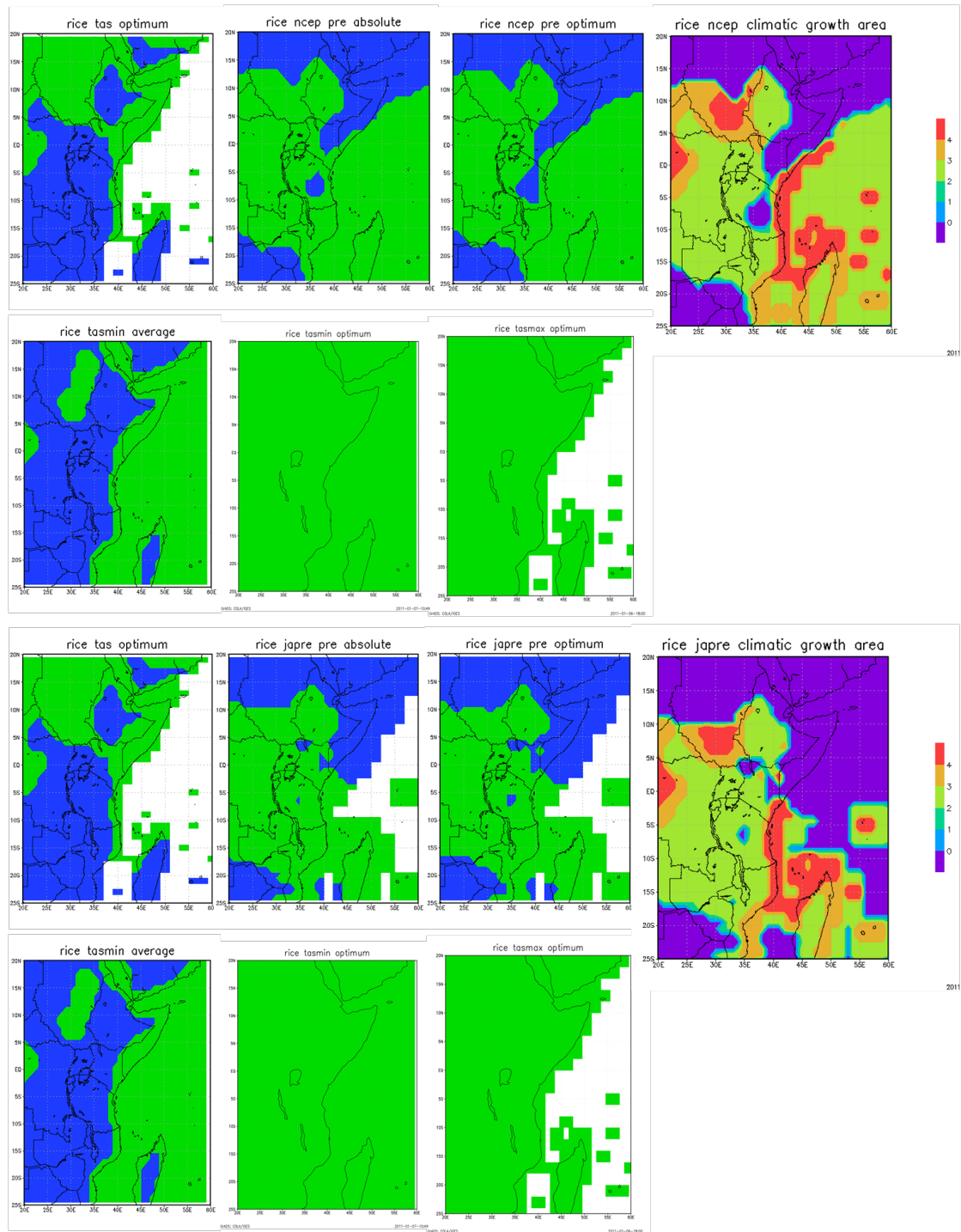


**Figure A8: Thresholds of production across the region, as realised from mean climatic conditions, for sorghum. Maps are provided using both the (a) NCEP and (b) JapRe precipitation reanalyses, both use the CRU temperature dataset.**

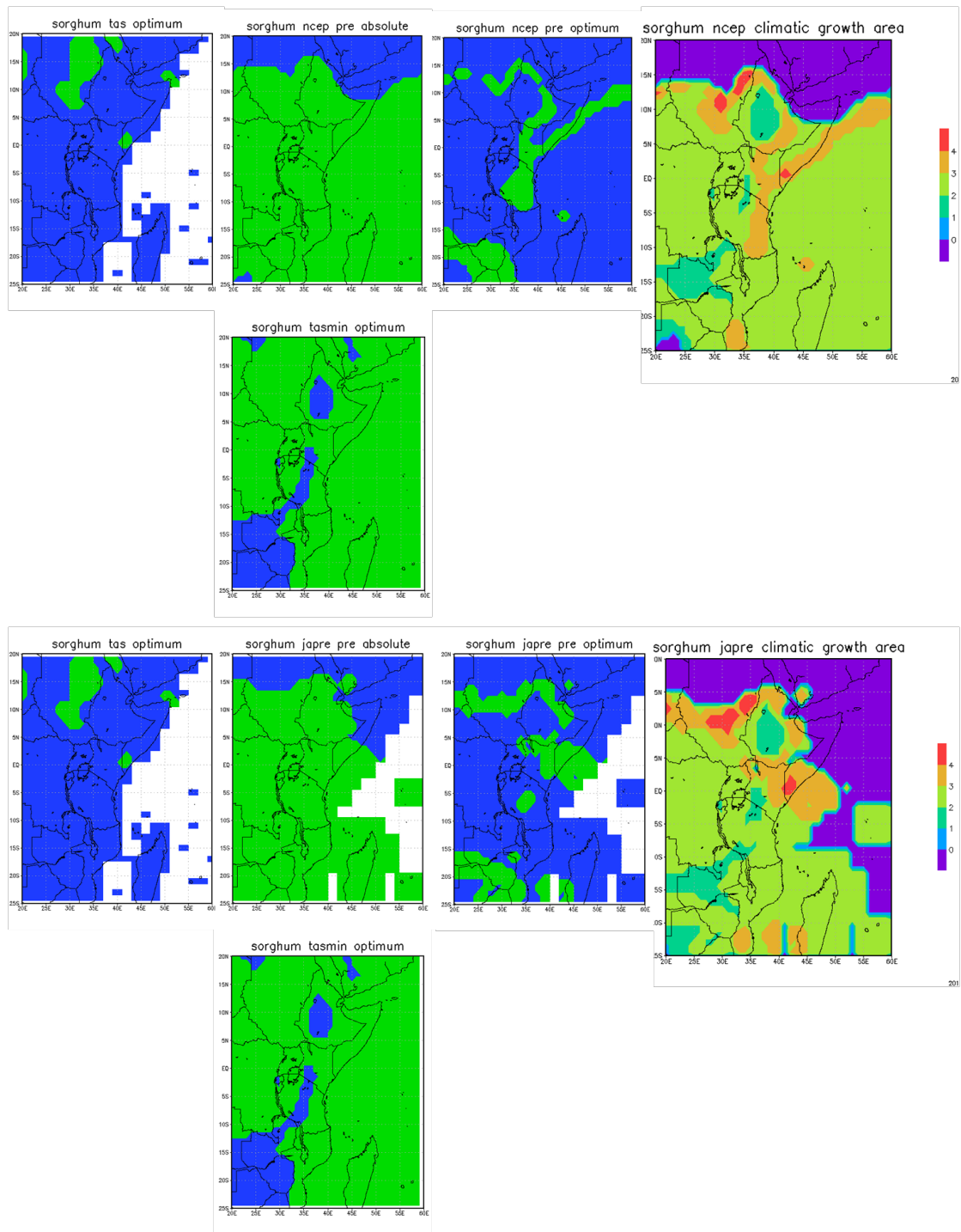


**Figure A9: Thresholds of production across the region, as realised from mean climatic conditions, for sweet potato. Maps are provided using both the (a) NCEP and (b) JapRe precipitation reanalyses, both use the CRU temperature dataset.**

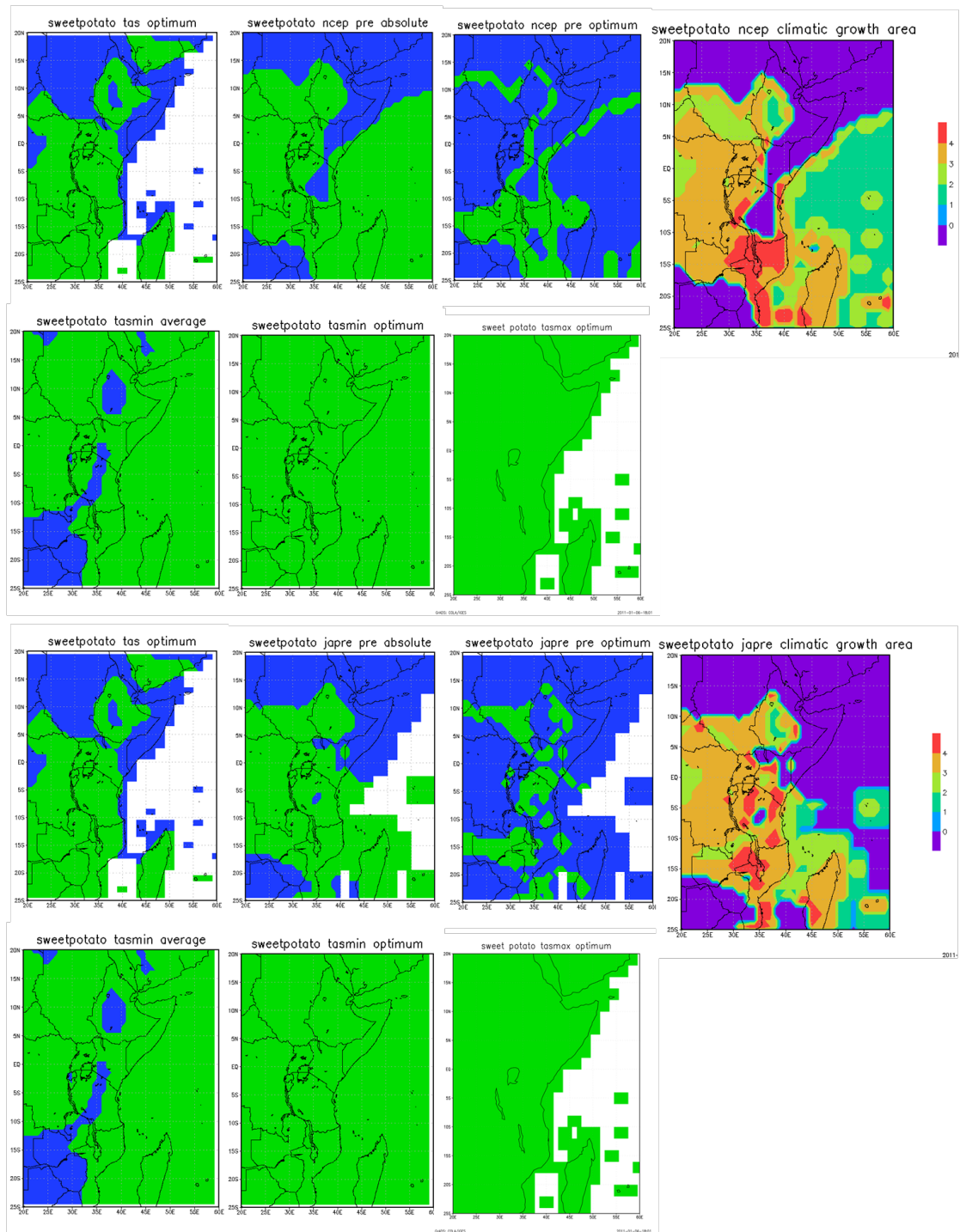
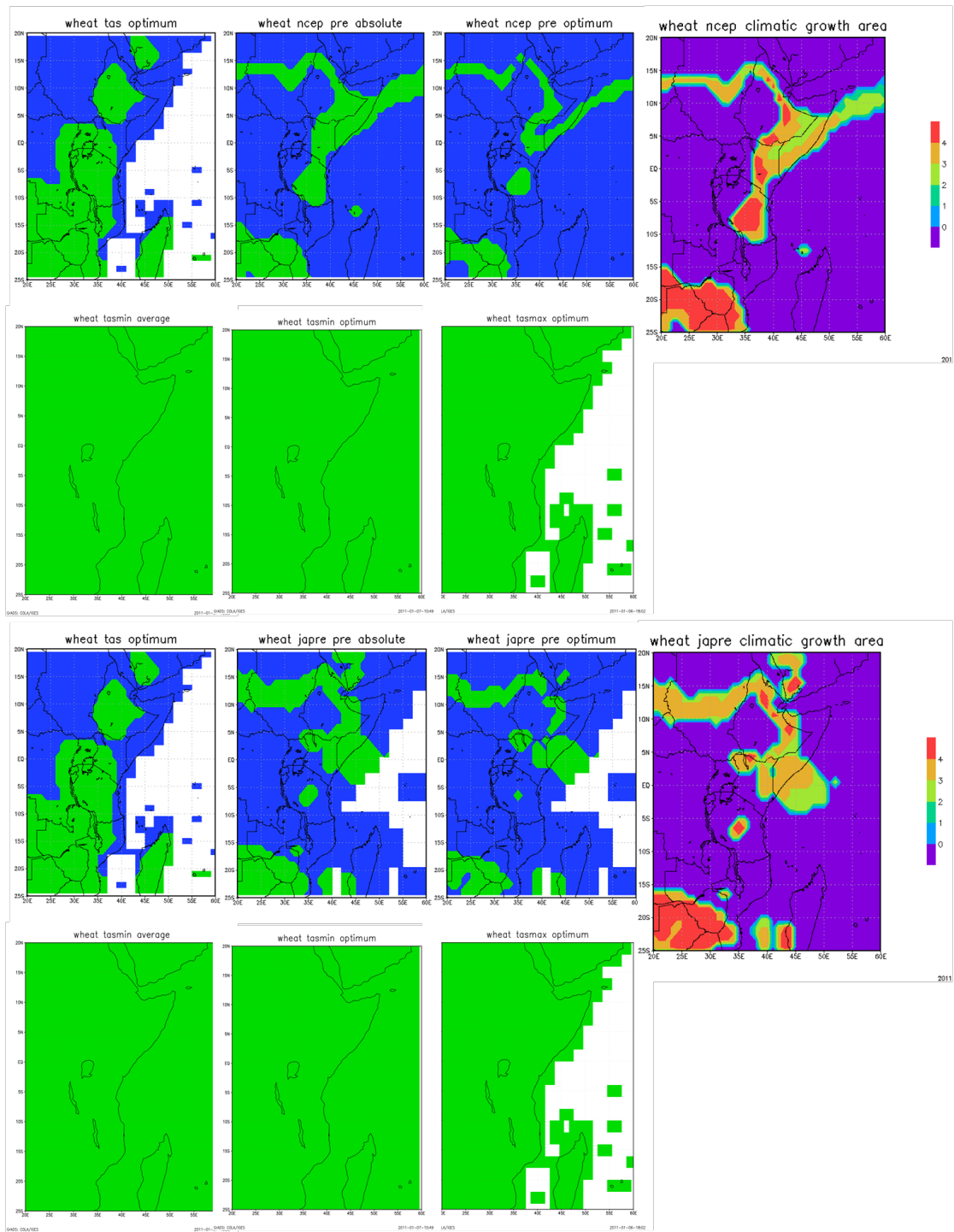


**Figure A10: Thresholds of production across the region, as realised from mean climatic conditions, for wheat. Maps are provided using both the (a) NCEP and (b) JapRe precipitation reanalyses, both use the CRU temperature dataset.**



## Appendix 2

Figure B1: Model derived crop domains for banana created using climatology data for the 1970-99 period. The NCEP and JapRe domains are included for comparison.

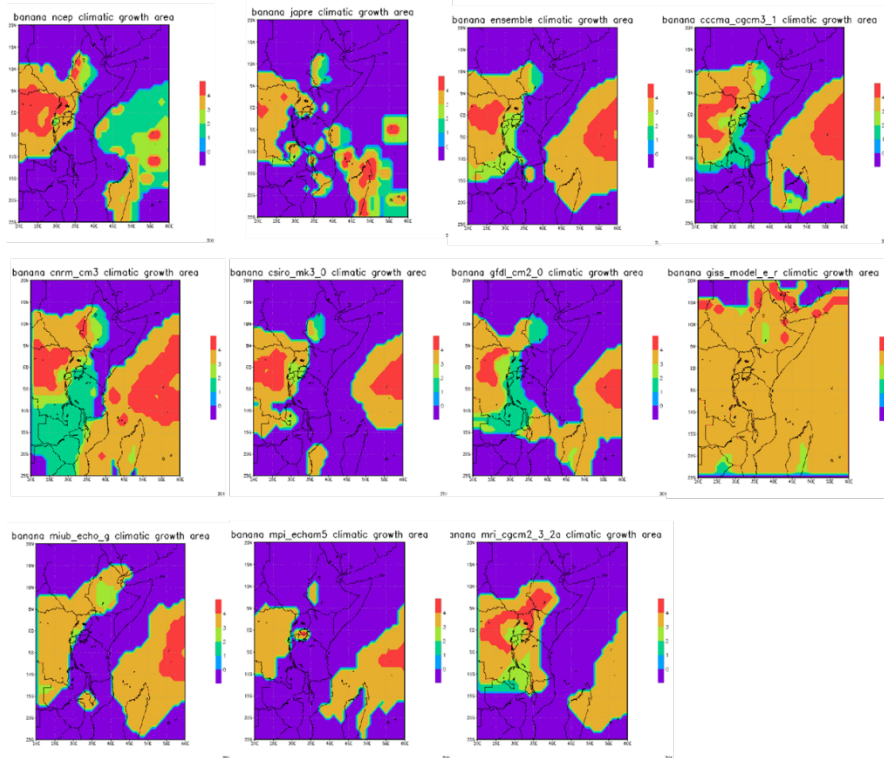


**Figure B2: Model derived crop domains for cassava created using climatology data for the 1970-99 period. The NCEP and JapRe domains are included for comparison.**

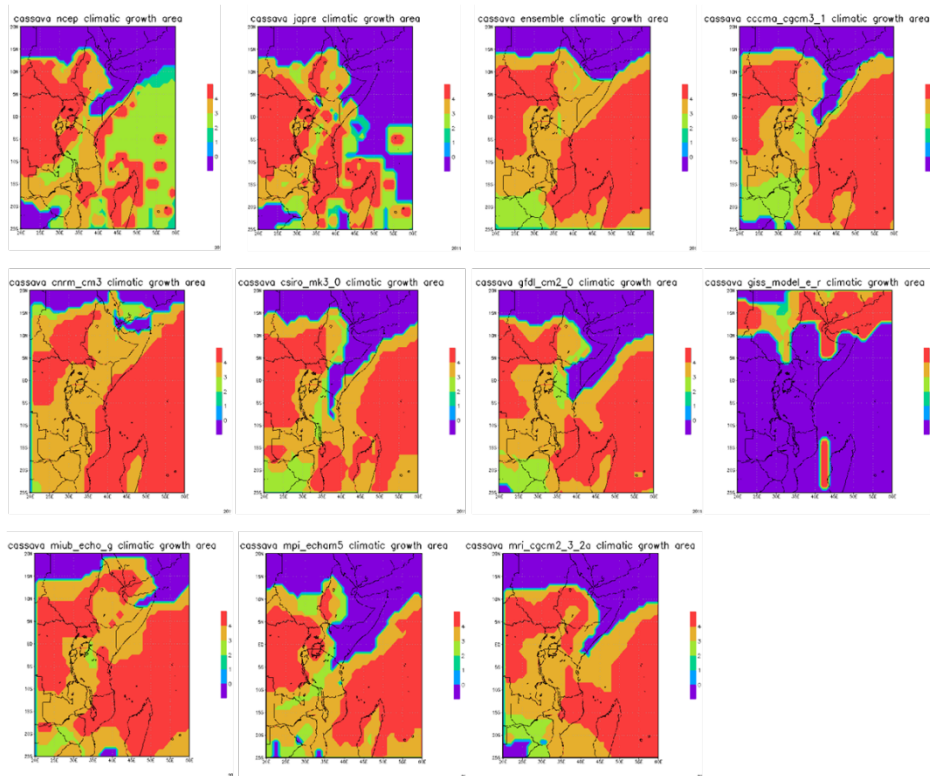


**Figure B3: Model derived crop domains for maize created using climatology data for the 1970-99 period. The NCEP and JapRe domains are included for comparison.**

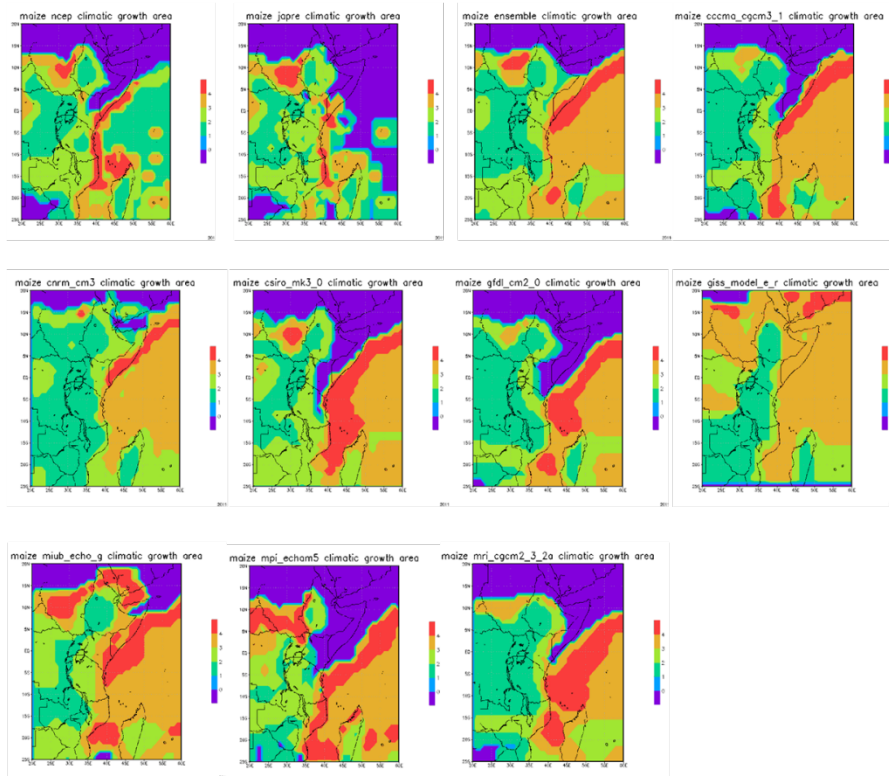


**Figure B4: Model derived crop domains for millet created using climatology data for the 1970-99 period. The NCEP and JapRe domains are included for comparison.**

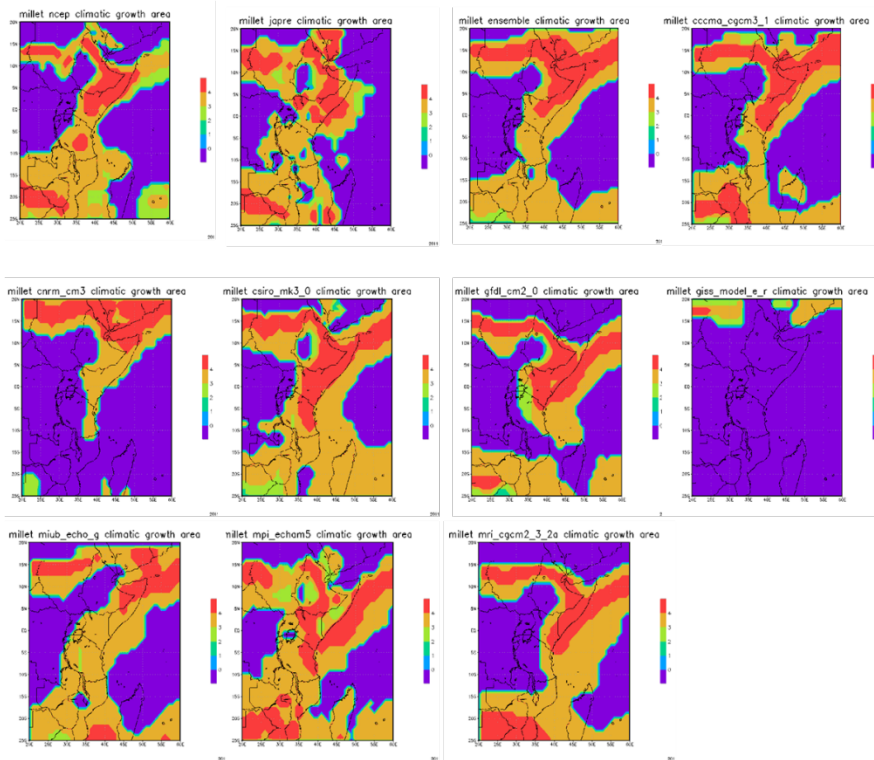


**Figure B5: Model derived crop domains for pigeonpea created using climatology data for the 1970-99 period. The NCEP and JapRe domains are included for comparison.**

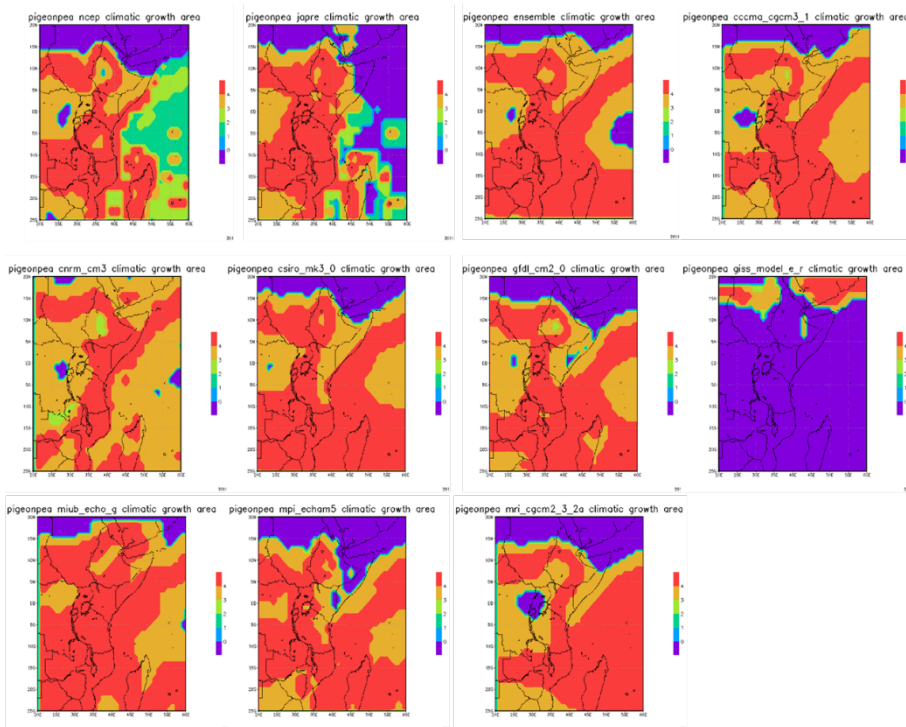


**Figure B6: Model derived crop domains for potato created using climatology data for the 1970-99 period. The NCEP and JapRe domains are included for comparison.**

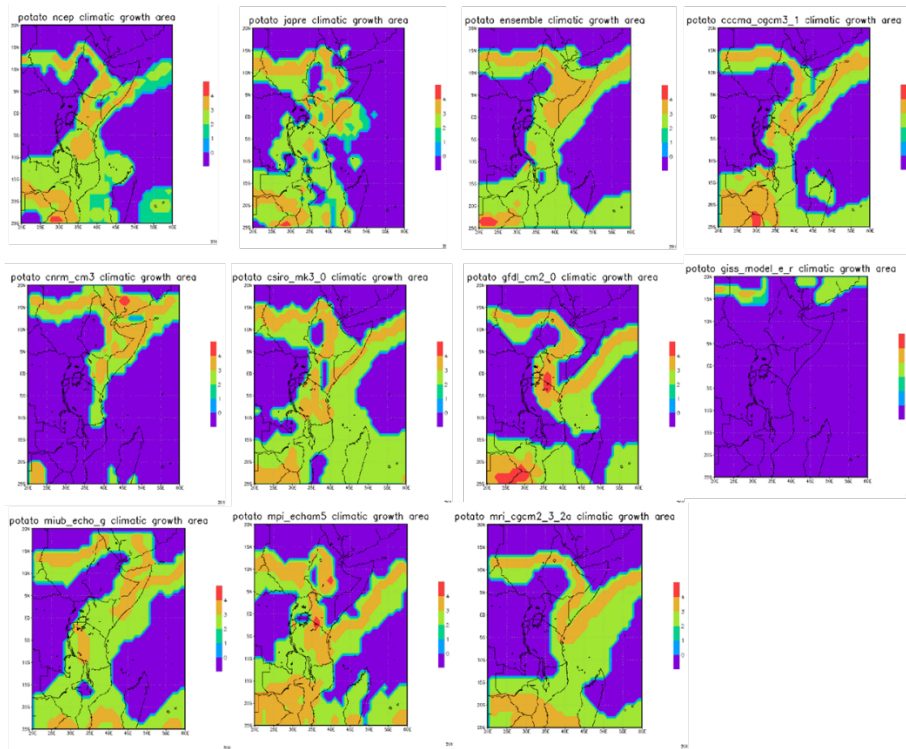


**Figure B7: Model derived crop domains for rice created using climatology data for the 1970-99 period. The NCEP and JapRe domains are included for comparison.**

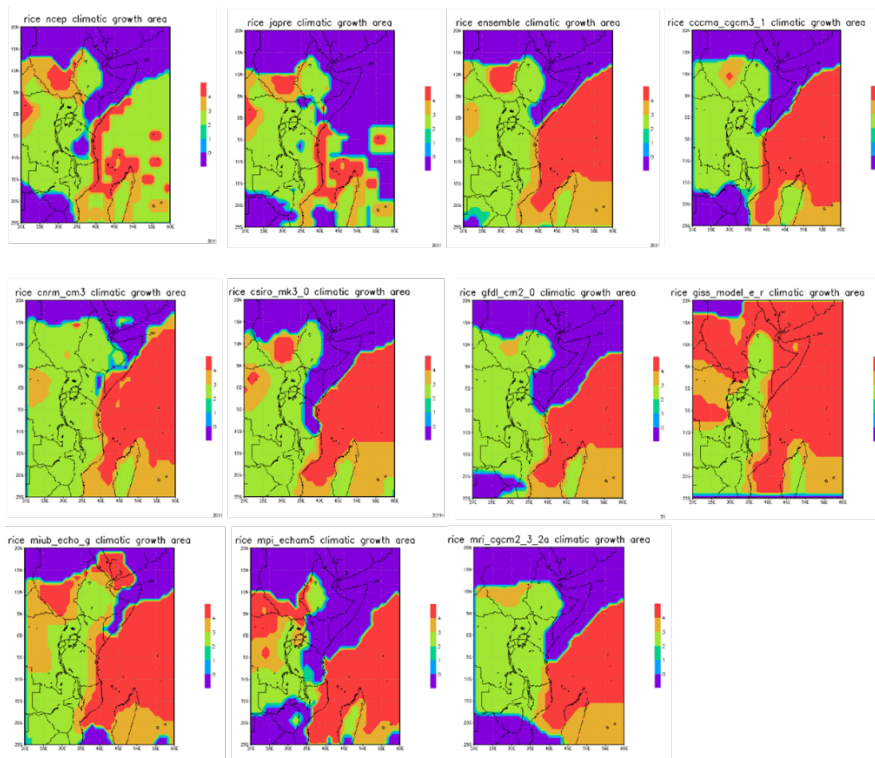


**Figure B8: Model derived crop domains for sorghum created using climatology data for the 1970-99 period. The NCEP and JapRe domains are included for comparison.**

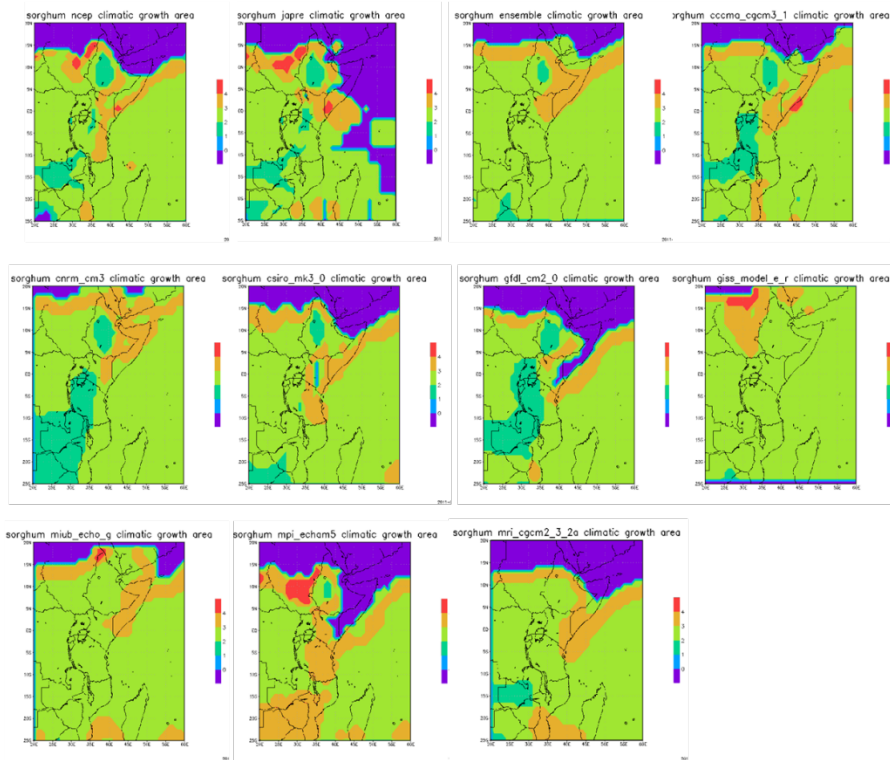


**Figure B9: Model derived crop domains for sweet potato created using climatology data for the 1970-99 period. The NCEP and JapRe domains are included for comparison.**

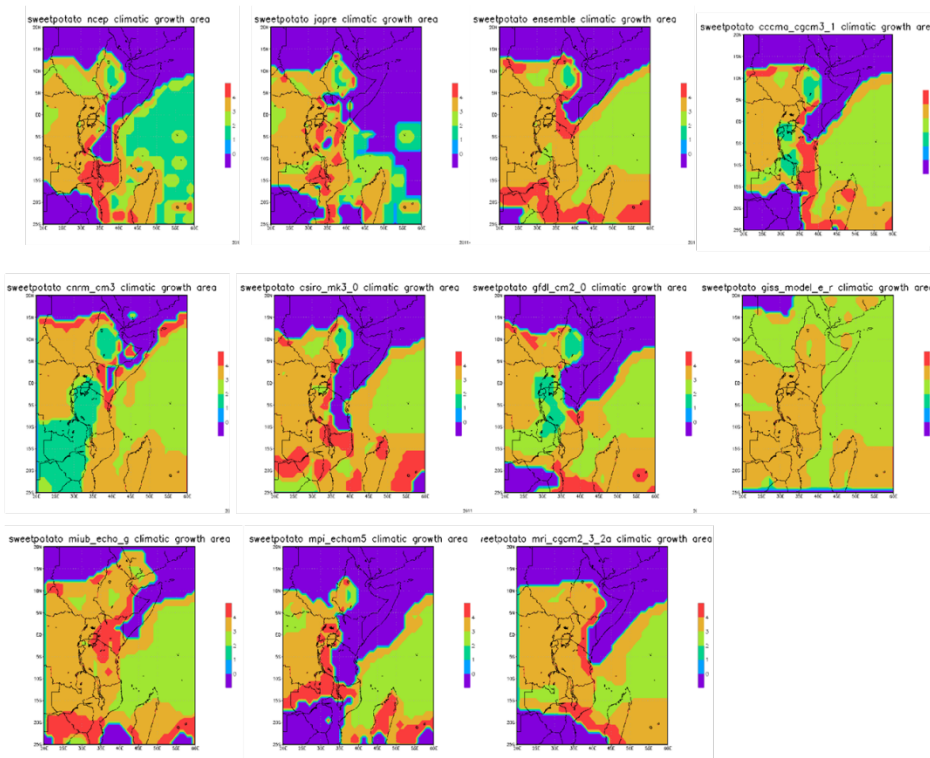
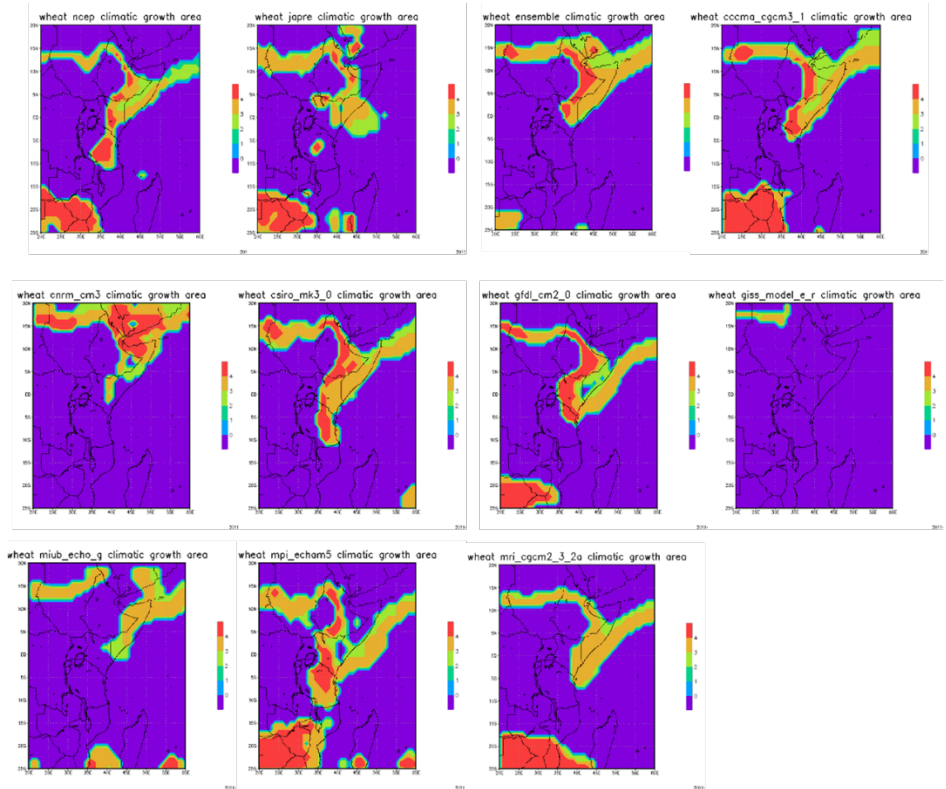
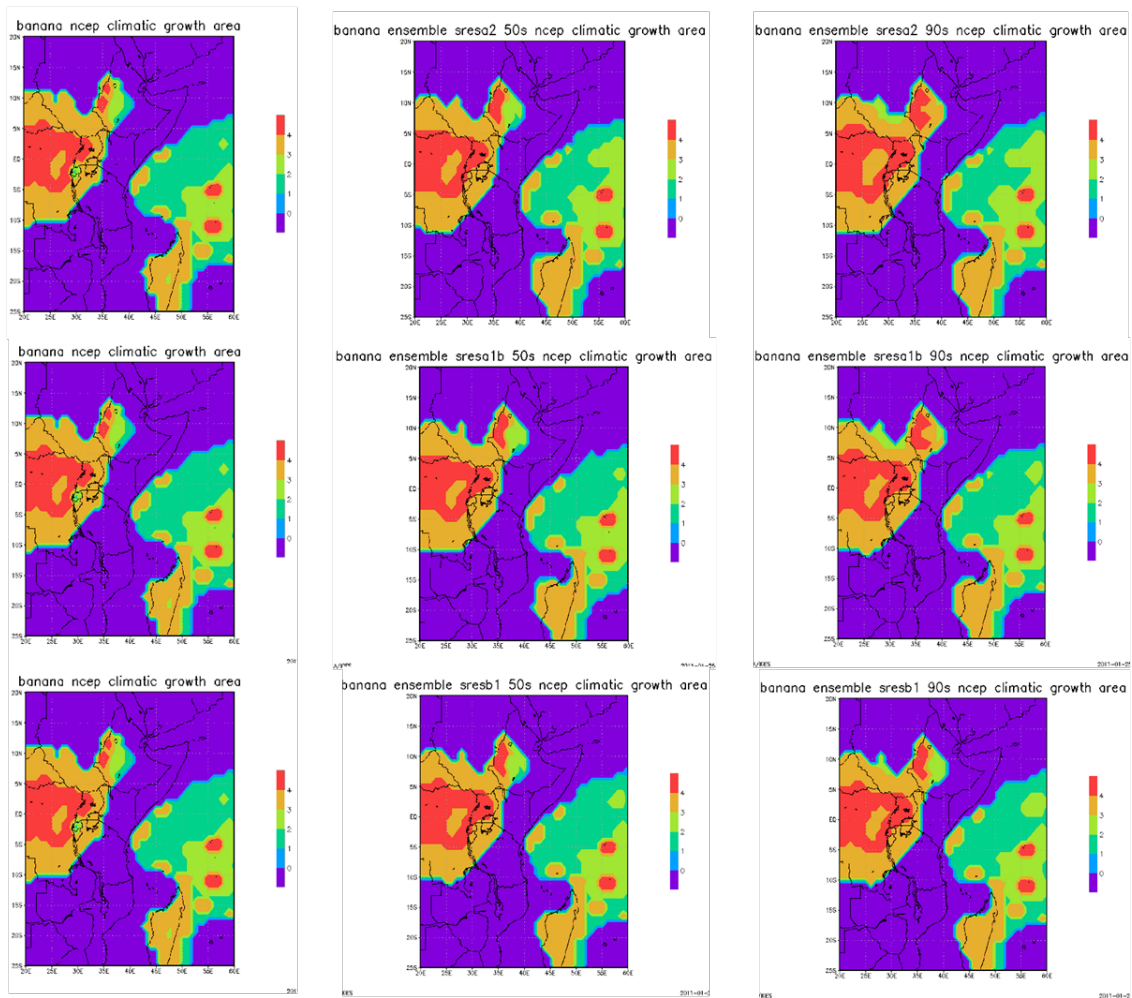


Figure B10: Model derived crop domains for wheat created using climatology data for the 1970-99 period. The NCEP and JapRe domains are included for comparison.



# Appendix 3

Figure C1 (this and following 2 pages): Model ensemble derived crop domains for banana for the 3 periods and 3 forcing scenarios used in this study. Two sets of projections are provided—based on anomalies relative to the NCEP data and the JapRe data, providing a form of initial condition uncertainty. Projections are provided firstly for the 2050s and 2090s including this data and then for 2030s, 2050s and 2090s without minimum temperature data.



(Figure C1 continued)

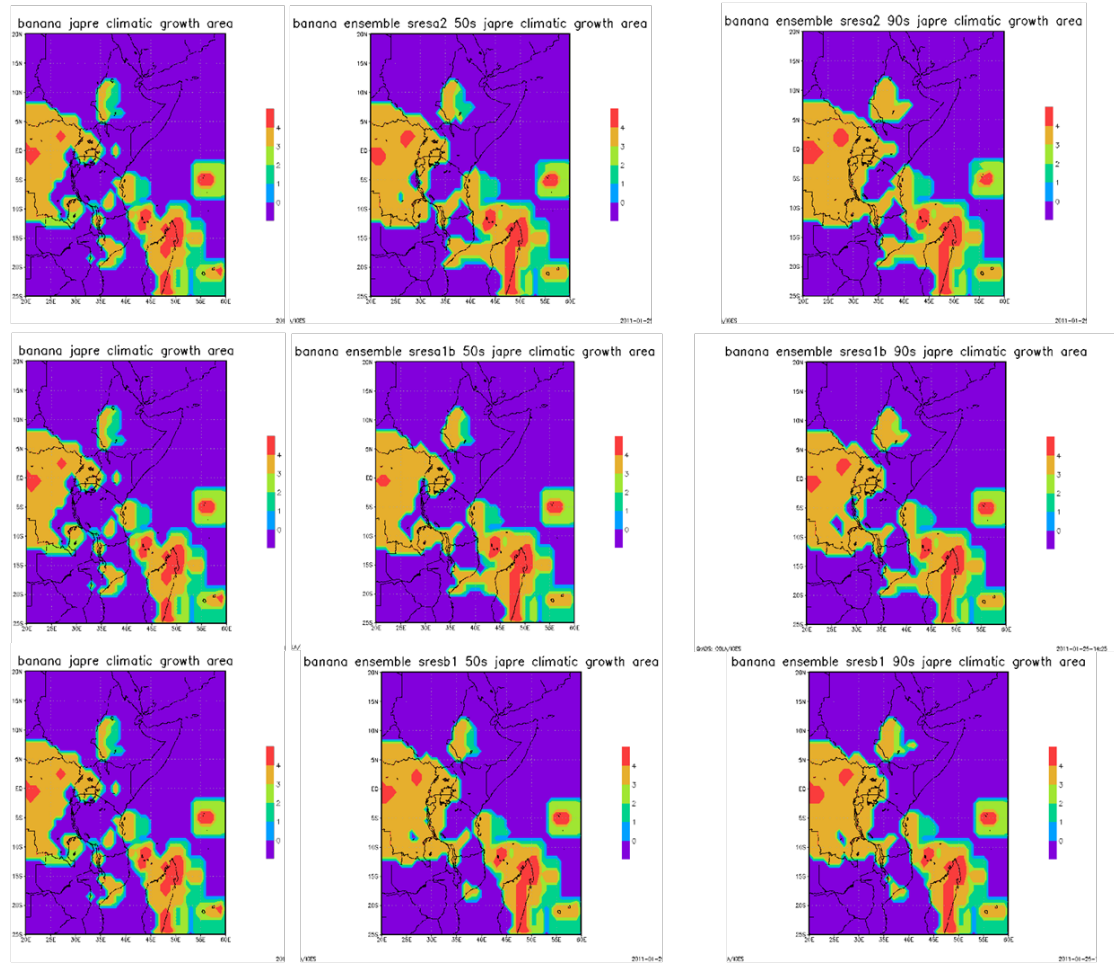


(Figure C1 continued)

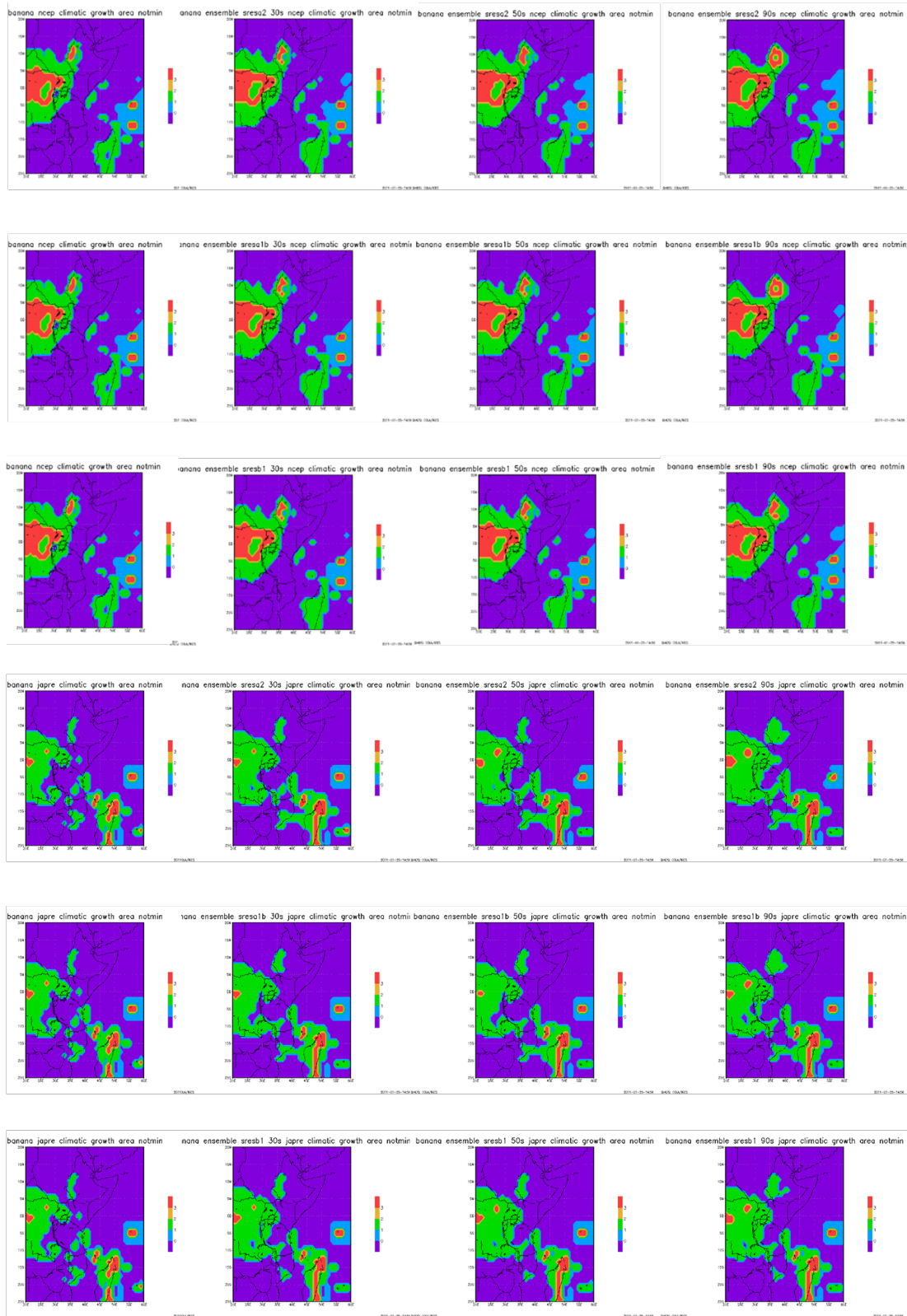
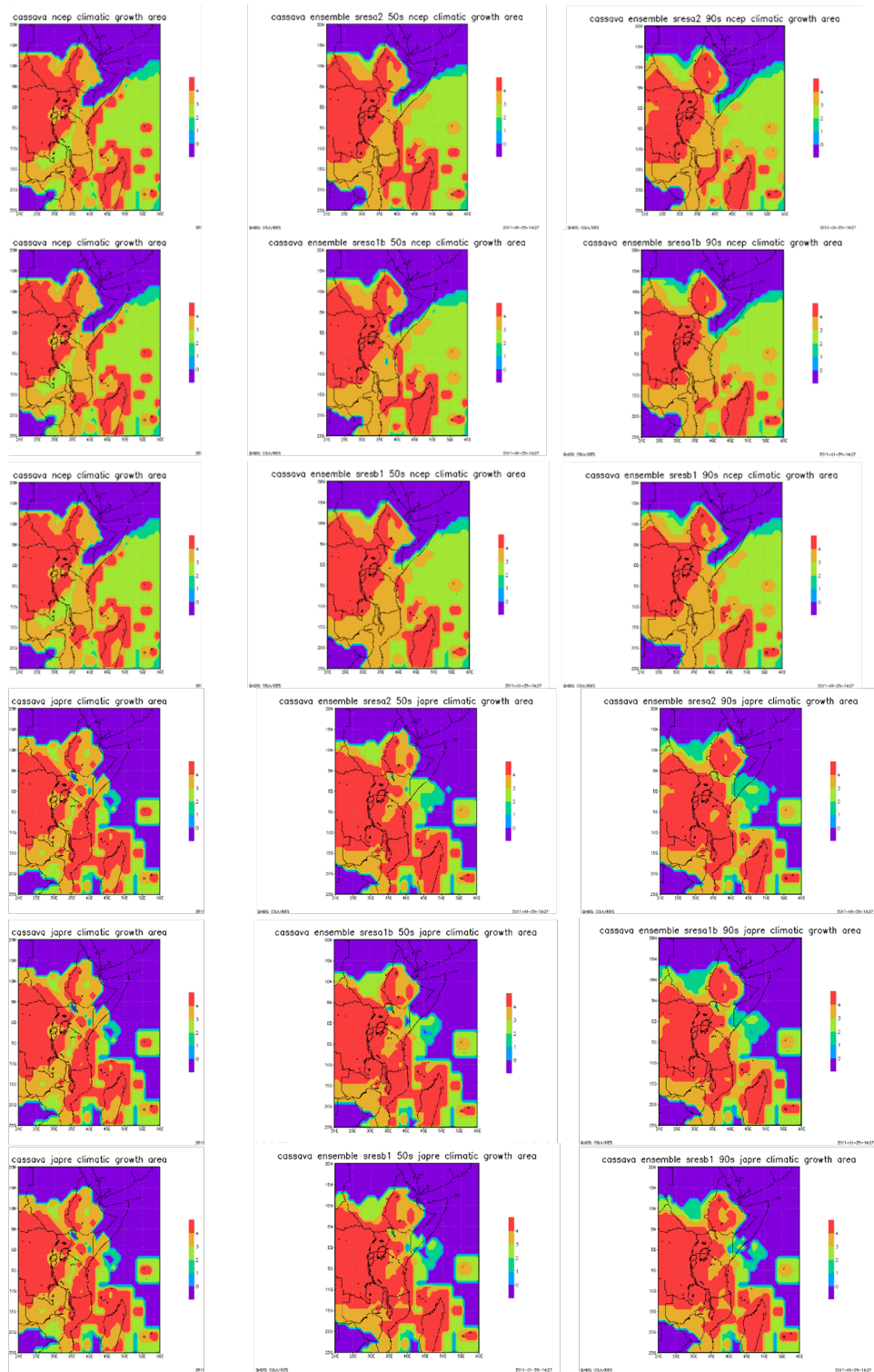


Figure C2 (this and following page): Model ensemble derived crop domains for cassava for the 3 periods and 3 forcing scenarios used in this study. Two sets of projections are provided—based on anomalies relative to the NCEP data and the JapRe data, providing a form of initial condition uncertainty. Projections are provided firstly for the 2050s and 2090s including this data and then for 2030s, 2050s and 2090s without minimum temperature data.



(Figure C2 continued)

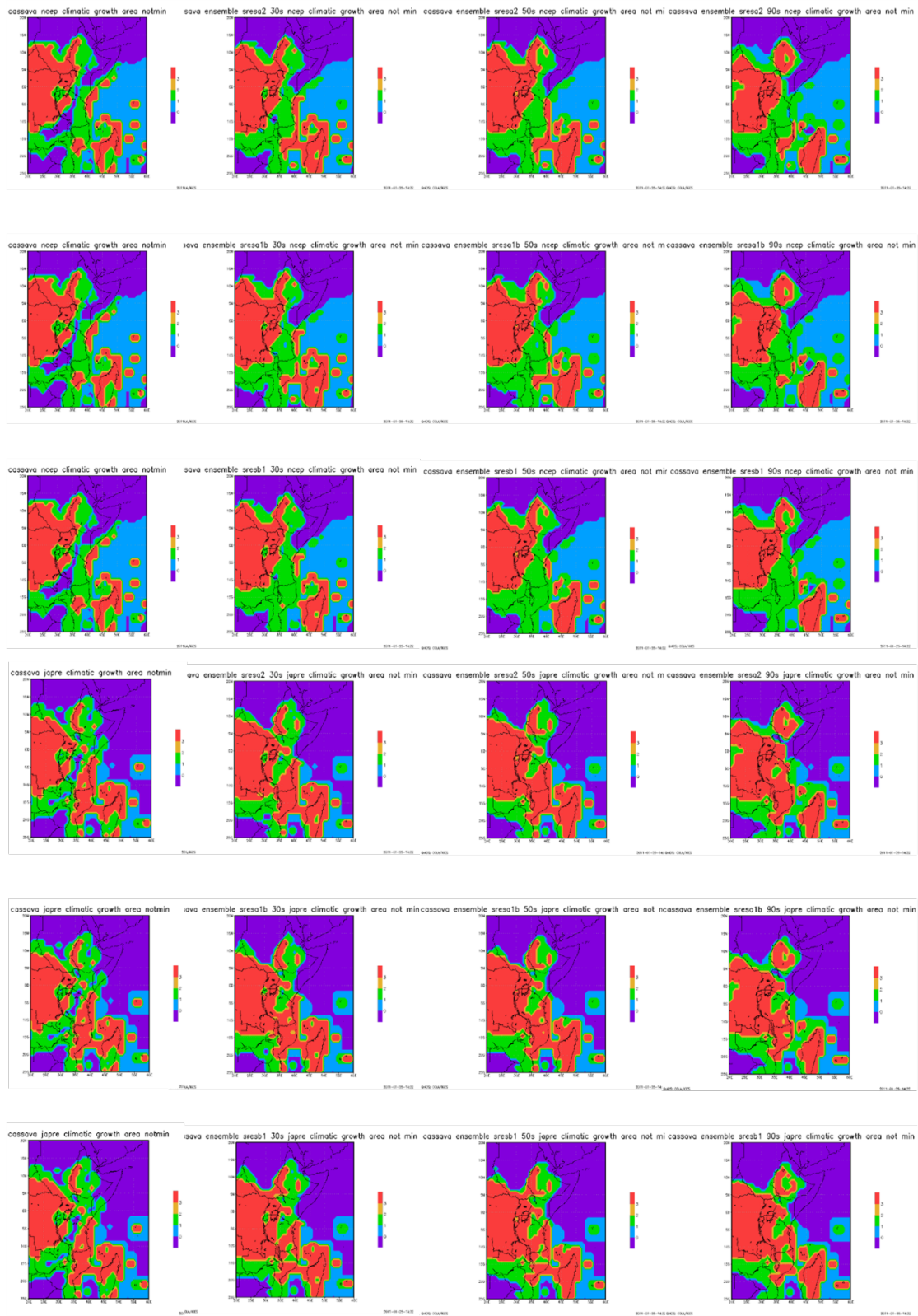
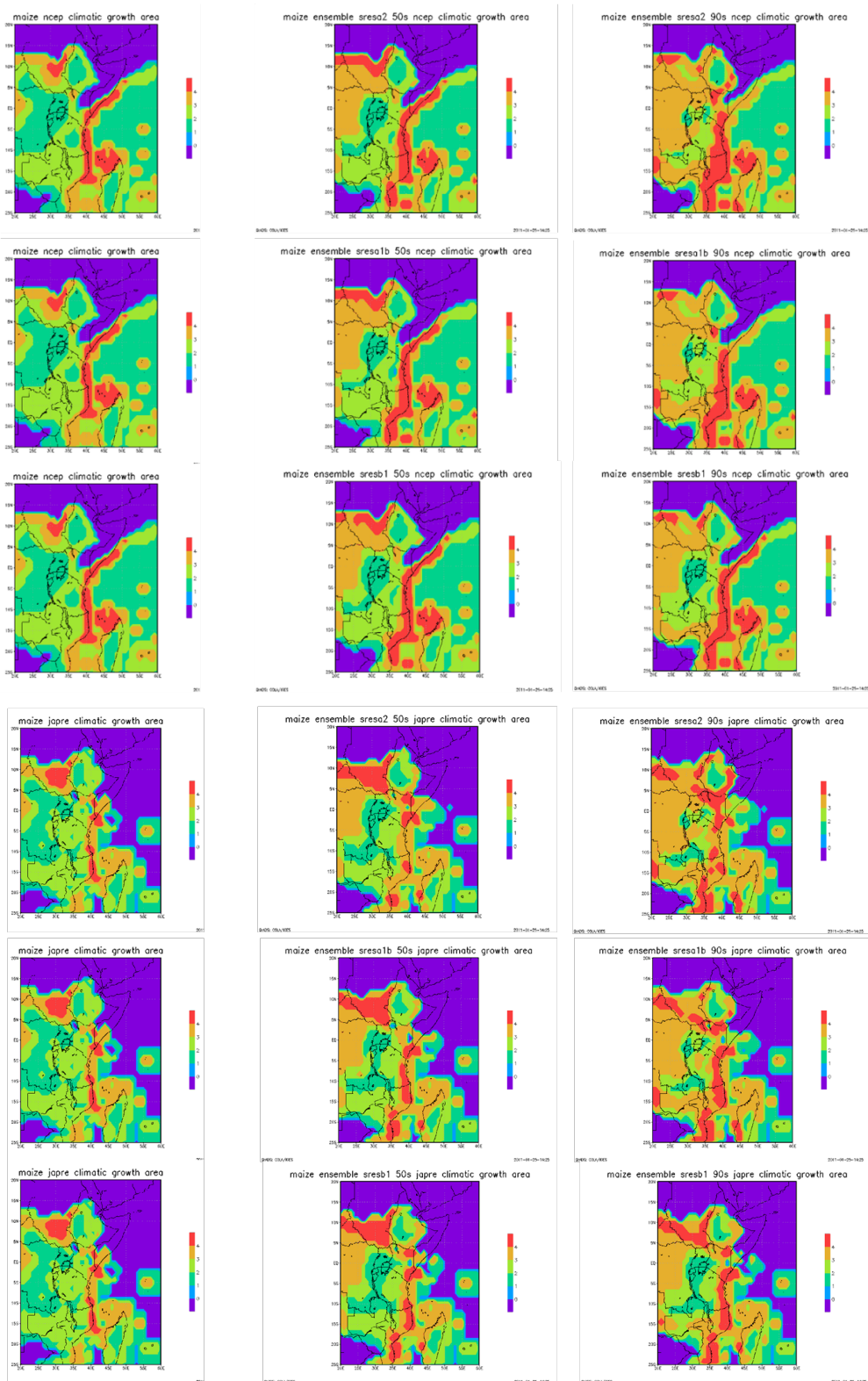


Figure C3 (this and following page): Model ensemble derived crop domains for maize for the three periods and three forcing scenarios used in this study. Two sets of projections are provided—based on anomalies relative to the NCEP data and the JapRe data, providing a form of initial condition uncertainty. Projections are provided firstly for the 2050s and 2090s including this data and then for 2030s, 2050s and 2090s without minimum temperature data.



(Figure C3 continued)

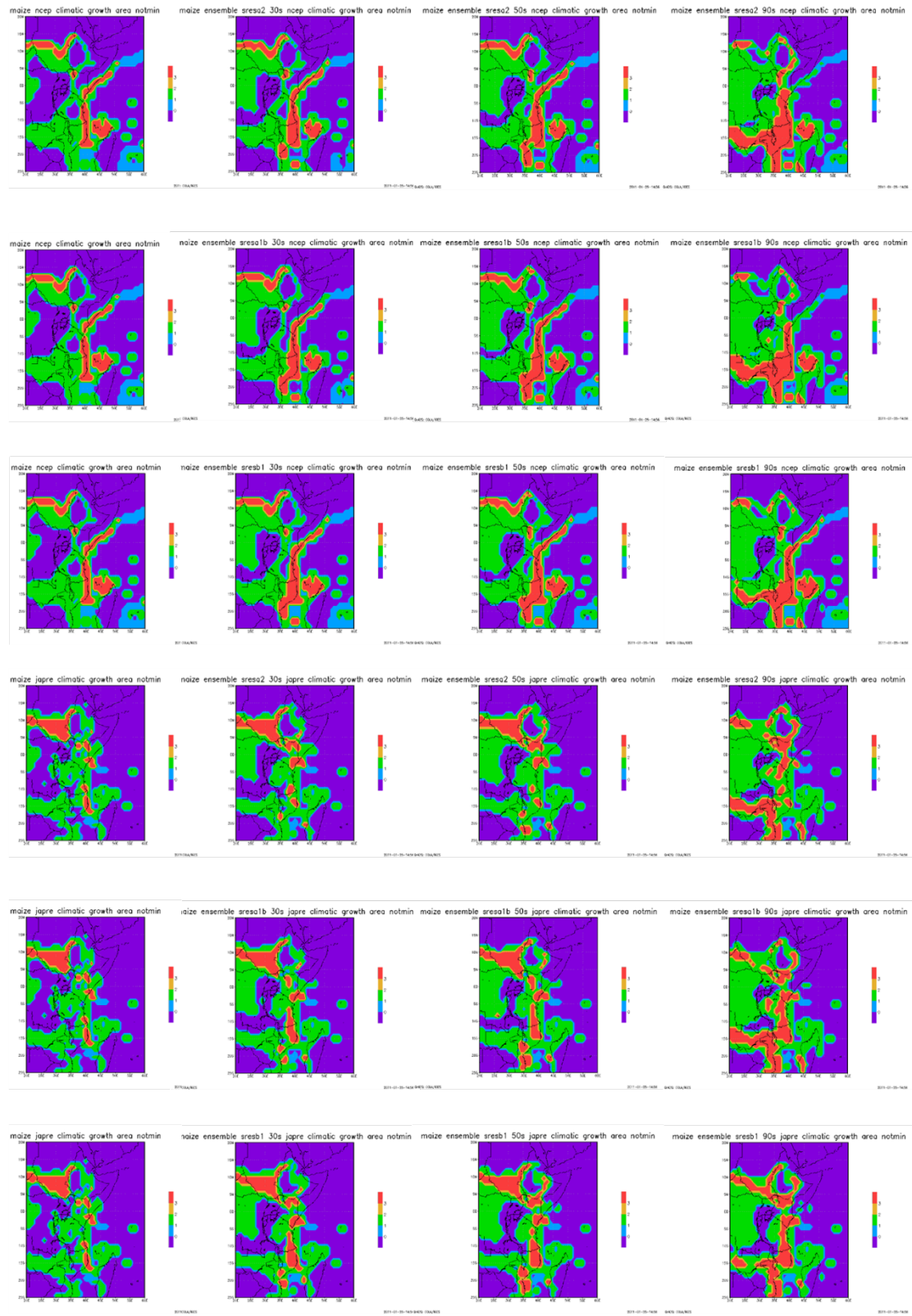
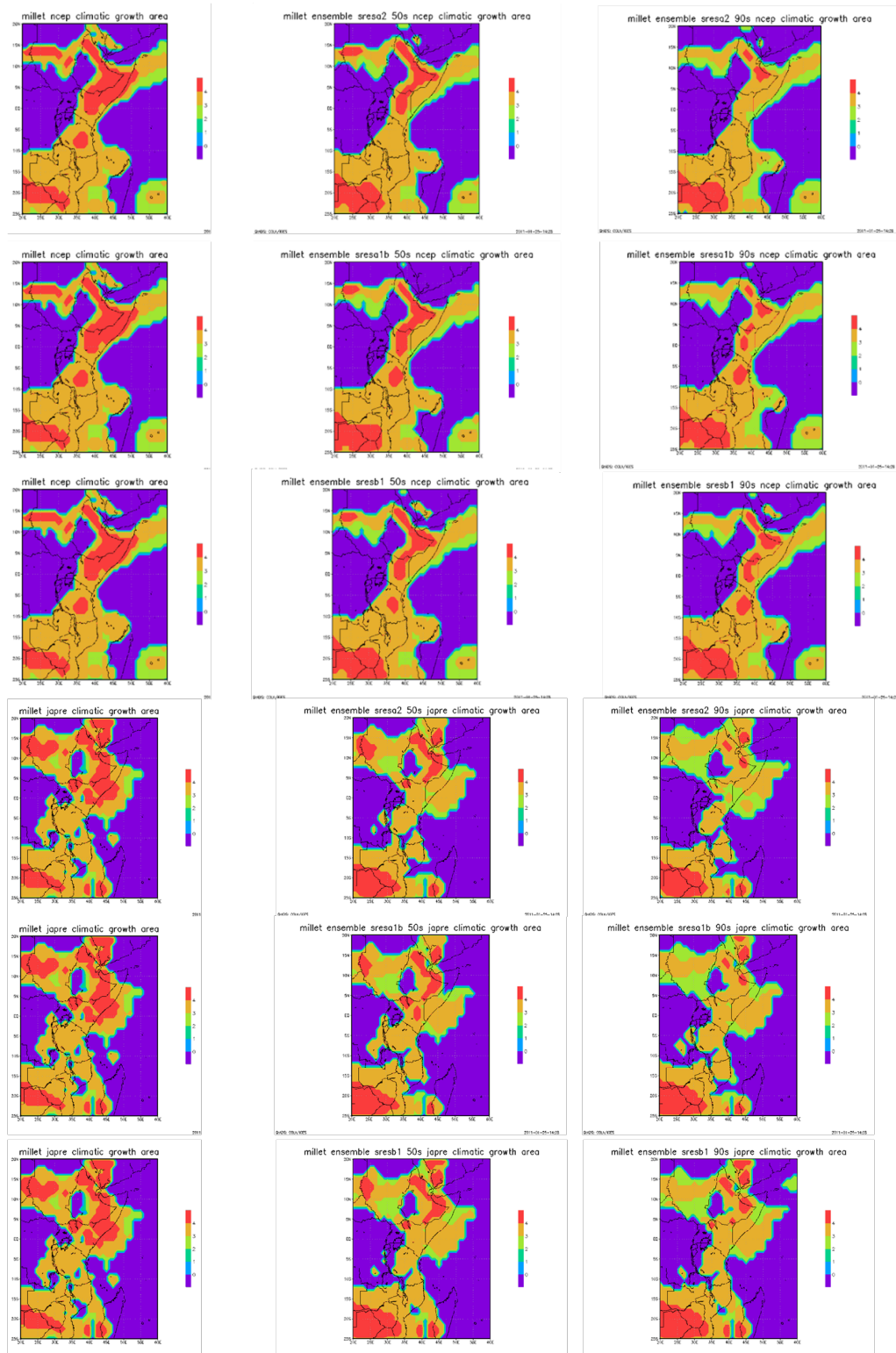


Figure C4 (this and following page): Model ensemble derived crop domains for millet for the 3 periods and 3 forcing scenarios used in this study. Two sets of projections are provided—based on anomalies relative to the NCEP data and the JapRe data, providing a form of initial condition uncertainty. Projections are provided firstly for the 2050s and 2090s including this data and then for 2030s, 2050s and 2090s without minimum temperature data.



(Figure C4 continued)

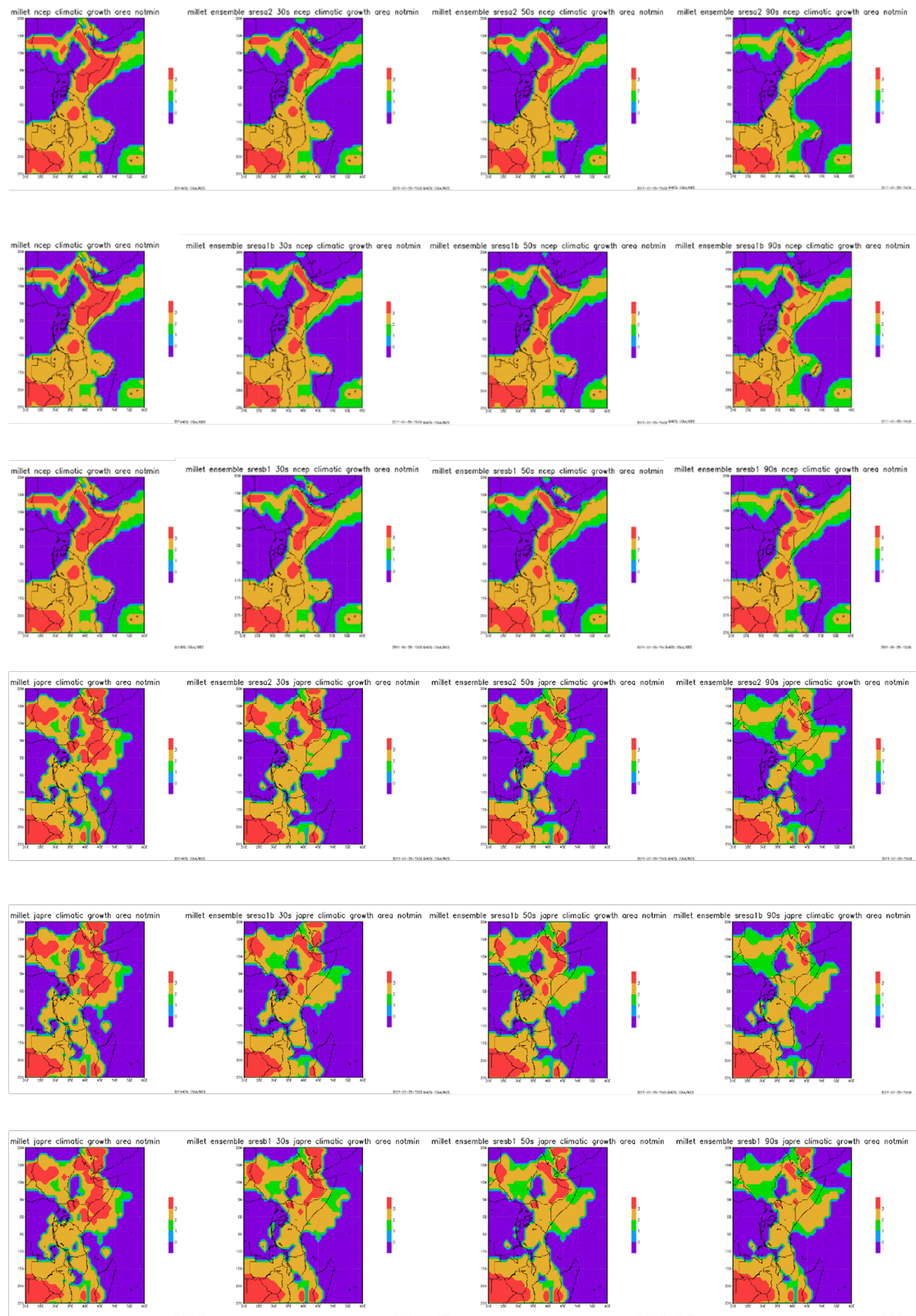
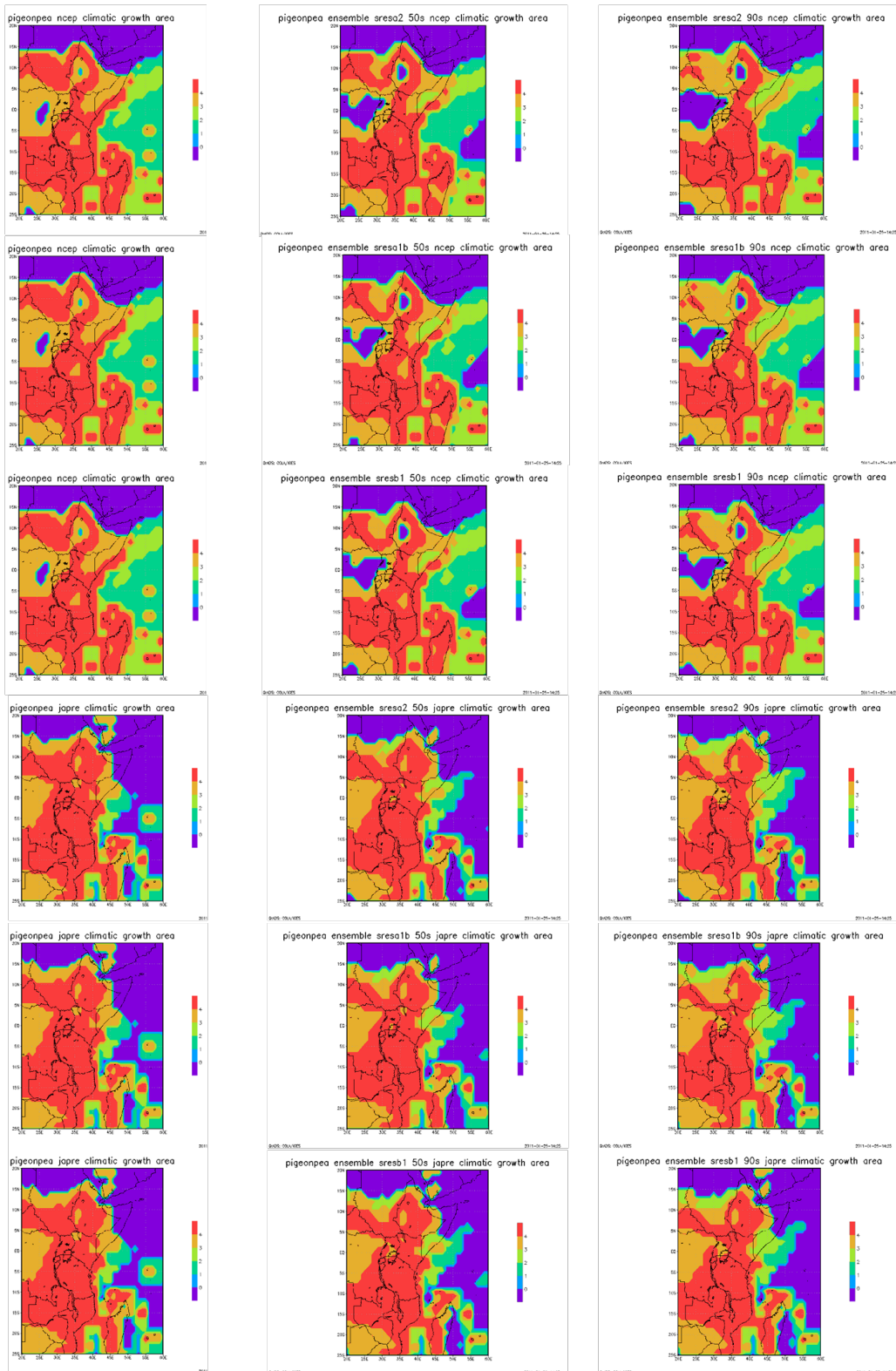
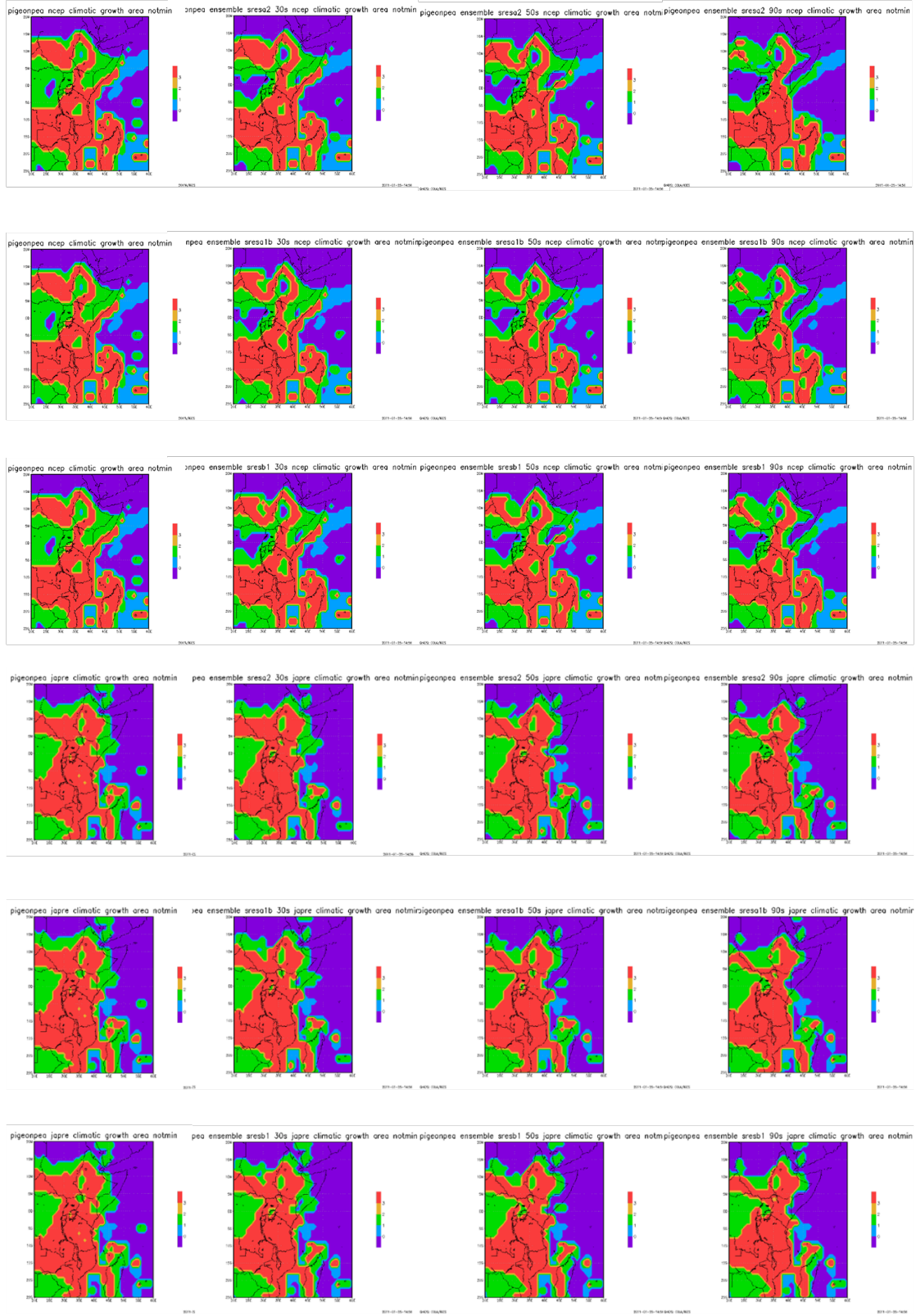


Figure C5 (this and following page): Model ensemble derived crop domains for pigeonpea for the 3 periods and 3 forcing scenarios used in this study. Two sets of projections are provided—based on anomalies relative to the NCEP data and the JapRe data, providing a form of initial condition uncertainty. Projections are provided firstly for the 2050s and 2090s including this data and then for 2030s, 2050s and 2090s without minimum temperature data.



(Figure C5 continued)



**Figure C6 (this and following page): Model ensemble derived crop domains for potato for the 3 periods and 3 forcing scenarios used in this study. Two sets of projections are provided—based on anomalies relative to the NCEP data and the JapRe data, providing a form of initial condition uncertainty. Projections are provided firstly for the 2050s and 2090s including this data and then for 2030s, 2050s and 2090s without minimum temperature data.**

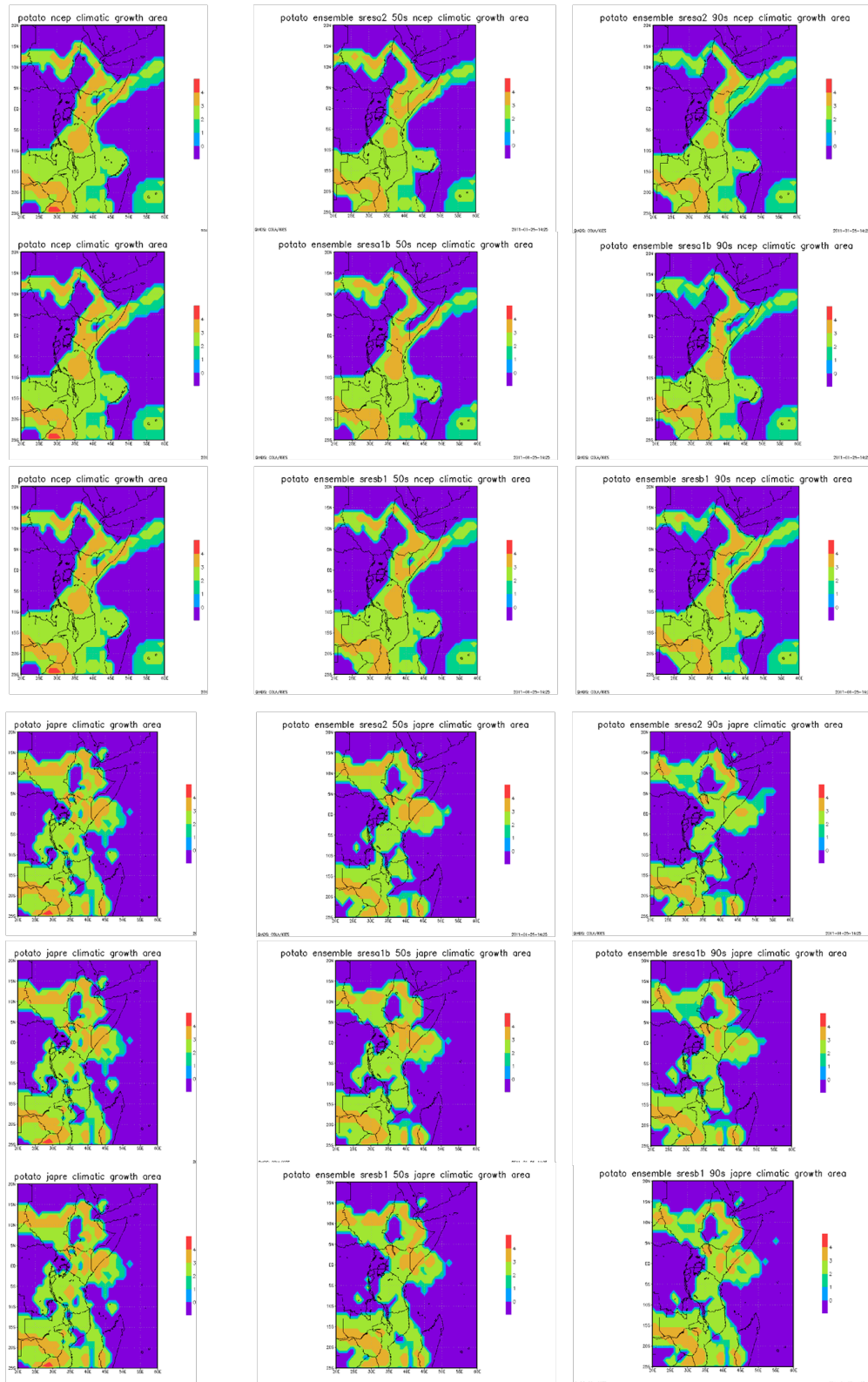


(Figure C6 continued)

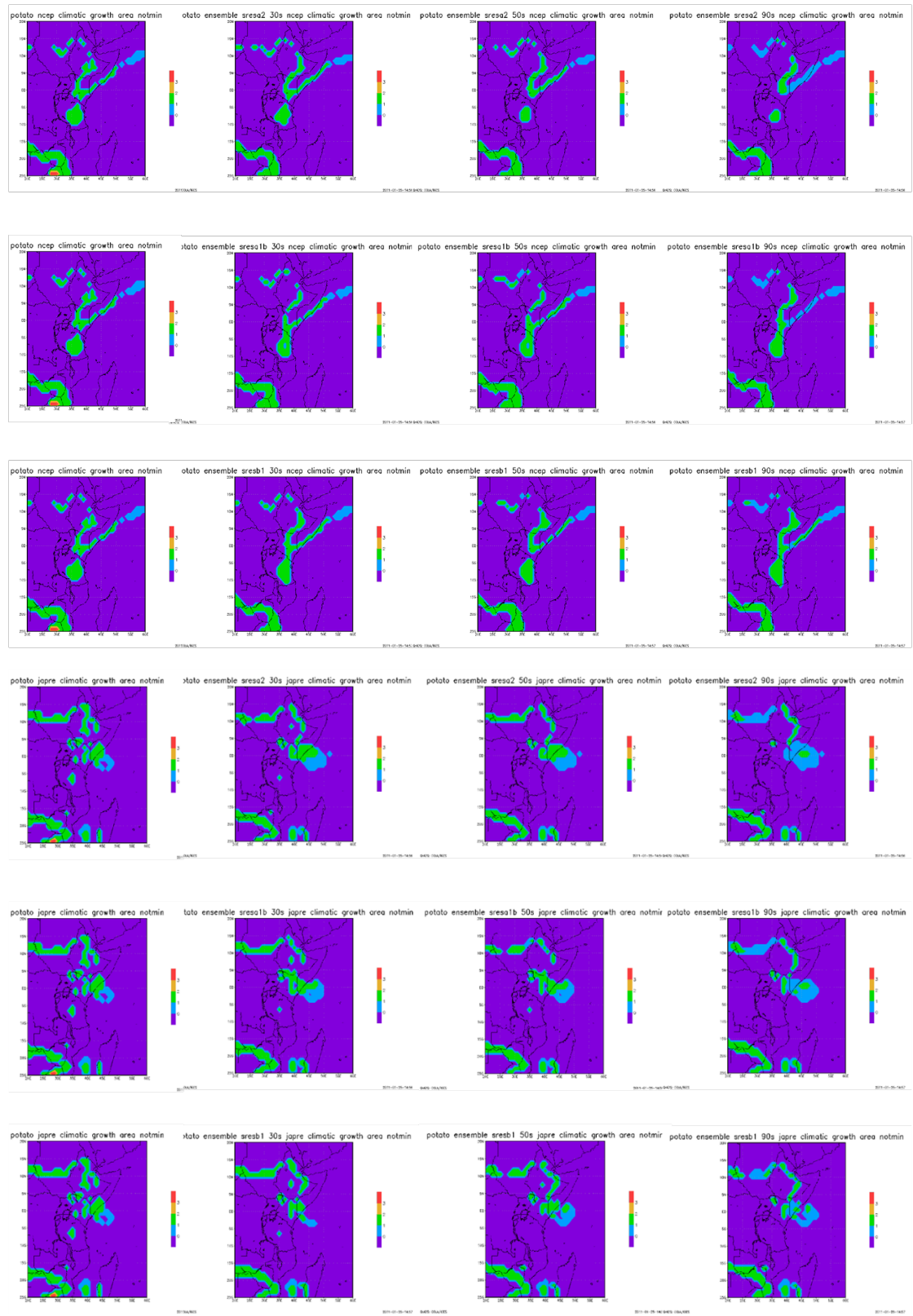
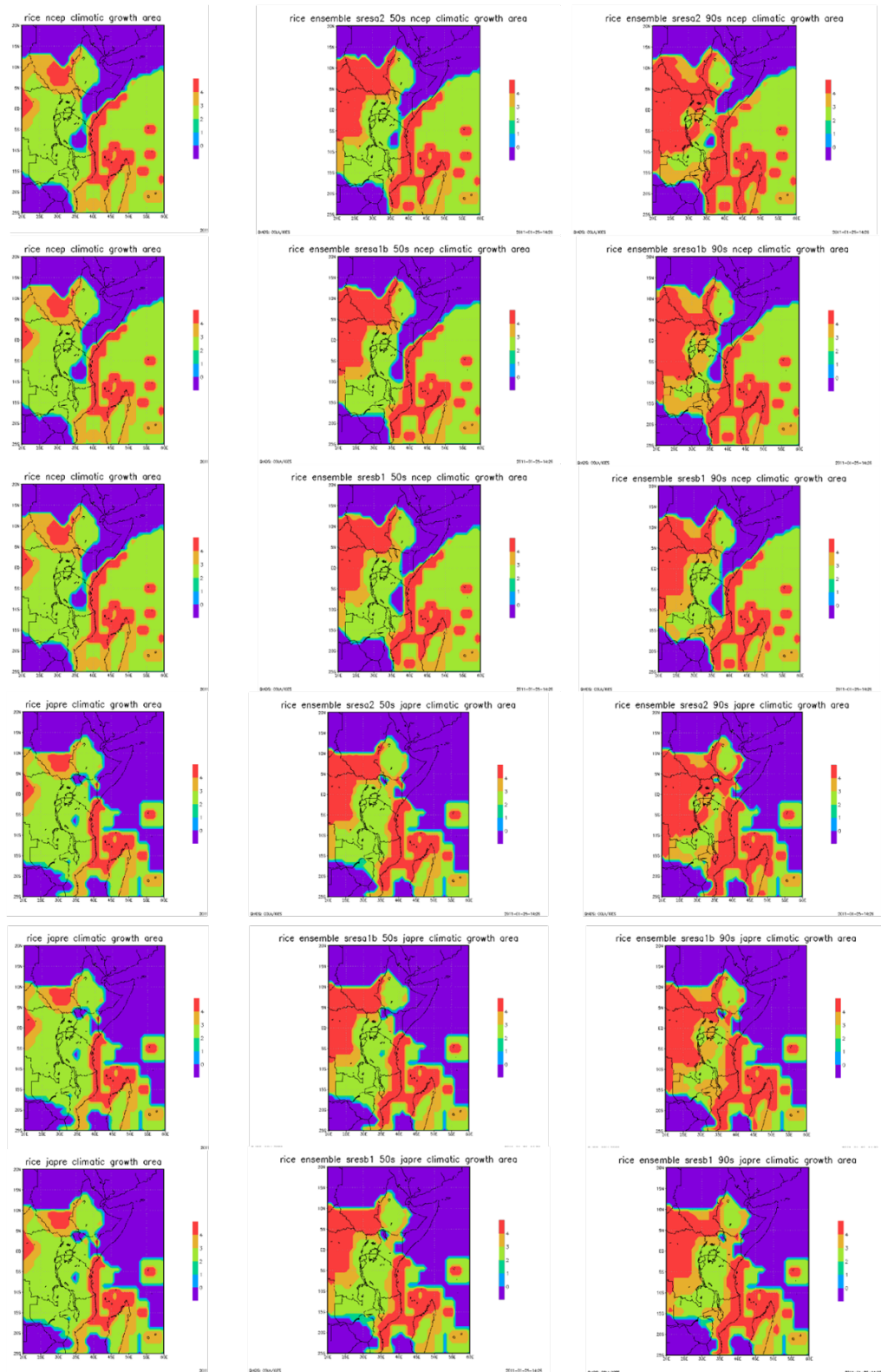
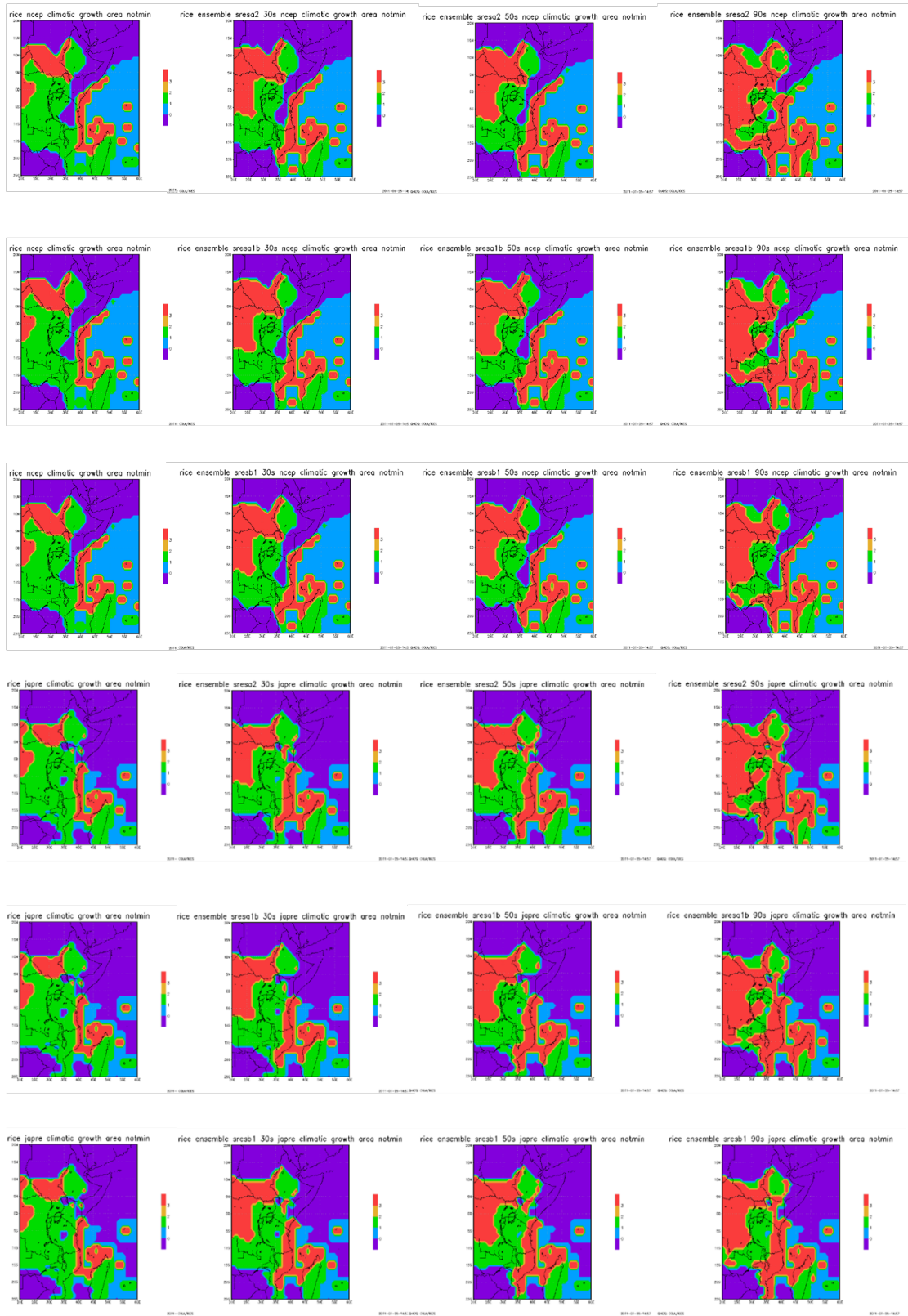


Figure C7 (this and following page): Model ensemble derived crop domains for rice for the 3 periods and 3 forcing scenarios used in this study. Two sets of projections are provided—based on anomalies relative to the NCEP data and the JapRe data, providing a form of initial condition uncertainty. Projections are provided firstly for the 2050s and 2090s including this data and then for 2030s, 2050s and 2090s without minimum temperature data.



(Figure C7 continued)



**Figure C8 (this and following page): Model ensemble derived crop domains for sorghum for the 3 periods and 3 forcing scenarios used in this study. Two sets of projections are provided—based on anomalies relative to the NCEP data and the JapRe data, providing a form of initial condition uncertainty. Projections are provided firstly for the 2050s and 2090s including this data and then for 2030s, 2050s and 2090s without minimum temperature data.**

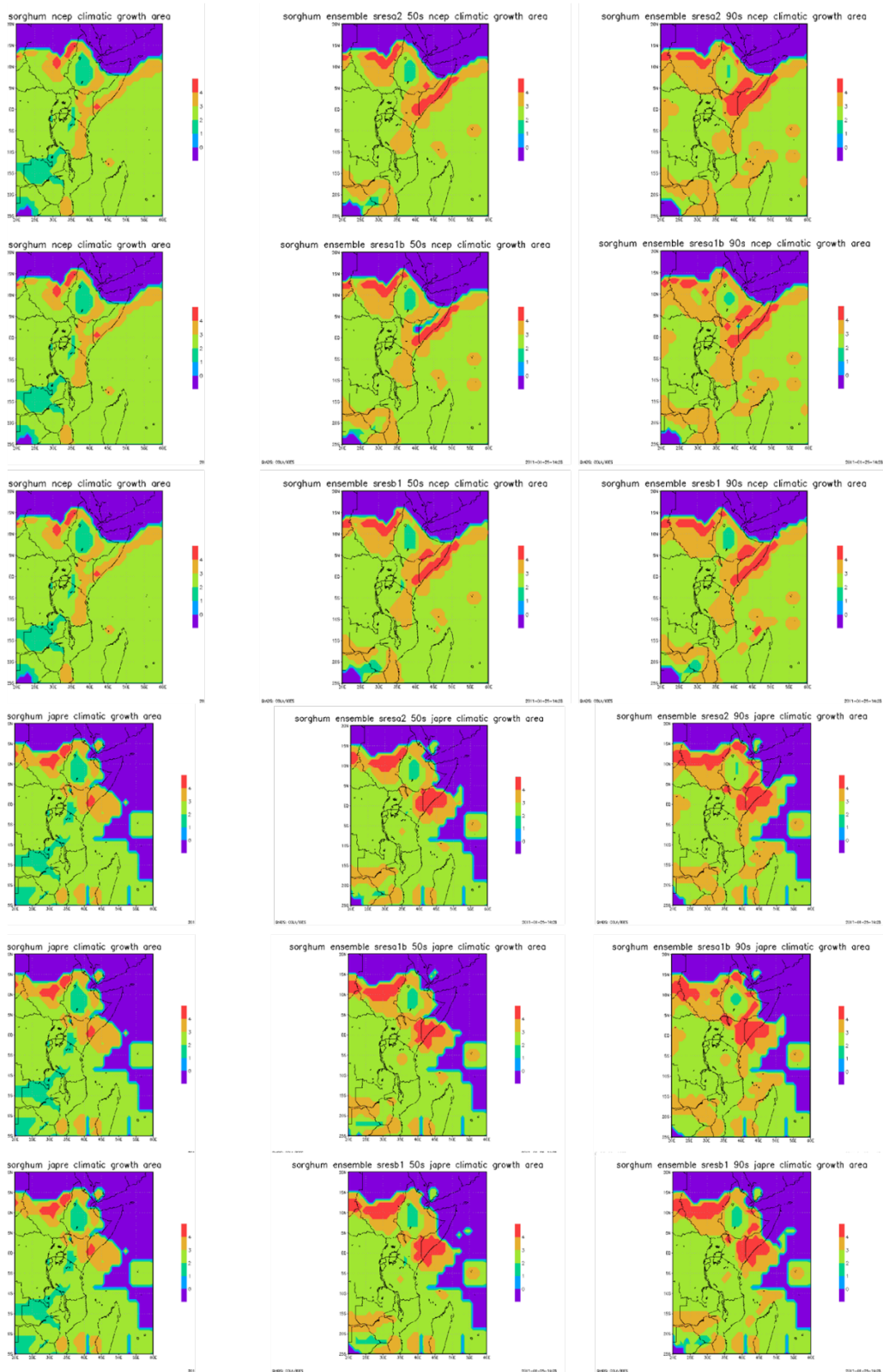


(Figure C8 continued)

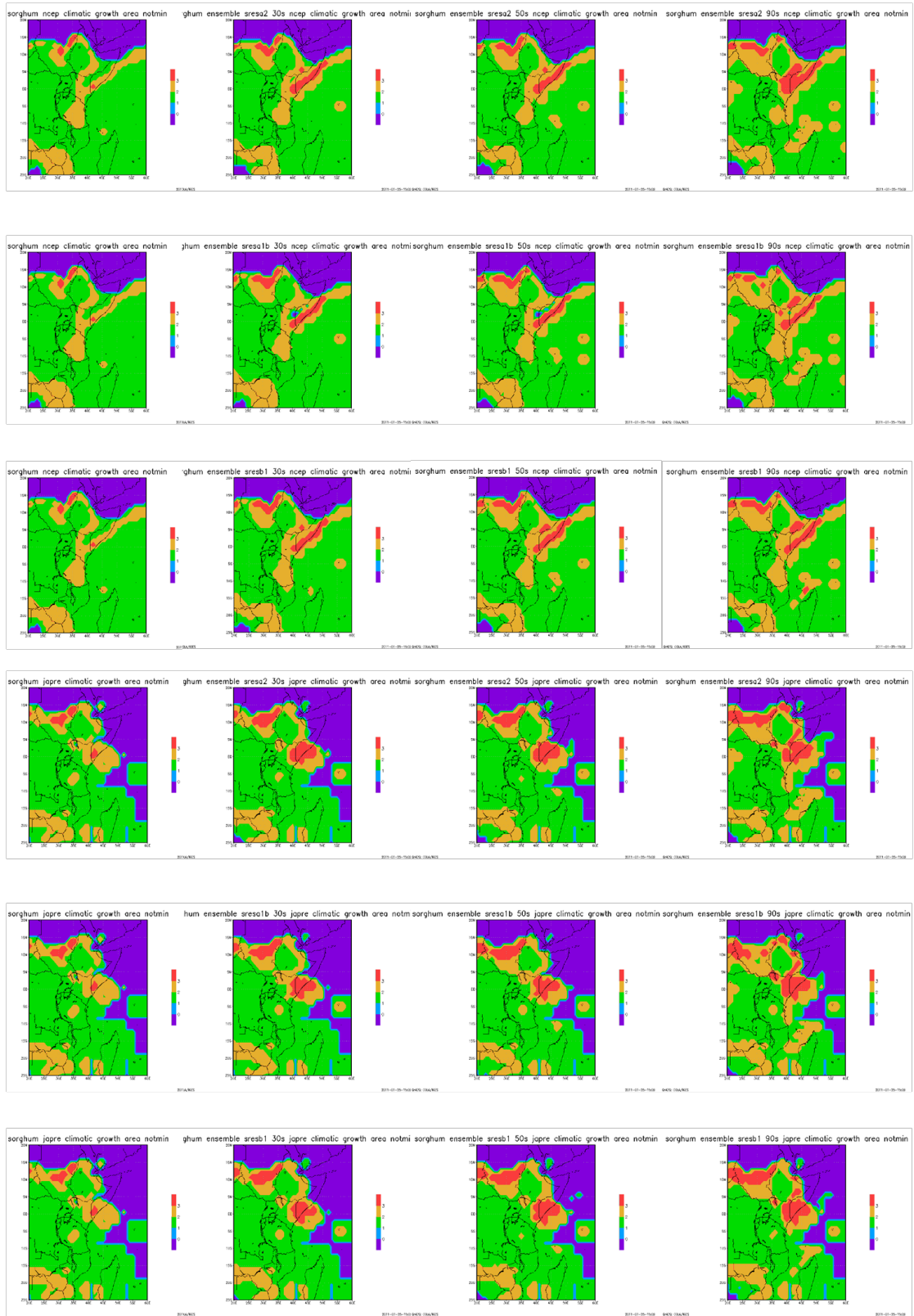
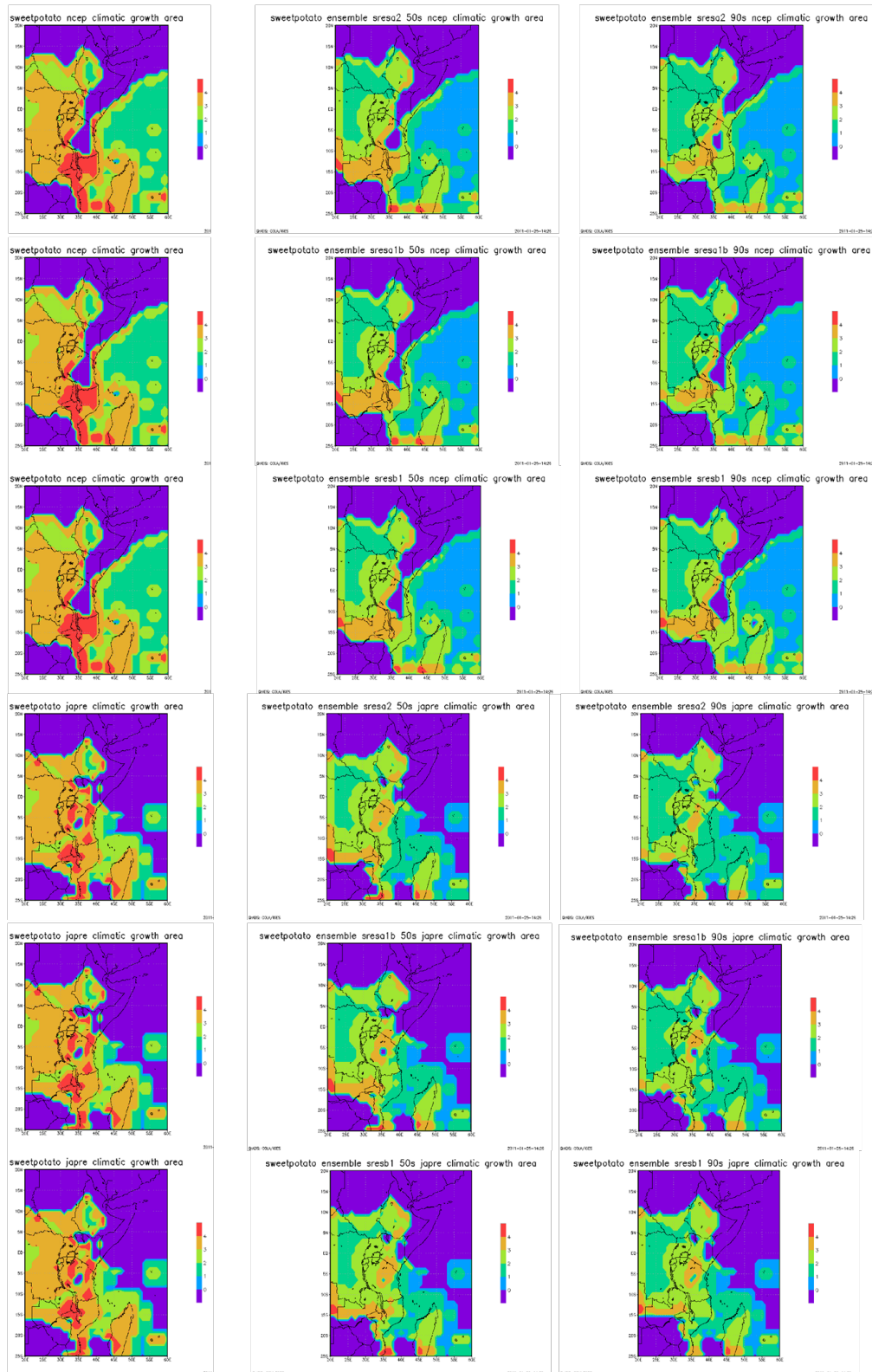
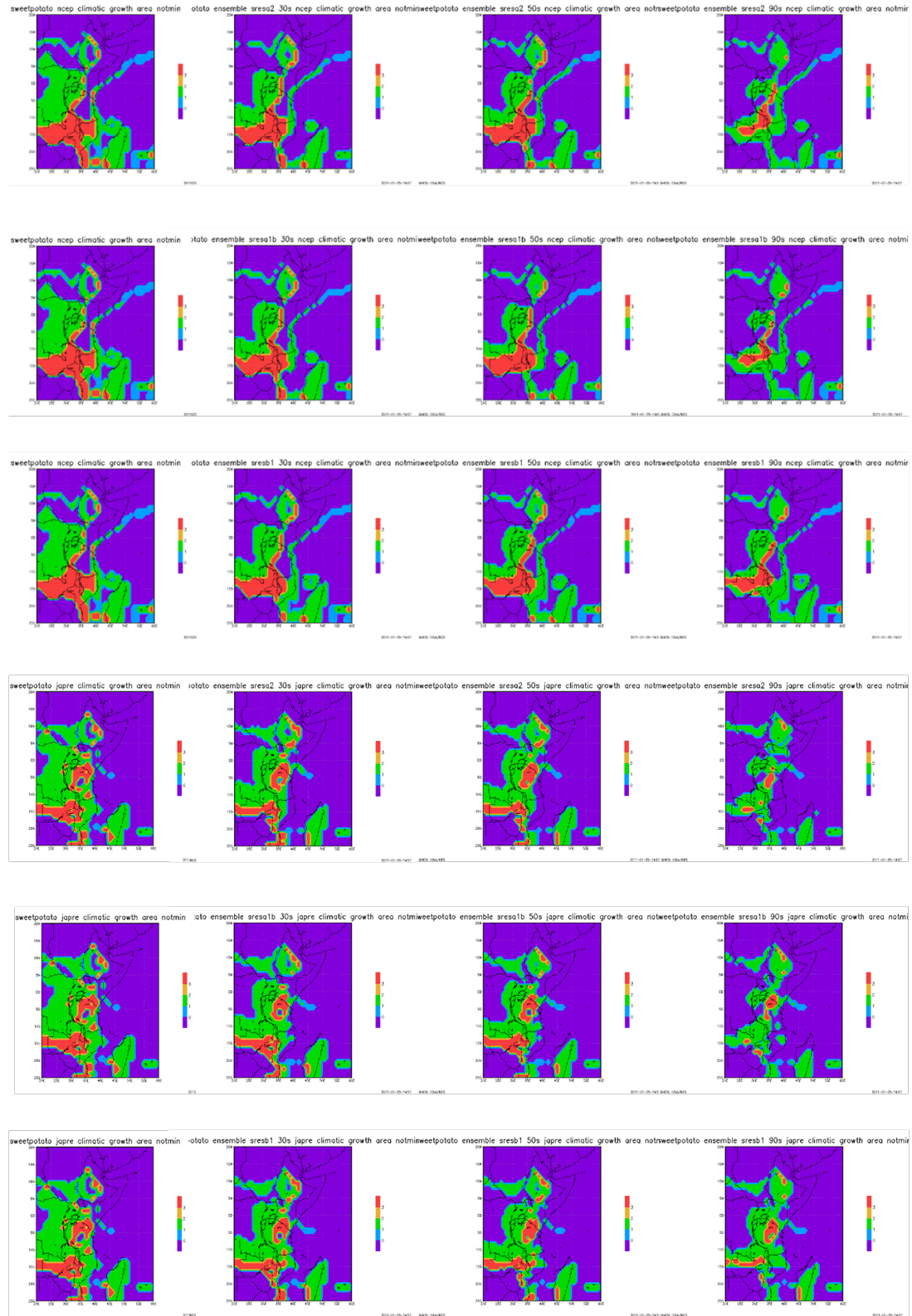


Figure C9 (this and following page): Model ensemble derived crop domains for sweet potato for the 3 periods and 3 forcing scenarios used in this study. Two sets of projections are provided—based on anomalies relative to the NCEP data and the JapRe data, providing a form of initial condition uncertainty. Projections are provided firstly for the 2050s and 2090s including this data and then for 2030s, 2050s and 2090s without minimum temperature data.



(Figure C9 continued)



**Figure C10 (this and following page): Model ensemble derived crop domains for wheat for the 3 periods and 3 forcing scenarios used in this study. Two sets of projections are provided—based on anomalies relative to the NCEP data and the JapRe data, providing a form of initial condition uncertainty. Projections are provided firstly for the 2050s and 2090s including this data and then for 2030s, 2050s and 2090s without minimum temperature data.**

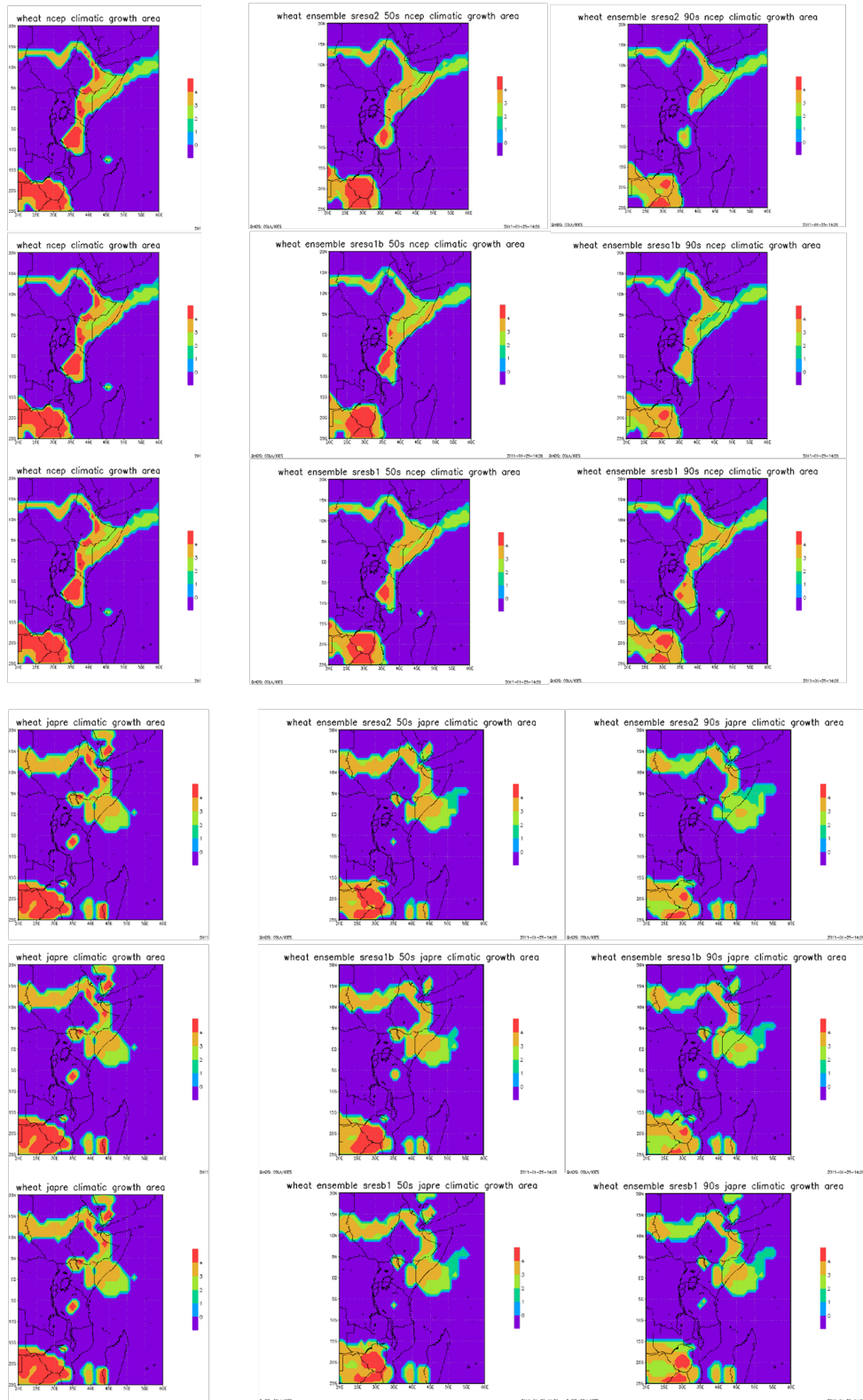
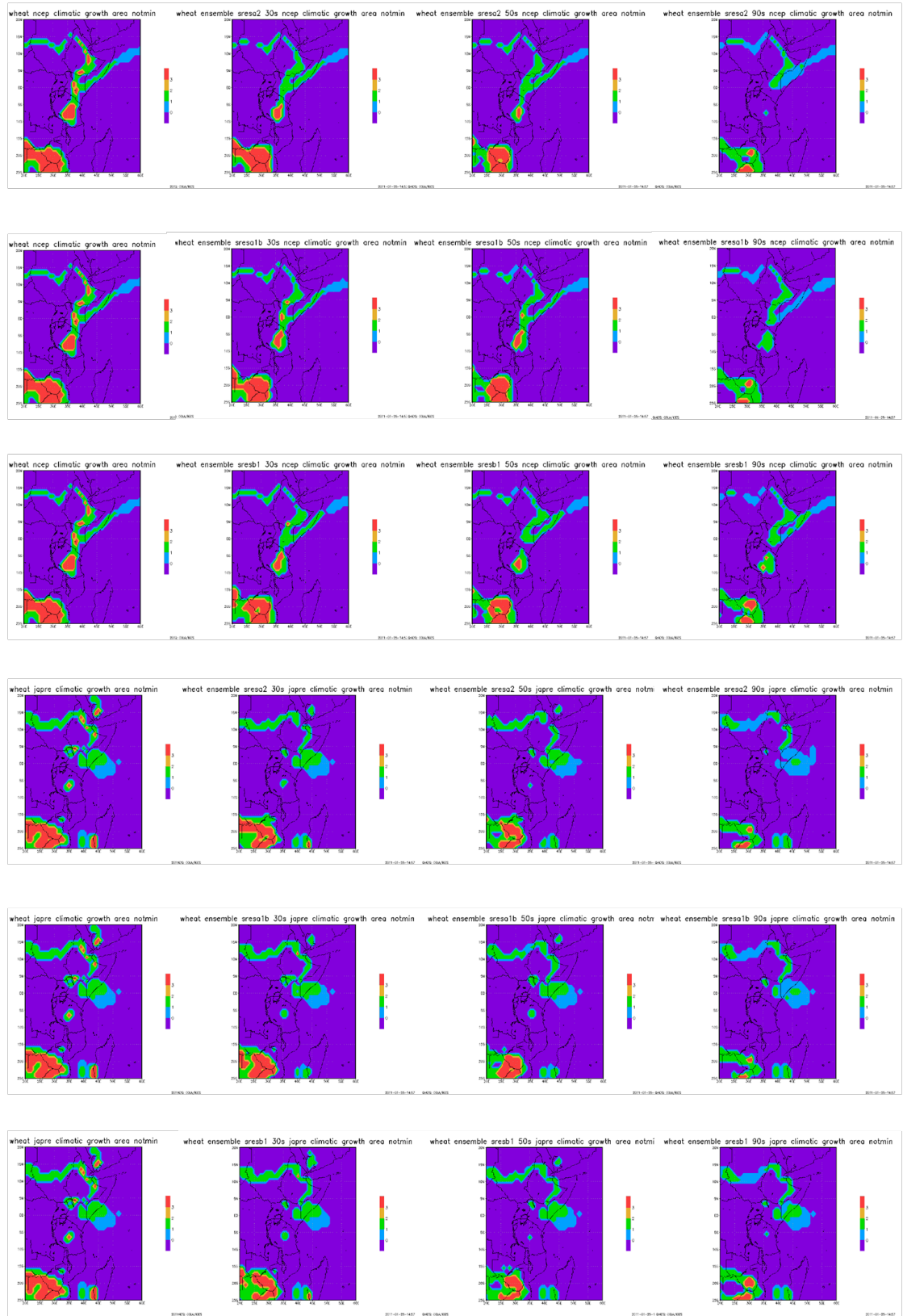


(Figure C10 continued)



## References

- Anyah RO, Semazzi FHM. 2006. Climate variability over the Greater Horn of Africa based on NCAR AGCM ensemble. *Theoretical and Applied Climatology* 86(1-4): 39–62.
- Anyah RO, Semazzi FHM. 2007. Variability of East African rainfall based on multiyear RegCM3 simulations. *International Journal of Climatology* 27(3): 357–371.
- Behera SK, et al. 2005. Paramount impact of the Indian Ocean dipole on the East African short rains: A CGCM study. *Journal of Climate* 18(21): 4514–4530.
- Black E, et al. 2003. An observational study of the relationship between excessively strong short rains in coastal East Africa and Indian Ocean SST. *Monthly Weather Review* 131(1): 74–94
- Camberlin P, Philippon N. 2002. The East African March–May rainy season: Associated atmospheric dynamics and predictability over the 1968–97 period. *Journal of Climate* 15(9): 1002–1019.
- Caminade C, Terray L. 2006. Influence of increased greenhouse gases and sulphate aerosols concentration upon diurnal temperature range over Africa at the end of the 20<sup>th</sup> century. *Geophysical Research Letters* 33 (15): L15703.
- Caminade C, Terray L. 2010. Twentieth century Sahel rainfall variability as simulated by the ARPEGE AGCM, and future changes. *Climate Dynamics* 35(1): 75–94.
- Christy JR, et al. 2009. Surface temperature variations in East Africa and possible causes. *Journal of Climate* 22(12): 3342–3356.
- Doherty RM, et al. 2010. Implications of future climate and atmospheric CO<sub>2</sub> content for regional biogeochemistry, biogeography and ecosystem services across East Africa. *Global Change Biology* 16(2): 617–640.
- Easterling DR, et al. 2000. Climate extremes: Observations, modeling, and impacts. *Science* 289(5487): 2068–2074.
- Funk C, et al 2008. Warming of the Indian Ocean threatens eastern and southern African food security but could be mitigated by agricultural development. *Proceedings of the National Academy of Sciences of the United States of America* 105(32): 11081–11086.
- Giannini A, et al. 2008. A global perspective on African climate. *Climatic Change* 90(4): 359–383.
- Gleckler PJ, et al. 2008. Performance metrics for climate models. *Journal of Geophysical Research-Atmospheres* 113(D6): D06104.

- Herrera E, et al. 2006. Downscaling methods applied to atmosphere-ocean general circulation models (AOGCM). [Méthodes de désagrégation Appliquées aux Modèles du Climat Global Atmosphère-Océan (MCGAO)] *Revue Des Sciences De L'eau* 19(4): 297–312.
- Hirabayashi Y, et al. 2008. A 59-year (1948–2006) global near-surface meteorological data set for land surface models. Part I: Development of daily forcing and assessment of precipitation intensity. *Hydrological Research Letters* 2: 36–40.
- Hulme M, et al. 2001. African climate change: 1900–2100. *Climate Research* 17(2): 145–168.
- Ingram JC, Dawson TP. 2005. Climate change impacts and vegetation response on the island of Madagascar. *Philosophical Transactions of the Royal Society of London Series A-Mathematical Physical and Engineering Sciences* 363(1862): 55–59.
- Jury MR, et al. 1995. Variability of summer rainfall over Madagascar: Climatic determinants at interannual scales. *International Journal of Climatology* 15(12): 1323–1332.
- Jury MR, et al. 2003. The climate of Madagascar. In: Goodman SM, Benstead JP, eds. *The Natural History of Madagascar*. Chicago: University of Chicago Press. p 75–87.
- Kalnay E, et al. 1996. The NCEP/NCAR 40-year reanalysis project. *Bulletin of the American Meteorological Society* 77(3): 437–471.
- Kaspar F, Cubasch U. 2008. Simulation of East African precipitation patterns with the regional climate model CLM. *Meteorologische Zeitschrift* 17(4): 511–517.
- Kharin VV, et al. 2007. Changes in temperature and precipitation extremes in the IPCC ensemble of global coupled model simulations. *Journal of Climate* 20(8): 1419–1444.
- Kiktev D, et al. 2003. Comparison of modeled and observed trends in indices of daily climate extremes. *Journal of Climate* 16(22): 3560–3571.
- Kizza M, et al. 2009. Temporal rainfall variability in the Lake Victoria Basin in East Africa during the twentieth century. *Theoretical and Applied Climatology* 98(1–2): 119–135.
- Kniveton DR, et al. 2009. Trends in the start of the wet season over Africa. *International Journal of Climatology* 29(9): 1216–1225.
- McHugh MJ. 2006. Impact of South Pacific circulation variability on east African rainfall. *International Journal of Climatology* 26(4): 505–521.
- Mitchell TD, Jones PD. 2005. An improved method of constructing a database of monthly climate observations and associated high-resolution grids. *International Journal Of Climatology* 25(6): 693–712.
- Molg t, et al. 2009. Quantifying Climate Change in the Tropical Midtroposphere over East Africa from Glacier Shrinkage on Kilimanjaro. *Journal of Climate* 22(15): 4162–4181.
- Mutai CC, Ward MM. 2000. East African rainfall and the tropical circulation/convection on intraseasonal to interannual timescales. *Journal of Climate* 13(22): 3915–3939.

- Oettli P, Camberlin P. 2005. Influence of topography on monthly rainfall distribution over East Africa. *Climate Research* 28(3): 199–212.
- Osman YZ, Shamseldin A. 2002. Qualitative rainfall prediction models for central and southern Sudan using El Nino-southern oscillation and Indian Ocean sea surface temperature indices. *International Journal of Climatology* 22(15): 1861–1878.
- Riddle EE, Cook KH. 2008. Abrupt rainfall transitions over the Greater Horn of Africa: Observations and regional model simulations. *Journal of Geophysical Research-Atmospheres* 113(D15): D15109.
- Schreck CJ, Semazzi FHM. 2004. Variability of the recent climate of eastern Africa. *International Journal of Climatology* 24(6): 681–701.
- Solomon S, et al. 2007. Climate Change 2007: The Physical Science Basis. Contribution of Working Group I to the Fourth Assessment Report of the Intergovernmental Panel on Climate Change.
- Song Y, et al. 2004. A coupled regional climate model for the Lake Victoria basin of East Africa. *International Journal of Climatology* 24(1): 57–75.
- Sun L, et al. 1999. Application of the NCAR Regional Climate Model to eastern Africa - 2. Simulation of interannual variability of short rains. *Journal of Geophysical Research-Atmospheres* 104(D6): 6549–6562.
- Tadross M, et al. 2008. *Climate change in Madagascar; recent past and future*. Washington DC: World Bank.
- Thornton PK, et al. 2009. Spatial variation of crop yield response to climate change in East Africa. *Global Environmental Change-Human and Policy Dimensions* 19(1): 54–65.
- Trenberth KE, et al. 2003. The changing character of precipitation. *Bulletin of the American Meteorological Society* 84(9): 1205–1217.
- Ummenhofer CC, et al. 2009. Contributions of Indian Ocean sea surface temperatures to enhanced East African rainfall. *Journal of Climate* 22(4): 993–1103.
- Verdin J, et al. 2005. Climate science and famine early warning. *Philosophical Transactions of the Royal Society B-Biological Sciences* 360(1463): 2155–2168.
- Williams AP, Funk C. 2010. *A Westward Extension of the Tropical Pacific Warm Pool Leads to March through June Drying in Kenya and Ethiopia*. U.S Geological Survey Open-File Report 2010–1199.